Universidad Carlos III de Madrid
www.uc3m.es

TESIS DOCTORAL

Three Essays on Network Theory Applied to Capital Markets

Autor:

Gustavo Angel Peralta

Directores:

José María Marín Vigueras

Christian Brownlees

Tutor:

José María Marín Vigueras

Departamento de Economía de la Empresa

Getafe, Mayo de 2016

Universidad Carlos III de Madrid
www.uc3m.es

TESIS DOCTORAL

Three Essays on Network Theory Applied to Capital Markets

Autor: **Gustavo Angel Peralta**

Directores: ***José María Marín Vigueras y Christian Brownlees***

Firma del Tribunal Calificador:

Firma

Presidente:

Vocal:

Secretario:

Calificación:

Getafe, de de

"Todas las teorías son legítimas y ninguna tiene importancia.
Lo que importa es lo que se hace con ellas."

Jorge Luis Borges

Index

Agradecimientos

Quiero expresar mi gratitud a todas aquellas personas que me han acompañado a lo largo de este proceso que culmina con la lectura de esta tesis doctoral, sin su apoyo y comprensión estoy seguro que hubiera sido imposible concluir mi investigación.

En primer lugar, quiero agradecer a mis Directores, José María Marín Vigueras y Christian Brownlees, tanto por sus contribuciones estrictamente técnicas como por su apoyo personal en aquellos momentos difíciles del doctorado. Quiero agradecer también a mi co-autor pero sobre todo amigo, Abalfazl Zareei, por haberme acompañado en esta travesía.

Agradezco al personal del Departamento de Estudios, Estadísticas y Publicaciones de la Comisión Nacional de Mercado de Valores (CNMV). Ciertamente, mi investigación se ha beneficiado de sus continuos feedbacks y sugerencias. En particular, quiero expresar mi gratitud a Pablo Gasós Casao y a Elías López Blanco por depositar su confianza en este trabajo.

Quiero dar las gracias a todo el profesorado del Departamento de Economía de Empresas de la Universidad Carlos III de Madrid; particularmente agradezco a Sergio Vicente por su gran predisposición y cercanía, principalmente durante los primeros pasos de mi investigación. No quiero dejar de agradecer a mis compañeros y amigos con los que he compartido innumerables experiencias de vida a lo largo de este tiempo. Cada uno de estos recuerdos quedará guardados en mi memoria con mucho aprecio.

Por último, pero no por ello menos importante, quiero dar las gracias a mis padres, Nestor y María del Carmen y a mi hermana Luciana por confiar siempre en mí y en este proyecto. Han sido, son y serán personas fundamentales en mi vida. Con toda certeza, puedo decir que no hubiera sido posible llegar hasta aquí sin su continuo apoyo.

Gustavo

Madrid, Mayo 2016

Introduction

In simple terms, a network is a set of elements called *nodes* that are connected among them with *links*. Such stylized structures are flexible enough to represent the patterns of interconnectivity of systems as different as the internet, social networks, interbank networks, distribution network, etc. The main focus of the network theory is to identify the essential properties that characterize a network and to determine to which extent those properties affect the performance of the processes taking place upon it. This dissertation can be thought of as an application of network theory to capital markets. Therefore, the main goal of this study is to contribute to the financial research from this novel perspective by providing new insights about well-established financial concepts and by highlighting those empirical findings that become evident through the lens of this approach.

The first chapter reinterprets fundamental results of the modern theory of portfolios from the perspective of the network theory. Specifically, it is proven the negative relationship between the centrality of the securities comprising the financial network and their optimal portfolio's weights. Additionally, a network-based investment strategy is proposed showing enhanced risk-adjusted returns compared to well-known benchmarks.

The second chapter investigates the Spanish financial network by identifying its fundamental features. In particular, it is shown the disproportional importance of the banking sector for the Spanish capital market given its relatively large centrality. The most relevant finding of this chapter regards to the identification of certain network-based measures acting as leading indicators of market instability.

Finally, the third chapter analyzes the nature of volatility spillovers across major international financial markets. To this end, a particular network is in place whose nodes account for specific countries while the links correspond to significant correlation between their volatilities. Two salient findings are worth mentioning: *i)* the empirical evidence indicates that the volatility tends to spread across economically connected countries and *ii)* the pattern of volatility's interconnectivity is more likely and stronger among countries from the same continent than across them. The latter observation is consistent with the hypothesis of gradual diffusion of information that is tested and empirically supported by the data.

Introducción

En términos simples, una *red* es conjunto de elementos denominados *nodos* conectados entre sí mediante vínculos o *links*. Dicha estructura estilizada es suficientemente flexible para representar el patrón de interconectividad de sistemas tan diversos como son internet, redes sociales, redes interbancarias, redes de distribución de mercancías, etc. El foco de teoría de redes es identificar aquellas propiedades esenciales que caracterizan una red y determinar en qué medida estas propiedades afectan la performance de los procesos que tienen lugar sobre la misma. Esta tesis doctoral debe ser entendida como una aplicación de teoría de redes al ámbito de los mercados de capitales. De esta manera, el objetivo principal del trabajo es contribuir con la investigación financiera desde una perspectiva innovadora proveyendo tanto nuevas intuiciones sobre conceptos financieros tradicionales como remarcando aquellos hallazgos empíricos que solo se evidencian mediante la aplicación de este enfoque.

En el primer capítulo, se reinterpretan resultados fundamentales de la teoría moderna de carteras desde la perspectiva de teoría de redes. En particular, se prueba la relación inversa entre la centralidad de los activos que conforman la red financiera y su peso en una cartera óptima. Adicionalmente, se propone una estrategia de inversión basada en la red financiera que muestra mejores rendimientos ajustados por riesgo en comparación con otras estrategias de referencia para la industria.

En el segundo capítulo, se investiga la red financieras del mercado de capitales español identificando sus características esenciales. De esta caracterización se revela, por ejemplo, la importancia desproporcionada del sector bancario en el mercado español dado su alto nivel de centralidad. La contribución más destacada de este capítulo consiste en la identificación de ciertas medidas basadas en la red financieras española que asumen el rol de indicadores adelantados de estrés financiero.

Finalmente, en el tercer capítulo se analiza la naturaleza del derrame de volatilidad entre los principales mercados financieros internacionales. Para ello, se construye una red donde cada nodo corresponde a un país mientras que cada link identifica una fuerte correlación entre sus volatilidades. Vale la pena mencionar dos hallazgos significativos de este estudio: *i)* el análisis muestra como la volatilidad entre países tiende a propagarse hacia otros mercados económicamente relacionados y *ii)* los datos indican que el patrón de interconectividad es marcadamente más fuerte y probable entre países que pertenecen al mismo continente. Esta última observación es consistente con la hipótesis de difusión gradual de información la cual es contrastada y respaldada empíricamente.

Chapter 1: A Network Approach to Portfolio Selection†

Co-authored with Abalfazl Zareei[a]

Abstract

In this study, a financial market is conceived as a network where the securities are nodes and the links account for returns' correlations. We theoretically prove the negative relationship between the centrality of assets in this financial market network and their optimal weights under the Markowitz framework. Therefore, optimal portfolios overweight low-central securities to avoid the large variances that result when highly influential stocks are included in the investor's opportunity set. Next, we empirically investigate the major financial and market determinants of stock's centralities. The evidence indicates that highly central nodes tend to coincide with older, larger-cap, cheaper and financially riskier securities. Finally, we explore by means of in-sample and out-of-sample analysis the extent to which the structure of the stock market network can be employed to improve the portfolio selection process. We propose a network-based investment strategy that outperforms well-known benchmarks while presenting positive and significant Carhart alphas. The major contribution of the paper is to employ the financial market network as a useful device to improve the portfolio selection process by targeting a group of assets according to their centrality.

Keywords: Network Theory, Centrality, Portfolio Selection

JEL Classification: C00, C45, C55, G10, G11, G17

† We thank Francisco J. Nogales, Jesús D. Moreno, Ricardo Crisóstomo and the participants in the 22nd Finance Forum of the Spanish Finance Association (AEFIN) and in the internal seminars at both CNMV and Universidad Carlos III de Madrid for helpful comments.

[a] Abalfazl Zareei (corresponding author) is with Department of Business Administration at Universidad Carlos III de Madrid, *Address:* Calle Madrid, 126, 28903, Getafe, Madrid, Spain.

1. Introduction

In his seminal paper, Markowitz (1952) laid the foundation of modern portfolio theory. In this static framework, investors optimally allocate their wealth across a set of assets considering only the first and second moment of the returns' distribution. Despite the profound changes derived from this publication, the out-of-sample performance of Markowitz's prescriptions is not as promising as expected. The poor performance of Markowitz's rule stems from the large estimation errors on the vector of expected returns (Merton, 1980) and on the covariance matrices (Jobson and Korkie, 1980) leading to the well-documented error-maximizing property discussed by Michaud and Michaud (2008). The magnitude of this problem is evident when we acknowledge the modest improvements achieved by those models specifically designed to tackle the estimation risk (DeMiguel et al., 2009). Moreover, the evidence indicates that the simple yet effective equally-weighted portfolio rule has not been consistently out-performed by more sophisticated alternatives (Bloomfield et al., 1977; DeMiguel et al., 2009; Jorion, 1991).

Recently, researchers from different fields have characterized financial markets as networks in which securities correspond to the nodes and the links relate to the correlation of returns (Barigozzi and Brownlees, 2014; Billio et al., 2012; Bonanno et al., 2004; Diebold and Yilmaz, 2014; Hautsch et al., 2015; Mantegna, 1999; Onnela et al., 2003; Peralta, 2015; Tse et al., 2010; Vandewalle et al., 2001; Zareei, 2015). In spite of the novel and interesting insights obtained from these network-related papers, most of their results are fundamentally descriptive and lack concrete applications in portfolio selection process. We contribute to this line of research by investigating the extent to which the underlying structure of this financial market network can be used as an effective tool in enhancing the portfolio selection process.

Our theoretical results establish a bridge between Markowitz's framework and the network theory. On the one hand, we show a negative relationship between optimal portfolio weights and the centrality of assets in the financial market network. The intuition is straightforward: those securities that are strongly embedded in a correlation-based network greatly affect the market and their inclusion in a portfolio undermines the benefit of diversification resulting in larger variances. We refer to the centrality of stocks as their systemic dimension. On the other hand, each security is also characterized by an individual dimension such as Sharpe ratio or volatility depending on the specific portfolio formation objective. Next, we theoretically show a positive relationship between the assets' individual performances and their optimal portfolio weights. In a nutshell, optimal weights from the Markowitz framework can be interpreted as an optimal trade-

off between the securities' systemic and individual dimensions in which the former is intimately related to the notion of network centrality.

From a descriptive perspective and relying on US data, we present evidence indicating that financial stocks are the most central nodes in the financial market network in accordance with Peralta (2015) and Tse et al., (2010). Additionally, we document a positive association between the centrality of a security and its corresponding beta from CAPM pointing out the large, although not perfect, correlation between this network indicator and the standard measure of systematic risk. In order to identify the salient financial and market features affecting securities' centrality, we estimate several specifications of a quarterly-based panel regression model upon a set of 200 highly capitalized stocks in the S&P500 index from Oct-2002 to Dec-2012. Our results present some empirical evidence indicating that highly central stocks correspond to firms that are older, cheaper, higher capitalized and financially riskier.

Finally, by means of in-sample and out-of-sample analysis, we investigate the extent to which the structure of the financial market network can be used to enhance the portfolio selection process. In order to check the robustness of our results and to avoid data mining bias, four datasets are considered, accounting for different time periods and markets. We propose a network-based investment rule, termed as ρ-dependent strategy, and report its performance against well-known benchmarks. The evidence shows that our network-based strategy provides significant larger out-of-sample Sharpe ratios compared to the ones obtained by implementing the $1/N$ rule or Markowitz-based models. Moreover, these enhanced out-of-sample performances are not explained by large exposures to the standard risk factors given the reported positive and statistically significant Carhart alphas. Finally, it is worth mentioning that our results are robust to different portfolio settings and transaction cost. We argue that our network-based investment policy captures the logic behind Markowitz's rule while making more efficient use of fundamental information, resulting in a substantial reduction of wealth misallocation.

The contribution of the paper is twofold. On the one hand, this paper sheds light on the connection between the modern theory of portfolios and the emerging literature on financial networks. On the other hand, our network-based investment strategy attempts to simplify the portfolio selection process by targeting a group of stocks within a certain range of network centrality. As far as we are aware, Pozzi et al. (2013) is the only paper that attempts to take advantage of the topology of the financial market network for investment purposes. They argue in favor of an unconditional allocation of wealth towards the outskirts of the structure. We depart from their results by proposing the ρ-dependent strategy which is contingent on the

correlation between the systemic and individual dimensions of the assets comprising the financial market network. Moreover, and in contrast to their synthetic centrality index, we show that our measure of centrality is strongly rooted in the principles of portfolio theory.

The remainder of the paper is organized as follows. Section 2 presents the notion of assets' centrality in the financial network and its connection to Markowitz framework. Section 3 describes the datasets used in the empirical applications. Section 4 provides a detailed statistical description of stocks in accordance to their centrality. Section 5 addresses the interaction between assets' centrality and optimal portfolio weights by relying on an in-sample analysis. Section 6 presents the ρ-dependent strategy and compares its out-of-sample performance to various conventional portfolio strategies. Finally, section 7 concludes and outlines future research lines.

2. A Bridge between Optimal Portfolio Weights and Network Centrality

The notion of centrality, intimately related to the social network analysis, aims to quantify the influence/importance of certain nodes in a given network. As discussed in Freeman (1978), there are several measurements in the literature each corresponding to the specific definition of centrality. The so-called eigenvector centrality, firstly proposed by Bonacich (1972), has become standard in network analysis. This section formally defines this measure and determines its relationship with optimal portfolio weights.

2.1 Defining network centrality

We denote by $G = \{N, \omega\}$, a network composed by a set of nodes $N = \{1,2, \dots, n\}$ and a set of links, ω, connecting pairs of nodes. If there is a link between nodes i and j, we indicate it as $(i,j) \in \omega$. A convenient rearrangement of the network information is provided by the $n \times n$ adjacency matrix $\Omega = [\Omega_{ij}]$ whose element $\Omega_{\mathrm{ij}} \neq 0$ whenever $(i,j) \in \omega$. The network G is said to be undirected if no-causal relationships are attached to the links implying that $\Omega = \Omega^{\mathrm{T}}$ since $(i,j) \in \omega \Leftrightarrow (j,i) \in \omega$. When Ω_{ij} entails a causal association from node j to node i, the network G is said to be directed. In this case, it is likely that $\Omega \neq \Omega^T$ since $(i,j) \in \omega$ does not necessarily imply $(j,i) \in \omega$. For unweighted networks, $\Omega_{ij} \in \{0,1\}$ and therefore only on/off relationships exist. On the contrary, when $\Omega_{ij} \in \mathbb{R}$, the links track the intensity of the interactions between nodes giving rise to weighted networks. The reader is referred to Jackson (2010) for a comprehensive treatment of the network literature.

According to Bonacich (1987, 1972), the eigenvector centrality of node i, denoted by v_i, is defined as the proportional sum of its neighbors' centrality.[1] (Newman, 2004) extends this notion to weighted networks for which v_i is proportional to the weighted sum of the centralities of neighbors of node i with Ω_{ij} as the corresponding weighting factors. It is computed as follows.

$$v_i \equiv \lambda^{-1} \sum_j \Omega_{ij} v_j \quad (1)$$

Note that node i becomes highly central (large v_i) by being connected either to many other nodes or to just few highly central ones. By restating equation (1) in matrix terms, we obtain $\lambda v = \Omega v$ indicating that the centrality vector v is given by the eigenvector of Ω corresponding to the largest eigenvalue, λ.[2] More formally:

Definition 1: Consider the undirected and weighted network $G = \{N, \Omega\}$, with N as the set of nodes and Ω as the adjacency matrix. The eigenvector centrality of node i in G denoted by v_i is proportional to the ith-component of the eigenvector of Ω corresponding to the largest eigenvalue λ_1.

2.2 Key results from the modern portfolio theory

The mathematical principles of modern portfolio theory were established in (Markowitz, 1952). Given that our theoretical results strongly rely on this framework, this section briefly reviews two of its fundamental results: the minimum-variance and the mean-variance investment rules.

Let us assume n risky securities with expected returns vector, μ, and covariance matrix, $\Sigma = [\sigma_{ii}]$. Consider the problem of finding the vector of optimal portfolio weights, w, that minimizes the portfolio variance subject to $w^T \mathbf{1} = 1$ where $\mathbf{1}$ (in bold) corresponds to a column vector whose components are equal to one. This strategy is commonly known as minimum-variance or minv for short. Formally the problem is stated as:

$$\min_w \sigma_p^2 = w^T \Sigma w \ \ subject\ to\ w^T \mathbf{1} = 1 \quad (2)$$

The solution of equation (2) is given by:

$$w^*_{minv} = \frac{1}{\mathbf{1}^T \Sigma^{-1} \mathbf{1}} \Sigma^{-1} \mathbf{1} \quad (3)$$

[1] The terms eigenvector centrality and centrality are used interchangeably throughout this study.

[2] In principle, each eigenvector of Ω is a solution to equation (1). However, the centrality vector corresponding to the largest component in the network is given by the eigenvector corresponding to the largest eigenvalue (Bonacich, 1972).

Denoting by Ω the correlation matrix of returns, and by Δ the diagonal matrix whose ith-main diagonal element is $\sigma_i = \sqrt{\sigma_{ii}}$, the relationship between Ω and Σ can be written as $\Sigma = \Delta\Omega\Delta$. Then, equation (3) is restated in terms of the correlation matrix as follows.

$$\widehat{w}^*_{minv} = \varphi_{minv}\Omega^{-1}\epsilon \tag{4}$$

where $\widehat{w}^*_{i,minv} = w^*_{i,minv} * \sigma_i$, $\varphi_{minv} = \frac{1}{\mathbf{1}^T\Sigma^{-1}\mathbf{1}}$ and $\epsilon_i = 1/\sigma_i$.

The introduction of a risk-free security whose return is given by r_f allows us to account for the mean-variance investment rules. We denote the excess return of security i by $r_i^e \equiv r_i - r_f$ and the vector of expected excess returns by μ^e. The problem of finding the optimal portfolio weights that minimize the portfolio variance for a given level of the portfolio expected excess return R^e is established as follows:

$$\min_w \sigma_p^2 = w^T\Sigma w \ \ subject\ to\ \ w^T\mu^e = R^e \tag{5}$$

The strategy implied by equation (5) is commonly known in the financial literature as the mean-variance strategy or mv for short. Since an investor's wealth might be partially allocated to the risk-free security and short sales of the risk-free security are allowed, the restriction $w^T\mathbf{1} = 1$ is not included in equation (5).[3] The optimum mean-variance portfolio weights vector is computed as follows:

$$w^*_{mv} = \frac{R^e}{\mu^{eT}\Sigma^{-1}\mu^e}\Sigma^{-1}\mu^e \tag{6}$$

Following the same reasoning as before, equation (6) is written in terms of the correlation matrix as follows:

$$\widehat{w}^*_{mv} = \varphi_{mv}\Omega^{-1}\hat{\mu}^e \tag{7}$$

where $\widehat{w}^*_{i,mv} = w^*_{i,mv} * \sigma_i$, $\varphi_{mv} = \frac{R^e}{\mu^{eT}\Sigma^{-1}\mu^e}$ and $\hat{\mu}_i^e = \mu_i^e/\sigma_i$.

2.3 The relationship between optimal portfolio weights and asset centralities

By interpreting the correlation matrix of returns as the adjacency matrix of a given network, an overlapping region between portfolio theory and network theory is established. More formally:

[3] Nevertheless, when the tangency portfolio is considered, $w^T\mathbf{1} = 1$ must hold.

Definition 2: Consider N to be a set of securities in a given asset opportunity set and Ω the corresponding returns' correlation matrix. The undirected and weighted financial market network is $FMN = \{N, \Omega\}$, with N as the set of nodes and Ω as the adjacency matrix.

Throughout the study, we set the main diagonal of Ω to zero in order to discard meaningless self-loops in a given financial market network. Since the eigenvectors' structures and the ordering of eigenvalues are the same after performing this operation, our statements in terms of eigenvector centrality remain valid (see appendix A).

Proposition 1 and Corollary 1 establish the negative relationship between security i's optimal portfolio weight and its centrality in the respective financial market networks for both the minv and mv strategies. The reader is referred to appendix A for a detailed proof.

Proposition 1: Consider a financial market network $FMN = \{N, \Omega\}$ where $\{v_1, \dots v_n\}$ and $\{\lambda_1, \dots \lambda_n\}$ account for the sets of eigenvectors and eigenvalues (in descending order) of Ω, respectively. The optimal portfolio weights in the equations (4) and (7) can be written as:

$$\widehat{w}^*_{minv} = \varphi_{minv}\epsilon + \varphi_{minv}\left(\frac{1}{\lambda_1} - 1\right)\epsilon_M v_1 + \Gamma_{minv} \tag{8}$$

$$\widehat{w}^*_{mv} = \varphi_{mv}\hat{\mu}^e + \varphi_{mv}\left(\frac{1}{\lambda_1} - 1\right)\hat{\mu}^e_M v_1 + \Gamma_{mv} \tag{9}$$

where $\epsilon_M = ({v_1}^T\epsilon)$, $\Gamma_{minv} = \varphi_{minv}\left[\sum_{k=2}^{n}\left(\frac{1}{\lambda_k} - 1\right)v_k v_k^T\right]\epsilon$, $\hat{\mu}^e_M = {v_1}^T\hat{\mu}^e$ and $\Gamma_{mv} = \varphi_{mv}\left[\sum_{k=2}^{n}\left(\frac{1}{\lambda_k} - 1\right)v_k v_k^T\right]\hat{\mu}^e$.

Note that ϵ_M and $\hat{\mu}^e_M$ in equations (8) and (9) account for weighted averages of the inverted standard deviations of returns and Sharpe ratios, respectively, with weighting factors given by the elements of v_1. From a principal component perspective, we interpret them as the corresponding variables at market level. Moreover, since the empirical evidence indicates that only eigenvector elements corresponding to the largest eigenvalue have informational content (Green and Hollifield, 1992; Laloux et al., 1999; Trzcinka, 1986), we focus on v_1 and λ_1 by defining Γ_{minv} and Γ_{mv} in terms of v_j and λ_j for $j > 1$.

The first term in equations (8) and (9) considers simple investment rules that only take into account the performance of securities as if they were in isolation. Therefore, lower (higher) standard deviations of returns (Sharpe ratios) are consistent with higher optimal portfolio weights. We call this the individual dimension of securities. The second term in the same

expressions quantifies the extent to which optimal weights deviate from the previously mentioned rule due to the centrality of securities. We call this the systemic dimension of securities. Corollary 1 states that, under plausible conditions, there is a negative relationship between optimal portfolio weights and network centralities.

Corollary 1: Assuming that $\lambda_1 > 1$ and $\epsilon_M, \hat{\mu}_M^e \in \mathbb{R}_+$. Then, $\frac{\partial \hat{w}_{r,i}^*}{\partial v_{1,i}} < 0$ for $r = minv, mv$.

Based on Rayleigh's inequality (Van Mieghem, 2011), the assumption $\lambda_1 > 1$ in Corollary 1 requires a positive mean correlation of returns, which is not a strong condition in practical terms.[4] It is worth mentioning that centrality does not necessarily rank assets in the same way as the mean correlation (mean of the row or columns in Ω) does. It is straightforward to show that for a correlation matrix with equal off-diagonal entries, each security is given the same amount of centrality and mean correlation (the leading eigenvector is $\frac{1}{\sqrt{n}}\mathbf{1}$). However, this association breaks as the dispersion in the distribution of Ω_{ij} increases.[5]

Our theoretical results are consistent with Pozzi et al. (2013) in establishing that optimal portfolio strategies should overweight low-central securities and underweight high-central ones. Therefore, optimal investors attempt to benefit from diversification by avoiding the allocation of wealth towards assets that are central in the correlation-based network. However, we depart from Pozzi et al. (2013) in two respects. First, our measure of centrality is derived from the investor's optimization problem, and thus is intimately associated with Markowitz's framework. Secondly, the individual performance of securities is overlooked in their study, leading to an incomplete analysis and potentially impairing the benefits of a network-based portfolio strategy.

3. Dataset Description and Stock Market Network Estimation

In order to avoid data mining bias and to test the robustness of our results, four datasets are considered throughout the empirical sections accounting for different markets and time periods. Unless otherwise stated, split-and-divided-adjusted returns and traded volumes are obtained from CRSP while quarterly financial data comes from COMPUSTAT. The dataset d-S&P contains daily returns for 200 highly capitalized constituents of the S&P-500 index at the end of year 2012 showing non-negative total equity in the period Oct-2002 to Dec-2012. The dataset m-NYSE

[4] Rayleigh's inequality states a classical lower bound for the largest eigenvalues as follows $\lambda_1 \geq \frac{u'\Omega u}{u'u}$ for $u \in \mathbb{R}^n$. If $u = \mathbf{1}$ then $\lambda_1 \geq 1 + \frac{\sum_i \sum_j \Omega_{ij}}{n} = 1 + (n-1)\bar{\Omega}_{ij}$ where $\bar{\Omega}_{ij}$ is the mean correlation of off-diagonal elements of Ω.

[5] In a non-reported simulated exercise, a positive correlation between centrality and mean correlation is observed for a mild dispersion in the distribution of Ω_{ij}.

considers monthly returns for the 200 firms that remain listed in NYSE normalized for capitalization and cheap stocks in the period Jan-64 to Dec-06. [6] The dataset d-FTSE accounts for daily stock returns of the 200 most capitalized constituents of FTSE-250 index during the period Feb-06 to Oct-13. For this particular sample, we rely on Datastream as the data provider. A large dataset named d-NYSE is mainly used for simulation purposes and it considers daily returns for 947 firms listed in NYSE (adjusted for capitalization and cheap stocks explain as in m-NYSE) in the period Jan-2004 to Jul-2007. Finally, the risk-free rates required to compute excess returns for the US and UK markets are gathered from Kenneth French's website and from Gregory et al. (2013), respectively.

The large estimation error of the sample correlation matrix is well-documented (Jobson and Korkie, 1980). Therefore, we implement the shrinkage estimator the correlation matrix $\hat{\Omega}$ upon excess returns as in Ledoit and Wolf (2004) to estimate the adjacency matrix of the corresponding financial market network.

4. Fundamental Drivers of Stock Centrality: Descriptive Analysis

Given the fundamental role assigned to the notion of centrality in this study, this section provides a set of descriptive results found in the d-S&P dataset. Table 1 reports the sample size, market capitalization and traded volume in 2012 (measured in millions of dollars) and the total and mean centrality by economic sectors (classified by firms' SIC codes). Although the manufacturing sector is the largest in terms of capitalization (48%) and traded volume (43%), financial firms are the most central nodes in the stock market network in accordance with reported evidence (Barigozzi and Brownlees, 2014; Peralta, 2015; Tse et al., 2010).

We also notice that the dispersion of the risk-adjusted returns' distribution is not constant across the network. The left panel of figure 1 plots the Sharpe ratio's boxplots conditioning on the low, middle and high terciles of the centrality distribution. Despite no significant difference in means, the Sharpe ratio's distribution shrinks as larger centralities are considered. Moreover, table B.1, included in Appendix B to preserve space, reports significantly greater mean volatility as we move from the bottom tercile (2.05%) to the middle (2.09%) and top tercile (2.24%) of the centrality distribution demonstrating larger risks among high-central securities. The relationship between the β-CAPM and the centrality of each security in the sample is plotted in right panel of figure 1.[7]

[6] The stocks are chosen to have capitalization more than 20th percentile of market capitalization and prices higher than \$5 (Penny stocks with prices lower than \$5 are discarded).

[7] The index S&P 500 is used as the market index for the estimation of the corresponding β from CAPM.

This graph shows an upward-sloping relationship that, although not perfect, indicates that central assets tend to correspond to high systematic risk securities.

Table 1. Market capitalization, traded volume, and centrality by economic sectors. This table reports the total and mean firms' centrality by economic sectors in the d-S&P500 dataset. Market capitalization and traded volume are in millions of dollars and correspond to the end of year 2012. The column Firms gives the number of companies in each economic sector. The columns denoted by % present the percentages with respect to the total of each of the preceding variables.

Economic Sector	Firms	%	Market Cap.	%	Traded Vol.	%	Centrality	
							Total	Mean
Finance, Insurance, And R. Estate	37	19%	2,254,158	20%	70,788	19%	2.74	0.0741
Mining	17	9%	656,688	6%	26,178	7%	1.23	0.0722
Transp., Comm., Elect, Gas, Sanit. S.	27	14%	1,145,092	10%	36,988	10%	1.88	0.0696
Manufacturing	87	44%	5,338,584	48%	156,881	43%	6.01	0.0691
Retail Trade	12	6%	745,486	7%	27,130	7%	0.82	0.0682
Services	13	7%	829,671	7%	37,314	10%	0.89	0.0682
Wholesale Trade	5	3%	142,423	1%	6,011	2%	0.33	0.0656
Construction	2	1%	44,905	0%	3,073	1%	0.13	0.0646
Total	200		11,157,008		364,364			

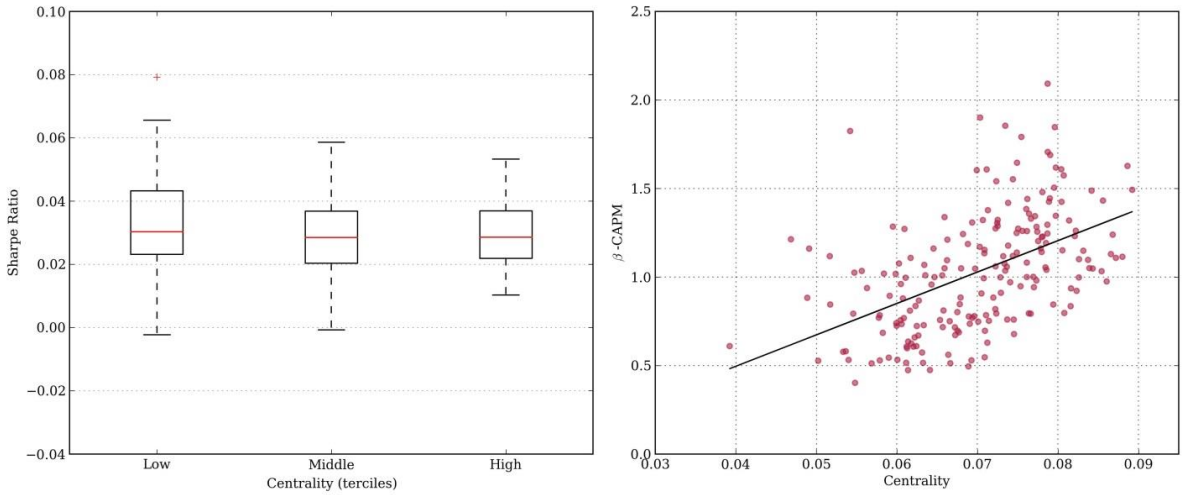

Figure 1. Sharpe ratio distributions for the high, middle and low terciles of securities' centrality (left panel). Relationship between the securities' centrality and the β from CAPM (right panel). Both panels consider the d-S&P dataset.

In order to identify the key financial and market drivers of stocks' centralities, we estimate an unbalanced quarterly-based panel regression largely inspired by Campbell et al. (2008) for the selection of relevant regressors. The study of Green and Hollifield (1992) rejects at a very high level of confidence the hypothesis that the first eigenvector of the covariance matrix is a constant vector. Our empirical exercise attempts to provide an economic content to their result. As before, the dataset used is d-S&P dataset comprising 7,931 firms-quarter data points.

The dependent variable is the centrality of a security (firm) i in quarter t.[8] The financial explanatory variables are ROA_{it}, Lev_{it} and Liq_{it} accounting for the ratio of net income, total liability and cash and short term assets to total assets, respectively. As market explanatory variables, we include $ln(MV_{it})$ and $ln(P_{it})$, denoting the logarithms of the market capitalization on a common-shares basis and the stocks' market price at the end of quarter t, respectively. In addition, $ln(TV_{it})$, Ret_{it} and Std_{it}, referring to the logarithm of total trades, the excess return and the daily standard deviation of returns during quarter t, are additional market explanatory variables. The variable M/B_{it} denotes the Market-to-Book ratio on a common-shares basis at the end of quarter t and is incorporated in the regressions as well. Finally, the logarithm of firms' age indicated as $ln(Age_{it})$ comprises the last independent variable of the model. It is computed by counting the number of quarters elapsed since the appearance of the first market price in CRSP until period t as in Fama and French (2004). To control for the effects of outliers, 1% winsorizing is implemented on regressors except for the case of $ln(Age_{it})$. Table 2 reports summary statistics.

Table 2. Descriptive statistics for the quarterly panel regression variables included in the d-S&P dataset. The description of the variables is as follows: *ROA* is net income/total assets at the end of period *t*, *Lev* is total liability/total assets at the end of period *t*, *Liq* is cash and short term assets over the total assets at the end of period *t*, *ln(MV)* is the logarithm of market capitalization on a common-share basis at the end of period *t, ln(TV)* is the logarithm of total trades during period *t*, *Ret* is the excess return during period *t*, *ln(P)* is the logarithm of stocks' prices at the end of period *t*, *Std* is the return variance during period *t*, *M/B* is the market-to-book ratio on a common-share basis at the end of period *t* and *ln(Age)* is the logarithm of the firms' age computed as in Fama and French (2004) and corresponding to the end of period *t*. The descriptive statistics are reported after 1% winsorising except for *ln(Age)*

Variables	Mean	Std	Percentiles					Skew	Kurtosis
			Min	5%	50%	95%	Max		
Independent									
Financial									
ROA	1.7%	1.7%	-5.0%	-0.1%	1.5%	4.7%	7.5%	0.1	2.7
Lev	59.0%	19.5%	12.2%	23.2%	59.6%	90.8%	94.5%	-0.2	-0.4
Liq	12.1%	13.4%	0.2%	0.7%	6.9%	41.2%	67.0%	1.9	3.7
Market									
ln(MV)	16.98	1.02	14.20	15.34	16.88	18.91	19.42	0.1	0.2
ln(TV)	12.47	1.04	9.95	10.83	12.41	14.28	15.21	0.2	0.1
Ret	2.6%	13.6%	-35.1%	-20.5%	2.8%	25.0%	45.1%	0.1	1.0
ln(P)	3.69	0.58	2.23	2.72	3.70	4.58	5.54	0.1	0.6
Std	1.8%	1.1%	0.7%	0.8%	1.5%	3.9%	6.8%	2.4	6.9
M/B	3.32	2.50	0.59	0.95	2.57	8.50	14.71	2.11	5.42
ln(Age)	4.84	0.77	1.79	3.43	4.96	5.81	5.86	-0.66	-0.12
Dependent									
Centrality	7.01	0.93	4.01	5.27	7.11	8.41	8.95	-0.69	0.86

[8] Only the data corresponding to quarter t is considered for computing the centralities. Additionally, we rescaled centrality by multiplying it by 100 for exposition purposes.

Table 3 presents OLS estimations for various specifications of the panel regression described above. Model I includes dummy variables by quarter and economic sector (first 2 digits of SIC codes) and considers only robust-heteroskedastic standard errors (White, 1980). To tackle the bias induced by autocorrelation and heteroskedasticity in the error term, two-way clustering correction by Cameron et al. (2011) is included in model II. As suggested by Petersen (2009), we also report estimations of model III that considers economic sector dummy variables while clustering the error term by quarters.

Table 3. OLS estimations of three specifications of the quarterly panel regression model implemented upon the d-S&P dataset. Each specification depends on the particular standard error correction method. *t-statistics* are in parentheses and the statistical significance is as follows: * at 5% level, ** at 1% and *** at 0.1% level. Model I combines economic sector and quarterly dummies with robust-heteroscedastic standard errors (White, 1980). Model II considers two-way clustered standard errors (Cameron et al., 2011). Model III includes economic sector dummies while clustering standard errors by quarters.

	Models		
	I	II	III
ROA	-1.128	-0.746	-1.062
	(-1.44)	(-0.41)	(-1.03)
Lev	0.111	0.484	0.111
	(1.31)	(2.30)*	(1.29)
Liq	-0.481	0.200	-0.582
	(-4.36)***	(0.49)	(-4.13)***
M/B	-0.00523	-0.0412	-0.00865
	(-0.90)	(-3.25)**	(-1.15)
ln(MV)	0.239	0.201	0.216
	(8.96)***	(2.23)*	(8.32)***
ln(TV)	-0.230	-0.150	-0.186
	(-7.88)***	(-1.62)	(-6.10)***
Ret	0.401	0.215	0.196
	(4.23)***	(1.15)	(1.16)
ln(P)	-0.239	-0.0106	-0.168
	(-6.40)***	(-0.11)	(-4.02)***
Std	-5.029	5.074	2.399
	(-2.50)*	(1.22)	(0.97)
ln(Age)	0.104	0.0574	0.124
	(5.53)***	(1.23)	(6.78)***
N	7931	7931	7931
R^2	0.174	0.055	0.165
Dummies	*Econ. Sectors and Quarter*	-	*Econ. Sectors*
Std. errors' correction	*Robust Heteroscedastic*	*Clustering by Econ. Sectors and Quarters*	*Clustering by Quarters*

Starting with the analysis of financial explanatory variables, table 3 indicates that ROA's coefficient is negative in each specification, however, it is not significant at the conventional levels. The variable Lev stays positive across models and shows a statistically significant coefficient in Model II comparable to M/B but with the opposite sign. Finally, the coefficient for variable Liq is negative and strongly significant in models I and III. In summary, there is some evidence indicating that highly central stocks are associated with leveraged firms showing less liquid asset positions and low Market-to-Book ratios, suggesting that firms' centrality conveys information on the financial risk profile of the sampled firms.

Among market explanatory variables, $ln(MV)$ shows positive and strongly significant coefficients across specifications evidencing a size effect. The variables $ln(TV)$ and $ln(P)$ present a negative impact on centrality for each specification and remain significant for models I and II. Therefore, low-traded and cheaper securities tend to be highly central in the financial market network. The variable Ret is positive for each model but statistically significant only for the first model. In the case of Std, since it is marginally significant only for model I and changes its sign across specifications, we disregard its effects. Finally, $ln(Age)$ shows positive coefficients that are strongly significant for models I and III.[9]

In a nutshell, our empirical results identify central stocks with greater capitalization, lower price and older firms with riskier financial profiles in terms of leverage, liquid asset positions and Market-to-Book ratios. We argue that the findings in Green and Hollifield (1992), indicating the importance of the first principal component of the covariance matrix, can be explained in terms of the financial and market informational content embedded in assets' centralities.

In an additional analysis reported in Appendix F to save space, we elaborate on the relationships between stocks' centrality and their stability. Specifically, we associate the concept of a stock's stability to the tendency to remain listed in the market without any change in its relative centrality status across time. We find that among the stocks that remain listed in the market, there is a strong tendency to show the same level of centrality through time. Additionally, we investigate the consequences of the period size used in the estimation of the correlation-based network on the ordering of securities provided by centrality. Our results show the large correlations between the rankings of centralities for different lengths of sample periods indicating the robustness of this ordering.

[9] We are grateful to the anonymous referee for suggesting the inclusion of $ln(Age)$ in the analysis.

5. Stock Centrality and Optimal Portfolio Weights: In-Sample Evaluation

The interaction between the individual and the systemic dimensions of stocks is empirically investigated in this section. The dataset used is d-S&P and the results reported below come from both a cross-sectional and a time series in-sample analysis.

5.1 Cross sectional approach

The detailed pattern of co-movements across stocks is properly captured by $\hat{\Omega}$. This matrix conveys an excessive amount of information and leads to a fully connected stock market network that is difficult to analyze.[10] The Minimum Spanning Trees (MST), first introduced in the financial markets by Mantegna (1999), allows us to filter out this adjacency matrix with the aim of uncovering the market skeleton.[11] This technique has been widely applied to several country-specific stock markets including the US (Bonanno et al., 2004; Onnela et al., 2003), Korean (Jung et al., 2006), Greek (Garas and Argyrakis, 2007) and Chinese (Huang, Zhuang, and Yao, 2009) markets among others.

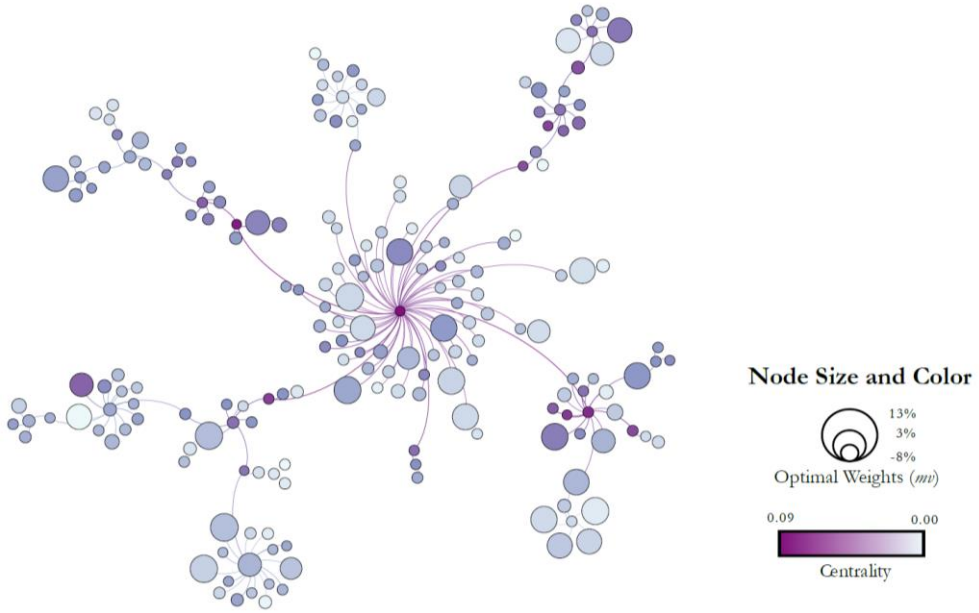

Figure 2. MST stock market network for the d-S&P dataset. The size of nodes corresponds to the optimal weights for the minimum-variance strategy (see equation 3) and the intensity of the colour accounts for the corresponding security's centrality.

Figure 2 plots the MST financial market network for our data where nodes are scaled to the optimal portfolio weights for the minv strategy (see equation (3)) while the colors account for the

[10] A fully connected network refers to a network structure in which each node is connected with the rest.

[11] MST connects the n stocks in a tree-like network by considering the highest $n-1$ paired correlations of returns as links to the extent that no loops are created.

respective security's centrality (darker colors imply greater centrality).[12] Note that investor's wealth is allocated toward lighter nodes (low-central securities) in accordance with Corollary 1. See Appendix C for the full list of stocks with their respective centrality.

The relation between the individual and systemic dimensions of assets is illustrated in figure 3. The horizontal and vertical axes of this plot account for the securities' centralities and the corresponding standard deviations of returns, respectively. Each security is represented by a bubble whose size and color are given by the optimal portfolio weight in the minv rule. Note that most of the investor's wealth is assigned toward stocks located in the bottom-left corner of the graph, thus overweighting low-central-&-low-volatile securities.

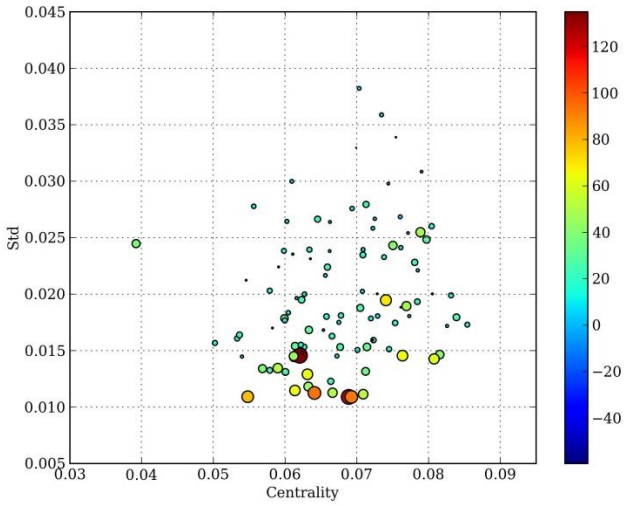

Figure 3. Relationship between standard deviation of returns (Std) and stocks' centrality. Stocks correspond to bubbles whose sizes and colours (colour bar) reflect their optimal portfolio weights in a minimum-variance (*minv*) weights specification. We use d-S&P dataset for this analysis.

Figure 4 presents a scatter plot of Sharpe ratios and centralities for a portfolio applying mv strategy as the investment rule. The left and right panel sets the expected portfolio return, R^e, equal to 10% and 40% of the maximum possible portfolio return, respectively (see equation (6)). As expected, the optimal portfolio for low R^e mainly comprises assets with middle-ranged Sharpe ratios while the investment set moves toward securities with higher Sharpe ratios for larger R^e. Note, however, that the mv strategy avoids the allocation of wealth towards high-central stocks, say stocks with $v_i > 0.08$.

[12] Short sales are allowed in the computation of optimal weights for both *minv* and *mv* strategies.

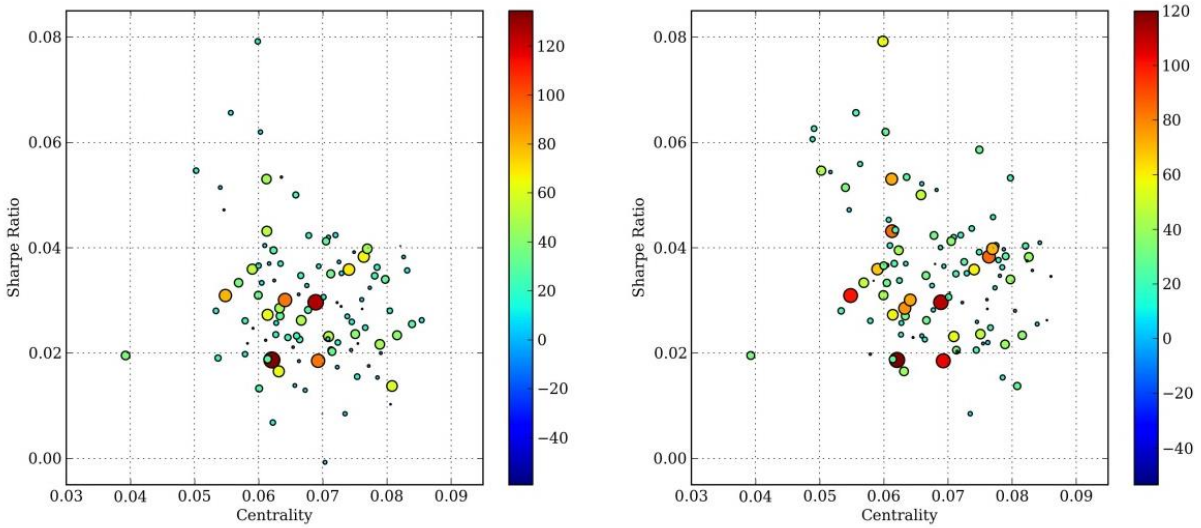

Figure 4. Relationship between Sharpe ratio and stock centrality. Stocks correspond to bubbles whose sizes and colours (colourbar) reflect their optimal portfolio weights in a mean-variance (*mv*) weights specification. The required expected portfolio return R^ein equation 6 is 10% (left panel) and 40% (right panel).of the maximum return in the dataset. We used the d-S&P dataset for this analysis.

To further disentangle the roles of stock dimensions in the determination of optimal portfolio weights, we report in table 4 the results from the OLS estimations of regressions (10) and (11). Equation (10) considers the case of the minv strategy where stock i's portfolio weight in a minimum-variance specification, $w^*_{i,minv}$, depends linearly on its centrality, v_i, and on its standard deviation of returns, σ_i. Similarly, equation (11) specifies a linear relationship between stock i's portfolio weight in a mean-variance specification, $w^*_{i,mv}$, with the corresponding stock centrality, v_i, and Sharpe Ratio, SR_i.[13] Therefore, the coefficients β_1 and β_2 stands for the effects of the systemic and individual dimensions of stocks upon optimal portfolio weights.

$$w^*_{i,minv} = \beta_0 + \beta_1 v_i + \beta_2 \sigma_i + \varepsilon_i \quad (10)$$

$$w^*_{i,mv} = \beta_0 + \beta_1 v_i + \beta_2 SR_i + \varepsilon_i \quad (11)$$

[13] In equation 11, optimal weights are obtained assuming R^e equals 40% of the maximum possible return.

Table 4. Optimal portfolio weights as a function of the individual and systemic stock's dimensions considering a cross-sectional approach. v_i is the centrality of stock i.. σ_i is the standard deviation of stock i. SR_i is the Sharpe ratio of stock i. N is the number of observations (stocks) in the cross-sectional regressions. The regression R^2 is adjusted for degrees of freedom. Each row of the table reports OLS estimations of equations (10) and (11), respectively, where *t-statistics* are in parentheses and the statistical significance is as follows: * at 5% level, ** at 1% and *** at 0.1% level.

	v_i	σ_i	SR_i	N	R^2
$w^*_{i,minv}$	-0.740 (-4.05)***	-1.755 (-6.38)***		200	0.231
$w^*_{i,mv}$	-0.778 (-3.64)***		0.761 (4.77)***	200	0.179

The coefficients reported in table 4 are strongly statistically significant and provide support to Proposition 1 and Corollary 1. The coefficient β_1 is negative for both regressions indicating that highly central stocks tend to be underweighted regardless of the specific investment objective. The coefficient β_2 is negative for the minv rule and positive for the mv case indicating the tendency to optimally allocate wealth towards low-standard deviation and high-Sharpe ratio securities, respectively.

5.2 Time series approach

Contrary to the static description provided by the cross-sectional analysis, this subsection takes a dynamic perspective on the portfolio selection by implementing a time series approach. The entire dataset is divided into 2,522 60-day-long rolling windows considering 1-day displacement steps. The vectors of stock centrality, v_t and portfolio weights for the minv and mv rules, $w^*_{minv,t}$ and $w^*_{mv,t}$, are computed for each rolling window and indexed by the time subscript t.

We introduce the mean stock centrality $\bar{v}_t$ and the weighted stock centrality $\bar{\bar{v}}_{r,t}$ as follows:

$$\bar{v}_t = \frac{1}{n}\sum_{i=1}^{n} v_{it} \tag{12}$$

$$\bar{\bar{v}}_{r,t} = \sum_{i=1}^{n} w^*_{r,it}\, v_{it} \;\; for\; r = minv,\; mv \tag{13}$$

By construction, the expression $\bar{\bar{v}}_{r,t} = \bar{v}_t$ for $r = minv,\; mv$ is satisfied when $w^*_{r,it} = 1/n$. In accordance with Corollary 1, it would be expected that $\bar{\bar{v}}_{r,t} < \bar{v}_t$ most of the time indicating a bias toward low-central stocks.

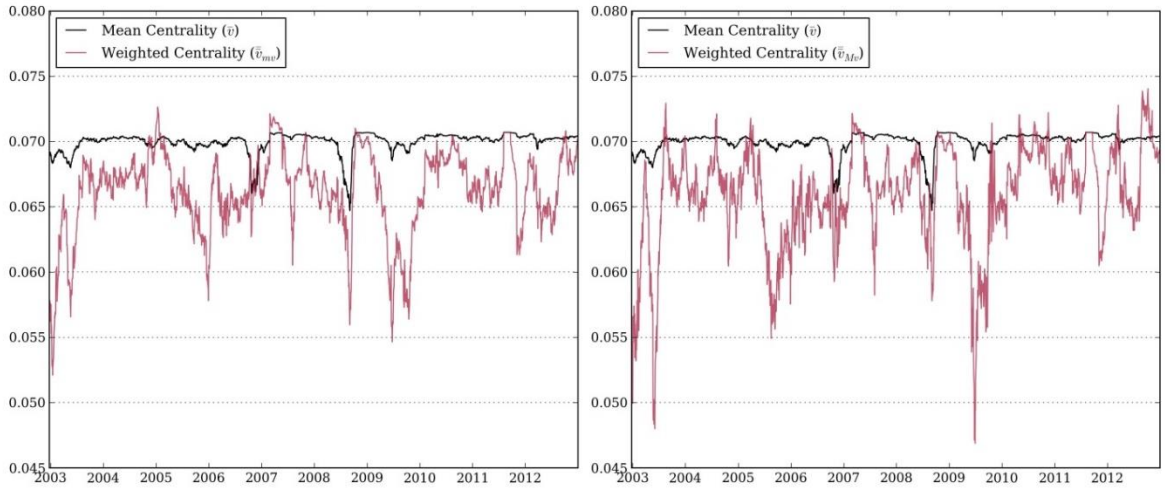

Figure 5. Mean centrality $\bar{v}_t$ and weighted centrality $\bar{\bar{v}}_{r,t}$ through time. We consider the *minv* strategy (left panel) and the *mv* strategy (right panel) for the d-S&P dataset. We divide the dataset into 2,522 of 60-days long rolling windows with 1-day displacement steps. The weight allocations of *minv* and *mv* strategies and the centrality rankings of stocks are computed for each rolling window. The mean centrality $\bar{v}_t$ is the average of centralities among stocks in each 60-days window and the weighted centrality, $\bar{\bar{v}}_{r,t}$, is computed by weighting each stock's centrality by their corresponding weights in *mv* and *minv* strategies.

Figure 5 plots the time series of $\bar{v}_t$ and $\bar{\bar{v}}_{r,t}$ presenting the pattern just described. Note, however, that $\bar{\bar{v}}_{r,t}$ shows values closer to, or even surpassing, $\bar{v}_t$ for some periods. The dynamic of the correlation between the individual and the systemic dimensions of stocks explains this time-dependent behavior of $\bar{\bar{v}}_{r,t}$. Let us denote by π_t the cross sectional correlation between v_{it} and σ_{it} and by ρ_t the cross-sectional correlation between v_{it} and SR_{it}, both at period t. When $\pi_t > 0$, the lowest standard deviation stocks tend to coincide with the weakly systemic ones, and as a consequence, overweighting these securities is certainly the optimal choice under the minv rule. For $\pi_t < 0$, a trade-off arises since low-central stocks also correspond to high-volatility securities. In this case, an optimal portfolios rule should balance these two confronting forces by adapting the investment set to include more central stocks. Considering the mv strategy, for $\rho_t < 0$, the assets with highest Sharpe ratios show the lowest centrality, and therefore, this leads to investing in non-systemic securities as the optimal portfolio choice. When $\rho_t > 0$, a trade-off between assets' dimensions takes place and an optimal wealth allocation should increase portfolio weights towards central securities. Figure 6 plots the time series of ρ_t and π_t and the corresponding 120-days moving averages evidencing the sign-switching nature of these two variables.

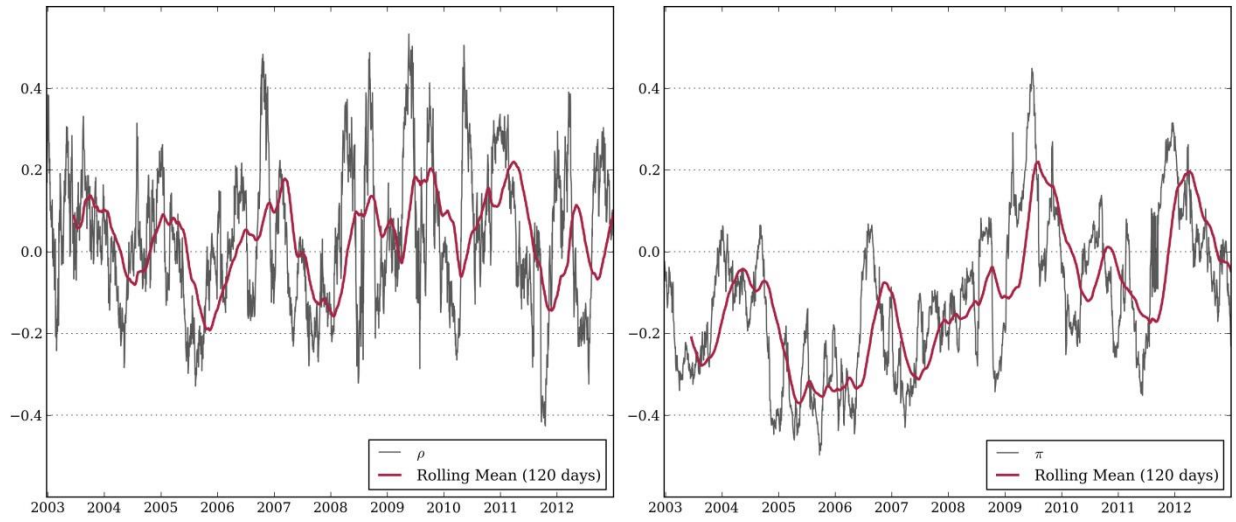

Figure 6. Time series of the cross-sectional correlations between the individual and the systemic dimensions of stocks. This figure presents the correlation between stocks' centralities and Sharpe ratios, $\rho_t = corr(v_{it}, SR_{it})$ (left panel) and stocks' centralities and standard deviation $\pi_t = corr(v_{it}, \sigma_{it})$ (right panel) for the d-S&P dataset. We also include the corresponding 120-day moving averages of ρ_t and π_t in each panel.

Further insights on the security selection process are gained by estimating the regressions (14) and (15) accounting for the time series versions of expressions (10) and (11). In (14), the optimally weighted centrality $\bar{\bar{v}}_{minv,t}$ for the minv strategy in period t is explained by the mean centrality, $\bar{v}_t$, the coefficient of variation of the centrality distribution, $\left(\frac{\sigma_{v,t}}{\bar{v}_t}\right)$, and π_t. Similarly, equation (15) considers the mv strategy and therefore, the dependent variable is $\bar{\bar{v}}_{mv,t}$ while ρ_t replaces π_t as explanatory variable.

$$\bar{\bar{v}}_{minv,t} = \beta_0 + \beta_1 \bar{v}_t + \beta_2 \left(\frac{\sigma_{v,t}}{\bar{v}_t}\right) + \beta_3 \pi_t + \varepsilon_t \tag{14}$$

$$\bar{\bar{v}}_{mv,t} = \beta_0 + \beta_1 \bar{v}_t + \beta_2 \left(\frac{\sigma_{v,t}}{\bar{v}_t}\right) + \beta_3 \rho_t + \varepsilon_t \tag{15}$$

Table 5 reports OLS estimations of (14) and (15) noting that all of the coefficients are strongly statistically significant. The coefficient β_1 is negative for both regressions indicating that higher $\bar{v}_t$ results in an overweighting of low-systemic assets as a mean to avoid the undesirable consequences of high-central securities in the portfolio. The negative signs of β_2 are interpreted as the benefits derived from a wider centrality distribution that allows an increased presence of assets with lower centrality scores in the portfolio after controlling for $\bar{v}_t$. The coefficient β_3 is negative for the minv rule (see equation (14)). In this case therefore, larger values of π, indicating no trade-off between assets' dimensions, are consistent with optimal wealth allocations away from central securities. In contrast, the coefficient β_3 shows a positive sign for the mv rule (see

equation (15)) explained by the trade-off between assets' dimensions arising for large ρ. As a consequence the increments of ρ rise $\bar{\bar{v}}_{mv}$ by moving the investment set toward central nodes.

Table 5. Optimal portfolio weights as a function of the individual and systemic stock dimensions taking a time series approach. We consider a 60-day rolling window estimation procedure for each variable. Each t denotes a 60-day rolling window. $\bar{v}_t$ is the mean centralities at each t. $\left(\frac{\sigma_{v,t}}{\bar{v}_t}\right)$ is the coefficient of variation of the centrality distribution at t. π_t is the correlation between centralities, v_{it} and standard deviations, σ_{it} at t. ρ_t is the cross-sectional correlation between centralities, v_{it}, and Sharpe ratios, SR_{it}, at t. N is the number of observations (stocks) in the cross-sectional regressions. The regression R^2 is adjusted for degrees of freedom. Each row of the table reports OLS estimation of equations (14) and (15). *t-statistics* are in parentheses and the statistical significance is denoted as follows: * at 5% level, ** at 1% and *** at 0.1% level.

	$\bar{v}_t$	$\frac{\sigma_{v,t}}{\bar{v}_t}$	π_t	ρ_t	N	R^2
$\bar{\bar{v}}_{minv}$	-3.324 (-19.04)***	-0.0707 (-33.80)***	-0.00613 (-26.34)***		2522	0.573
$\bar{\bar{v}}_{mv,t}$	-2.661 (-10.83)***	-0.0720 (-24.50)***		0.00627 (17.79)***	2522	0.457

6. Stock Centrality and Optimal Portfolio Weights: Out-of-Sample Evaluation

In DeMiguel et al. (2009), naïve strategy, commonly termed as $1/N$[14], is shown not to be consistently outperformed by Markowitz-based rules or their extensions designed to deal with the estimation error problem. This better out-of-sample performance of $1/N$ strategy relative to Markowitz's rule is also investigated and supported by Jobson and Korkie (1980), Michaud (2008) and Duchin and Levy (2009). Moreover, DeMiguel et al. (2009, p. 1936) report that among those models designed to tackle the estimation error problem, the constrained Markowitz rules might be considered as second-best alternatives to naïve diversification. Accordingly, naïve strategy and constrained Markowitz rules portray two reasonable benchmarks for out-of-sample portfolio evaluations.

Based on the insights obtained mainly from sections 2 and 5, we here propose a network-based investment strategy, termed as ρ-dependent strategy that targets groups of assets in accordance with their centrality rankings. We proceed to define this strategy in detail and evaluate its out-of-sample performance against the benchmarks.

[14] Naïve strategy assigns a fraction $1/N$ of wealth to each asset out of the N available assets.

6.1 The out-of-sample evaluation

The out-of-sample returns are computed as follows. For a T-period-long dataset, we implement several portfolio strategies (specified below) upon a set of M-period-long rolling windows indexed by the subscript t. We buy-and-hold the portfolios for H periods and the resulting out-of-sample return is recorded. The rolling window in period t is created by simultaneously adding the next H data points and discarding the H earliest ones from the previous rolling window in order to preserve its length. This process is repeated several times until the end of the dataset is reached thus accounting for $\lfloor (\mathrm{T}-\mathrm{M})/\mathrm{H} \rfloor$ rebalancing periods, vectors of portfolio's weights and out-of-sample returns for each portfolio strategy.

We introduce our network based investment policy, the so-called ρ-dependent strategy, as follows. The process estimates the correlation matrix $\hat{\Omega}_{\mathrm{t}}$, the vector of securities' centrality, v_t and the correlation between the systemic and individual dimensions of stocks, ρ_t, upon the rolling window corresponding to period t. Assuming a threshold parameter $\tilde{\rho}$, for a sufficiently large ρ, say $\rho > \tilde{\rho}$, we naively invest in the 20 stocks with the highest centrality. Conversely, for a sufficiently low ρ, say $\rho < \tilde{\rho}$, we naively invest in the 20 stocks with the lowest centrality. This strategy is designed to benefit from investing in low systemic stocks to the extent that the most central ones do not show significant individual performances, thus replicating Markowitz's logic to some extent.

In accordance with the previous literature (DeMiguel et al., 2009), the $1/N$ rule applied upon the entire investment opportunity set is a convenient benchmark with which to evaluate the performance of our network-based strategy. To ensure that the performance of ρ-dependent strategy does not happen by chance, we also includes the reverse ρ–dependent strategy that naively invests in the 20 lowest central stocks when $\rho > \tilde{\rho}$ and in the 20 highest central ones when $\rho < \tilde{\rho}$. Moreover, two Markowitz-related rules, the mean-variance and minimum-variance strategies with short-selling constraints are incorporated in the analysis as well. Finally, we consider three more investment rules as "control strategies" that naively invest in the 20 stocks with the Highest Sharpe Ratio, the Highest Centrality and the Lowest Centrality.[15]

[15] The decision to construct portfolios made up of 20 assets is based on Desmoulins-Lebeault and Kharoubi-Rakotomalala (2012) which highlights the fact that most diversification benefits are gained by investing in such a number of stocks.

The investment policies are compared using three out-of-sample performance measures: i) Sharpe ratio, ii) variance of return and iii) turnover. This latter measure averages the amount and size of the rebalancing operations as follows

$$turnover \quad = \frac{1}{T-M-1} \sum_{t=M}^{T-1} \sum_{j=1}^{N} |w_{j,t+1} - w_{j,t^+}| \tag{16}$$

where $w_{j,t+1}$ is the weight of security j at the beginning of period $t+1$ and w_{j,t^+} is the weight of that security just before the rebalancing occurring between the end of period t and the beginning of period $t+1$.[16]

We statistically test the difference in out-of-sample portfolios' Sharpe ratios and variances between each of the investment rules against the $1/N$ strategy following Ledoit and Wolf (2008) and Ledoit and Wolf (2011). More specifically, we implement a studentized circular block bootstrap with block size equal to 5 and bootstrap samples equal to 5.000 to compute the respective p-values.[17]

6.2 Determining the threshold parameter $\tilde{\rho}$

Before the application of our network-based strategies, the value of $\tilde{\rho}$ needs to be specified. In order to do that, we rely on an extensive simulation procedure using artificially created subsamples where ρ spans a broad range of values. Specifically, we generate 120 datasets by randomly selecting 150 stocks from the d-NYSE dataset (see section 3) with ρ ranging from -0.20 to 0.45. Then, we compute the out-of-sample Sharpe ratio where M and H are set to be equal to 500 days and 20 days, respectively.

Panels a, b and c from figure 7 plot the out-of-sample Sharpe ratios from three particular datasets with ρ equal to 0.45, -0.20 and 0.0, arising from a progressive percentage removal of stocks from the upper and lower tails of the centrality distribution (with 5% increments). Panel c from figure 7 (when $\rho = 0$) presents a scenario in which an intensive removal of high central stocks leads to better out-of-sample performance in terms of Sharpe ratio. This result is expected since highly individual performing stocks are randomly disseminated in the stock market network. Panel (b) from figure 7 (when $\rho = -0.20$) shows us the convenience of selecting among low-central stocks as the target region to invest. This is due to the absence of trade-off between the systemic and individual dimension of stocks. The opposite case is observed in panel (a) of figure 7 (when

[16] Note that in the expression (16), rebalancing is assumed in each investment period as if $H = 1$. However, with $H > 1$, we only consider the rebalancing periods in our *turnover* calculation.
[17] For the particular case of the variance, a stationary bootstrap is employed as in Politis and Romano (1994).

$\rho = 0.45$). In this case, the best performance is achieved by investing in high central stocks with an intense removal of securities from the left tail of the centrality distribution. This is explained given that the positive effect of the individual dimension of stocks over-compensates the negative effect of their systemic dimension.

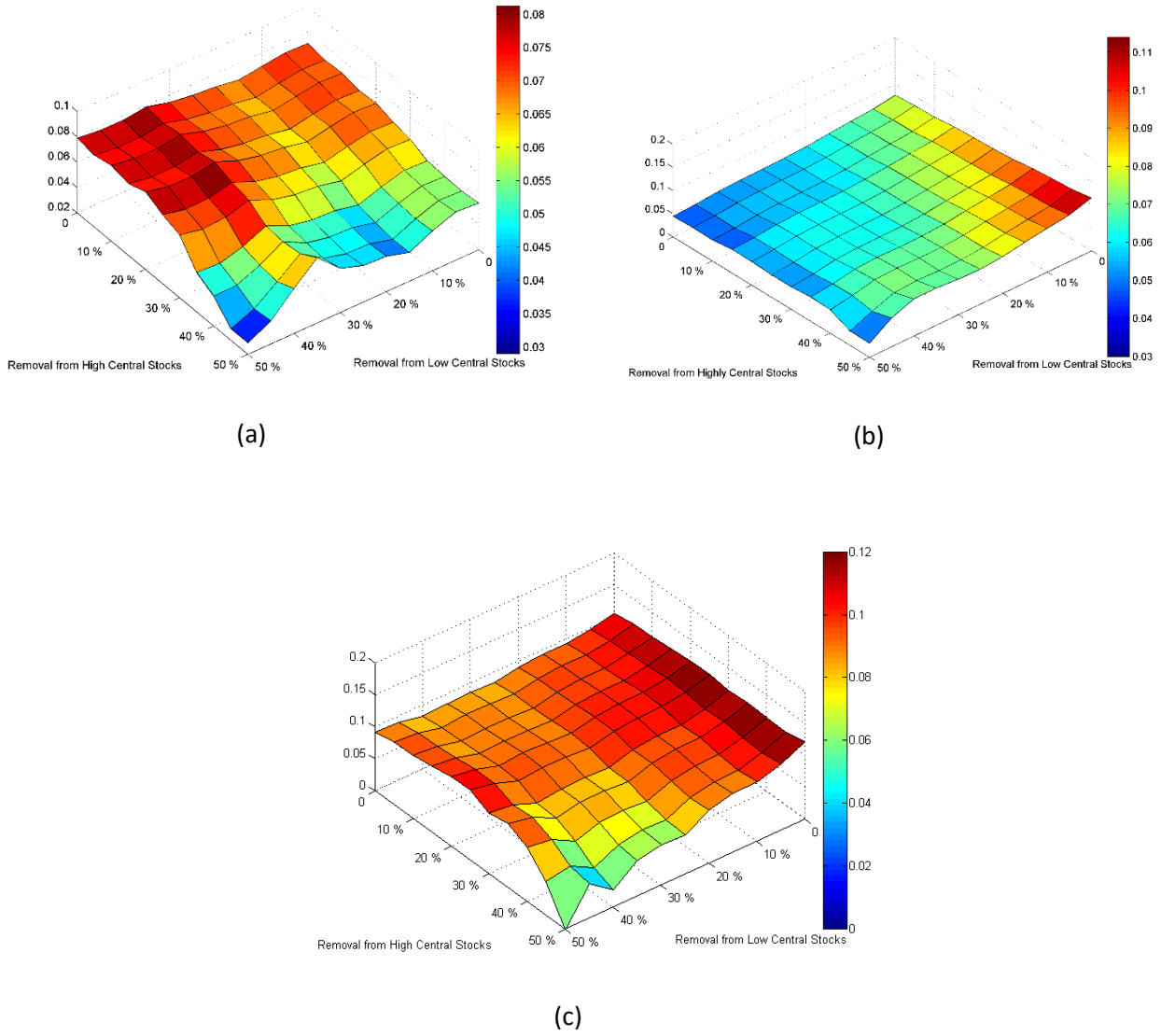

Figure 7. Out-of-sample Sharpe ratios resulting from progressive percentage removal of stocks from the lower tail and upper tail of the centrality distribution. Three specific randomly generated samples from d-NYSE dataset are considered with ρ values: (a) ρ = 0.4550, (b) ρ =-0.2010, (c) ρ =0.000. The out-of-sample Sharpe ratios are computed with $M = 500$ and $H = 20$.

In the next step, we investigate the break point of ρ that characterizes the region of the market network that is susceptible to being discarded from the investment opportunity set. Let us define the high central stock investment region as the set of securities arising from the deletion of 25% to 45% of assets from the left tail of the centrality distribution (starting from the lowest central security) and no more than 20% from its right tail (starting from the highest central security). In a

symmetric fashion, let us define the low central stock investment region as the set of stocks comprising the deletion of 25% to 45% of stock from the right tail of the centrality distribution and no more than 20% of its left tail. Then, from all of the 120 artificially-constructed data sets, we identify the investment region that generates the highest out-of-sample Sharpe ratio. The identification rule simply averages out the out-of-sample Sharpe ratios generated in each of the two investment regions and then selects the one with the highest average performance. Figure 8 plots the distribution of ρ conditional on the investment region that leads to the largest Sharpe ratio. In accordance with figure 8, low values of ρ are more consistent with high Sharpe ratio emerging from the low central investment region. In contrast, for large values of ρ, it is the high central stock investment region that generates the largest risk-adjusted returns.

With the aim of setting the value of $\tilde{\rho}$, note that such a threshold must be high enough to be worthwhile to move the optimal investment region from the low central securities towards more central ones.[18] Taking figure 8 into account, we consider 0.2 as a reasonable value for $\tilde{\rho}$ since it roughly coincides with the 75% percentile of ρ from the low central stock investment region and the 25% percentile of ρ from the high central stock investing region. We acknowledge that the determination of $\tilde{\rho}$ is the weakest point in our procedure since it implies ad-hoc rules. Other methodologies might be investigated in this regard and we leave them as future research lines.

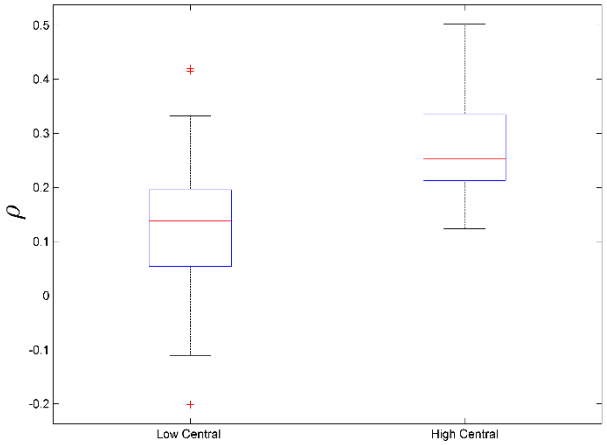

Figure 8. Distribution of ρ conditioning on the investment region generating the highest out-of-sample Sharpe ratio. 120 artificially-created datasets from d-NYSE dataset is considered. *High Central* refers to the investment region comprised of the set of stocks arising from the deletion of 25% to 45% of assets from the left tail of the centrality distribution and no more than 20% from its right tail. *Low Central* refers to the investment region with the set of stocks comprising the deletion of 25% to 45% of stocks from the right tail of the centrality distribution and no more than 20% of its left tail. The out-of-sample Sharpe ratios are computed with $M = 500$ and $H = 20$.

[18] The tendency is to invest in low-central stocks unless high-central ones show good individual performances.

6.3. Out-of-sample performance

The annualized out-of-sample performance measures originated from the two daily datasets d-S&P and d-FTSE and the monthly dataset m-NYSE are reported in table 6. Since the average ρs from these datasets are lower than $\tilde{\rho} = 0.20$, the performance of the ρ-dependent strategy is indistinguishable from an unconditional lowest-central investment rule. Therefore, we also include an additional sample (d-NYSE150) obtained by a random selection of 150 stocks from d-NYSE presenting an average ρ equal to 0.23. The setup for the out-of-sample evaluation assumes M=1000 and H=20 for the daily datasets and M=192 and H=12 for the monthly dataset.[19]

Table 6 shows the noticeable outperformance of the ρ–dependent strategy for the daily datasets. The Sharpe ratio from the $1/N$ naïve strategy reaches 0.471 and 1.153 for d-S&P and d-FTSE, respectively. The same measures rise to 0.724 and 2.584 when the ρ–dependent strategy is in place, showing a statistically significant difference with respect to the benchmark. Similar good performances are observed in terms of portfolio variance, presenting a statistically significant reduction from 0.066 to 0.051 and from 0.025 to 0.014, for d-S&P and d-FTSE. Considering the m-NYSE dataset, the ρ–dependent results are worse in terms of Sharpe ratio and variance in comparison to the benchmark but not to a statistically significant extent as indicated by the p-values. The benefit derived from the switching nature of ρ–dependent rules is explored by means of the d-NYSE150 dataset. In this case, a higher and statistically different Sharpe ratio (2.083) is obtained by following the proposed investment strategy in comparison to the naïve (1.241) and lowest-central (1.942) rules.

Table 6 also shows that ρ–dependent strategy implies distinctive and enhanced investment dynamics when it is compared to the unconditional strategies. In general terms, the Highest Sharpe Ratio, Highest Central Stocks and Lowest Central Stocks strategies present poorer outcomes in a portfolio's Sharpe Ratio in all of the datasets. In order to discard the possibility that our results were driven by chance, table 6 also reports the results for the reverse ρ–dependent strategy. In this case, none of the out-of-sample portfolio's Sharpe ratios show better results when compared either with the benchmark or with the ρ–dependent strategy. Moreover, in the d-NYSE150 dataset, we observe that the ρ–dependent rule significantly outperforms other strategies. Since the mean value of ρ in this dataset surpasses the threshold 0.2, the ρ–dependent strategy can exploit the benefit of moving the investment set from high-central to low-central nodes and vice versa.

[19] Due to data limitation, M=500 for the d-NYSE dataset.

Table 6. Out-of-sample Performance of Portfolio Strategies. We report the out-of-sample Sharpe ratio, variance and turnover for portfolio strategies. The benchmark strategy is denoted as "*All stocks*", that is naïve strategies applied to all of the stocks in the dataset. Following the ρ-*dependent* strategy, when ρ is higher than 0.2, we diversify among highest central stocks and otherwise, diversify among the lowest central stocks. The *Reverse* ρ-*dependent* approach takes an opposite investment decision to the ρ-dependent strategy. The *Highest Sharpe Ratio* strategy refers to diversifying naively among stocks with the highest level of Sharpe ratios. In *Lowest Central* and *Highest Central* strategies, we diversifying among lowest and highest central stocks, respectively. The *minv-cc* and *mv-cc* strategies refer to minimum-variance and mean-variance strategies with short-selling constraints. We considered 20 stocks for our portfolios. The p-values are computed following the procedure in Ledoit and Wolf (2008) and Ledoit and Wolf (2011) based on a studentized circular block bootstrap with block size equal to 5 and number of bootstrap samples equal to 5000.

Panel A	d-S&P (Avg ρ: -0.0556)			d-FTSE (Avg ρ: -0.1853)		
	Sharpe Ratio	Variance	Turnover	Sharpe Ratio	Variance	Turnover
All Stocks	**0.471**	**0.066**	**0.141**	**1.153**	**0.025**	**0.138**
ρ-dependent	0.724	0.051	0.149	2.523	0.014	0.164
	(0.0125)	(0.0010)		(0.0033)	(0.0009)	
Reverse ρ-dependent	0.315	0.110	0.126	0.549	0.026	0.061
	(0.1523)	(0.0009)		(0.0100)	(0.014)	
Highest Sharpe Ratio	0.438	0.038	0.141	1.201	0.018	0.138
	(0.8239)	(0.0009)		(0.8007)	(0.0009)	
Highest Central	0.315	0.110	0.126	0.549	0.026	0.061
	(0.1523)	(0.0009)		(0.0100)	(0.014)	
Lowest Central	0.724	0.051	0.149	2.523	0.014	0.164
	(0.0125)	(0.0010)		(0.0033)	(0.0009)	
minv_cc	0.448	0.040	0.115	1.589	0.015	0.127
	(0.9568)	(0.0020)		(0.5482)	(0.0010)	
mv-cc	0.573	0.067	0.148	1.089	0.025	0.137
	(0.8339)	(0.8951)		(0.9535)	(0.6563)	
Panel B	m-NYSE (Avg ρ: 0.1157)			d-NYSE150 (Avg ρ: 0.2323)		
	Sharpe Ratio	Variance	Turnover	Sharpe Ratio	Variance	Turnover
All Stocks	**0.754**	**0.019**	**0.057**	**1.241**	**0.021**	**0.127**
ρ-dependent	0.591	0.025	0.065	2.083	0.019	0.140
	(0.3997)	(0.2553)		(0.0664)	(0.3367)	
Reverse ρ-dependent	0.552	0.034	0.049	0.968	0.028	0.113
	(0.0233)	(0.0009)		(0.5216)	(0.0020)	
Highest Sharpe Ratio	0.531	0.017	0.039	1.0571	0.018	0.103
	(0.1694)	(0.2248)		(0.5781)	(0.0110)	
Highest Central	0.555	0.032	0.049	1.201	0.033	0.106
	(0.0299)	(0.0009)		(0.8671)	(0.0009)	
Lowest Central	0.583	0.028	0.065	1.942	0.014	0.147
	(0.0831)	(0.0009)		(0.1927)	(0.0009)	
minv_cc	0.777	0.015	0.046	1.310	0.013	0.109
	(0.9302)	(0.1558)		(0.9734)	(0.0110)	
mv-cc	0.456	0.054	0.053	1.353	0.039	0.122
	(0.3422)	(0.0010)		(0.9502)	(0.0010)	

Additionally, table 6 reports the performance of the two Markowitz-related strategies: mean-variance and mean-variance with short selling constraints denoted by minv-cc and mv-cc, respectively. In comparison with these strategies, the ρ–dependent rule shows a better performance except for the case of minv-cc in the m-NYSE. For example, in the case of d-S&P dataset, while the minv-cc strategy manages to earn a lower level of portfolio variance compared to the benchmark, it fails to improve the level of the Sharpe ratio. On the other hand, the mv-cc strategy results in a non-significant increase in the Sharpe ratio level while maintaining the

portfolio risk at the same level as the $1/N$ rule. In contrast, the ρ–dependent strategy manages to simultaneously increase the level of the Sharpe ratio and decrease the portfolio variance level as commented previously. This comparison highlights the poor out-of-sample performance of Markowitz rules reported in the literature and also shows the convenience of implementing the network-based portfolio strategy.[20]

Unfortunately, the major shortcoming of our proposed rule is that it tends to raise the number of rebalancing operations, a phenomenon captured by the increased portfolio turnover compared to the $1/N$ benchmark. The severity of this issue is further investigated in section 6.5 below. Two additional comments are worth mentioning. First, the relatively extreme and negative value of ρ (-0.1853 on average) for the d-FTSE dataset might explain the strikingly good results obtained in the UK market where no trade-off between the individual dimension and systemic dimension exists. Secondly, it should be mentioned that the prescription from Pozzi et al. (2013) in favor of unconditional allocation of wealth only towards the periphery of the stock market network shows clearly inferior results relative to the ρ–dependent rule when ρ assumes large values as in the d-NYSE150 dataset. Nevertheless, in the cases where ρ is relatively low, as in the d-S&P and d-FTSE datasets, our results are in line with theirs.

6.4. Carhart alpha for the $\boldsymbol{\rho}$*–dependent strategy*

The large risk-adjusted returns of the ρ–dependent strategy might result from large exposures to systematic risk factors. We investigate this hypothesis by estimating Carhart's alpha from the four risk factor models (Carhart, 1997; Fama and French, 1996, 1993) as in equation (17).

$$R_t^{\rho} - r_t^f = \alpha + \beta_{MKT}\left(R_t^M - r_t^f\right) + \beta_{HML}HML_t + \beta_{SMB}SMB_t + \beta_{MOM}MOM_t + \varepsilon_t \qquad (17)$$

where $R_t^{\rho} - r_t^f$ is the excess out-of-sample return from the ρ–dependent strategy, $R_t^M - r_t^f$ is the market risk premium, HML_t is the difference between the returns of high and low book-to-market portfolios, SMB_t is the difference between the returns of small-cap and large-cap portfolios and MOM_t is the momentum factor. The parameter α measures the abnormal risk-adjusted return capturing the excess return above what would be expected based solely on the portfolio's risk profile. The time series of the four risk factors are gathered from Ken French's website for the US market and from (Gregory et al., 2013) for the UK case. We correct the

[20] We also evaluate the performance of mean-variance and minimum-variance strategies without the short-selling constraints. However, our main conclusions remain unchanged. These results are available upon request.

standard errors in the estimation of equation (17) for heteroskedasticity and serial correlation in ε_t following Newey and West (1987).

Table 7 reports the estimated Carhart's alpha for three portfolio sizes (10, 20 and 50) and two holdings periods (1 and 20 days for the daily datasets and 1 and 12 months for the monthly dataset) across the US and UK samples. The reader is referred to Appendix D for a detailed results of the estimation of equation 17 without winsorizing. However, to account for outliers, table 7 reports results after 5% data winsorizing, noting that qualitative similar results are obtained either without winsorizing or by winsorizing at 10% (see table E.1 and E.2 in Appendix E). The estimations show positive and statistically significant alphas for each of the portfolio configurations. The weakest results stem from the monthly dataset where the reduced estimation window might undermine the statistical significance.

Table 7. Annualized risk-adjusted returns for ρ-dependent strategy with 5% winsorisation. We report annualised risk-adjusted returns for different settings of ρ-dependent strategy on the four Carhart (1997) factors, MKT, HML, SMB, MOM with 5% winsorisation. The estimation window is considered to be 1000 days (192 months) for daily (monthly) datasets. The t-statistics are reported in parentheses. ** and * indicate significance at 1% and 5% levels, respectively.

Portfolio Setting		Alpha (5% winsorizing)		
Stocks	Holding Period	d-S&P	d-FTSE	m-NYSE
10	1d/1m	14.75	35.97	5.1
		(3.37)**	(6.37)**	(2.26)*
	20d/12m	17.19	36.01	4.49
		(3.97)**	(6.21)**	(1.98)*
20	1d/1m	10.57	33.65	4.42
		(3.02)**	(6.65)**	(2.31)*
	20d/12m	11.97	32.84	4.37
		(3.45)**	(6.52)**	(2.36)*
50	1d/1m	10.52	28.07	5.45
		(3.63)**	(5.17)**	(3.23)**
	20d/12m	10.08	28.08	5.82
		(3.50)**	(5.18)**	(3.40)**

To sum up, the ρ-dependent rule is able to provide enhanced risk-adjusted returns that are not explained by exposure to traditional risk factors. Interestingly, the evidence also indicates a negative relationship between portfolio sizes and alphas for each of the considered holding periods and across datasets. For instance, considering the d-S&P dataset and a 20-day holding period, the Carhart's alphas of portfolios made of 10, 20 and 50 stocks are 17.19, 11.97 and 10.08, respectively. To confirm this regularity, however, further analyses are required.

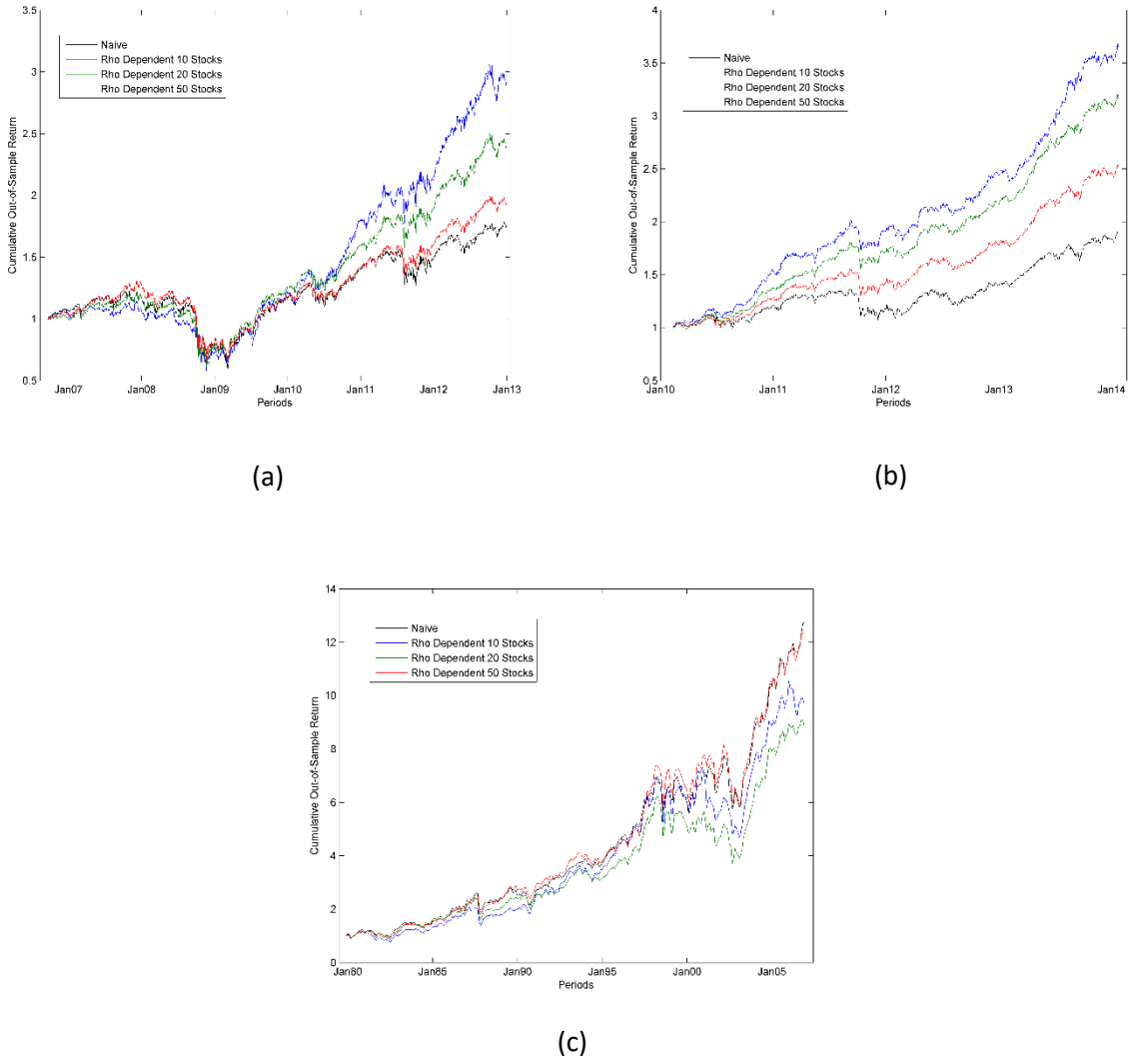

Figure 9. Cumulative return for the ρ–dependent strategy for (a) d-S&P, (b) d-FTSE, (c) m-NYSE datasets in comparison to the naïve strategy for 20 days and 12 month holding periods in daily and monthly datasets, respectively.

Finally, figure 9 plots the cumulative out-of-sample returns of the ρ–dependent strategy for different portfolio configurations. For the d-S&P dataset plotted in panel (a), we observe that investing in 10 stocks results in the largest payoffs while the $1/N$ rule produces the poorest performance. The same observation applies for the d-FTSE dataset captured in panel (b) from the same figure. The case of the m-NYSE dataset presented in panel (c) is different; the time series of cumulative returns of the naïve strategy outperforms the ρ–dependent strategy for portfolios made of 10 and 20 stocks while for a portfolio size equal to 50 they both tend to behave similarly.

6.5 Transaction cost

Since our ρ–dependent strategy is a dynamic strategy that requires rebalancing operations, it is important to investigate the impact of transaction costs. Following the approach provided in Han et al. (2013), we compute the breakeven transaction cost (BETC) that sets the average returns of the ρ–dependent strategy equal to zero. Denoting by R_t the out-of-sample return of the ρ–dependent strategy in period t, the breakeven transaction cost (BETC) is computed as follows:

$$BETC = \frac{\sum_{t=M+1}^{T} R_t}{T-M} \times H \tag{18}$$

As stated in Balduzzi and Lynch (1999), reasonable lower and upper bounds for the transition cost are 1 bp and 50 bps, respectively. Thus, obtaining a BETC higher than 50 bps means that a disproportionally abnormal transaction cost is required to wipe out the returns of the ρ–dependent strategy.

The results for BETC are reported in table 8 considering the d-S&P, d-FTSE and m-NYSE datasets and different portfolio settings (size and holding period). In general terms, we observe that for short holding periods, BETC assumes low values for any investment configuration. For instance, in a setting of a 1 day holding period and 10 stocks from the FTSE dataset, a transaction cost of only 13.79 bps is needed to wipe out the benefit of ρ–dependent strategy. However, for longer holding periods, our calculations indicate large values of BETC which supports the outperformance of the ρ–dependent strategy after controlling for transaction cost. For example, considering again the FTSE dataset, a portfolio size of 10 and a holding period of 20 days, a transaction cost of more than 264.56 bps is needed to wipe out the returns of the proposed strategy.

It should be noted that in this analysis, it is assumed that the investor faces a flat-transaction fee every time he/she wants to rebalance the portfolio regardless the size of the rebalancing operation. Appendix G provides a detailed analysis in a context in which the investor pays in proportion to the changes in portfolio's weights. The results reported in this appendix provide further support to the application of our proposed network-based investment rule.

Table 8. BETC for ρ–dependent strategy. We report the BETC for the ρ–dependent strategy in various strategy settings across the three datasets of d-S&P, d-FTSE and m-NYSE. The results are reported in basis points (bps).

Portfolio Setting		BETC		
Stocks	Holding Period	d-S&P	d-FTSE	m-NYSE
10	1d/1m	6.98	13.79	85.69
	20d/12m	156.74	264.56	937.18
20	1d/1m	5.42	12.12	79.69
	20d/12m	130.1	236.59	982.12
50	1d/1m	5.04	9.67	85.5
	20d/12m	102.06	191.76	1040.94

7. Conclusion and Future Research Lines

In this study, a stock market is conceived as a network where securities correspond to nodes while the paired returns' correlations account for the links. The paper establishes a bridge between Markowitz's framework and network theory by stating the tendency to overweight low-central stocks in order to build efficient portfolios. Therefore, optimal portfolio weights of highly influential securities in a correlation-based network are biased downward after controlling for their individual performance measured by either Sharpe ratios or the volatility of returns (depending on the specific portfolio's goal).

From a more descriptive point of view, we find that financial firms are the most central nodes in the market network and that both financial and market variables are major determinants of a stock's centrality. More precisely, we provide some evidence indicating that highly central securities correspond to large-capitalized, cheap and old firms presenting weak financial profiles.

We also investigate the extent to which network-based investment strategies might improve portfolio performance by means of in-sample and out-of-sample analysis. We propose the so-called ρ–dependent strategy and test its performances against the extremely simple yet effective $1/N$ naïve rule and two Markowitz-related policies. Our out-of-sample results show that the ρ–dependent strategy tends to present significant higher portfolio Sharpe ratios and lower portfolio variance relative to these well-known benchmarks. Additionally, this enhanced performance is not explained by large exposures to traditional risk factors as indicated by the reported positive and statistically significant Carhart's alphas. More importantly, our results are robust to several portfolio configurations, time periods and markets even after accounting for transaction costs.

There are several future research lines that could provide novel insights from the interaction between network theory and portfolio selection. However, it seems particularly appealing to

extend the approach by considering stock markets as directed and weighted networks. This framework may contribute to improve our understanding on the shock-transmission mechanisms across stocks and disentangling the differential role played by specific securities as an absorber or booster of initial impulses.

References

Balduzzi, P., Lynch, A.W., 1999. Transaction Costs and Predictability: Some Utility Cost Calculations. J. financ. econ. 52, 47–78.

Barigozzi, M., Brownlees, C., 2014. Nets: Network Estimation for Time Series. SSRN - Work. Pap. 1–43.

Billio, M., Getmansky, M., Lo, A.W., Pelizzon, L., 2012. Econometric measures of connectedness and systemic risk in the finance and insurance sectors. J. financ. econ. 104, 535–559. doi:10.1016/j.jfineco.2011.12.010

Bloomfield, T., Leftwich, R., Long, J., 1977. Portfolio Strategies and Performance. J. financ. econ. 5, 201–218.

Bonacich, P., 1972. Factoring and weighting approaches to status scores and clique identification. J. Math. Sociol. 2, 113–120.

Bonacich, P., 1987. Power and Centrality: A Family of Measures. Am. J. Sociol. 92, 1170–1182.

Bonanno, G., Caldarelli, G., Lillo, F., Miccichè, S., Vandewalle, N., Mantegna, R.N., 2004. Networks of equities in financial markets. Eur. Phys. J. B - Condens. Matter 38, 363–371.

Cameron, A., Gelbach, J., D., M., 2011. Robust Inference With Multiway Clustering. J. Bus. Econ. Stat. 29, 238–249.

Campbell, J.Y., Hilscher, J., Szilagyi, J., 2008. In Search of Distress Risk. J. Finance 63, 2899–2939.

Carhart, M., 1997. On Persistence in Mutual Fund Performance. J. Finance 52, 57–82.

DeMiguel, V., Garlappi, L., Uppal, R., 2009. Optimal Versus Naive Diversification: How Inefficient is the 1/N Portfolio Strategy? Rev. Financ. Stud. 22, 1915–1953.

Desmoulins-Lebeault, F., Kharoubi-Rakotomalala, C., 2012. Non-Gaussian diversification: When size matters. J. Bank. Financ. 36, 1987–1996.

Diebold, F.X., Yilmaz, K., 2014. On the network topology of variance decompositions: Measuring the connectedness of financial firms. J. Econom. 182, 119–134.

Duchin, R., Levy, H., 2009. Markowitz versus the Talmudic portfolio diversification strategies. J. Portf. Manag. 35, 71–74.

Fama, E., French, K., 1993. Common Risk Factors in the Returns on Stocks and Bonds. J. financ. econ. 33, 3–56.

Fama, E., French, K., 1996. Multifactor Explanations of Asset Pricing Anomalies. J. Finance 51, 55–84.

Fama, E., French, K., 2004. New lists: Fundamentals and survival rates. J. financ. econ. 73, 229–269. doi:10.1016/j.jfineco.2003.04.001

Freeman, L., 1978. Centrality in Social Networks Conceptual Clarification. Soc. Networks 1, 215–239.

Garas, A., Argyrakis, P., 2007. Correlation study of the Athens Stock Exchange. Phys. A Stat. Mech. its Appl. 380, 399–410.

Green, R., Hollifield, B., 1992. When Will Mean-Variance Efficient Portfolios Be Well Diversified? J. Finance 47, 1785–1809.

Gregory, A., Tharyan, R., Christidis, A., 2013. Constructing and Testing Alternative Versions of the Fama–French and Carhart Models in the UK. J. Bus. Financ. Account. 40, 172–214.

Han, Y., Yang, K., Zhou, G., 2013. A new anomaly: The cross-sectional profitability of technical analysis. J. Financ. Quant. Anal. 48, 1433–1461.

Hautsch, N., Schaumburg, J., Schienle, M., 2015. Financial Network Systemic Risk Contributions. Rev. Financ. 9, 685–738.

Huang, W.Q., Zhuang, X.T., Yao, S., 2009. A network analysis of the Chinese stock market. Phys. A Stat. Mech. its Appl. 388, 2956–2964.

Jackson, M.O., 2010. Social and Economic Networks. Princeton University Press.

Jobson, D.J., Korkie, B.M., 1980. Estimation for Markowitz efficient portfolios. J. Am. Stat. Assoc. 75, 544–554.

Jorion, P., 1991. Bayesian anc CAPM Estimators of the Means: Implications for Portfolio Selection. J. Bank. Financ. 15, 717–727.

Jung, W., Chae, S., Yang, J.S., Moon, H., 2006. Characteristics of the Korean stock market correlations. Phys. A Stat. Mech. its Appl. 361, 263–271.

Laloux, L., Cizeau, P., Bouchaud, J.P., Potters, M., 1999. Noise Dressing of Financial Correlation Matrices. Phys. Rev. Lett. 83, 1467–1470. doi:10.1103/PhysRevLett.83.1467

Ledoit, O., Wolf, M., 2004. Honey, I Shrunk the Sample Covariance Matrix. J. Portf. Manag. 30, 110–119.

Ledoit, O., Wolf, M., 2008. Robust performance hypothesis testing with the Sharpe ratio. J. Empir. Financ. 15, 850–859.

Ledoit, O., Wolf, M., 2011. Robust Performance Hypothesis Testing with the Variance. Wilmott 55, 86–89.

Mantegna, R.N., 1999. Hierarchical structure in financial markets. Eur. Phys. J. B - Condens. Matter 11, 193–197.

Markowitz, H., 1952. Portfolio Selection. J. Finance 7, 77–91.

Merton, R., 1980. On Estimating the Expected Return on the Market. J. financ. econ. 8, 323–361.

Michaud, R., 2008. Efficient Asset Management: A Practical Guide to Stock Portfolio Optimization and Asset Allocation., Second. ed. Oxford University Press. New York.

Michaud, R., Michaud, R.O., 2008. Efficient Asset Management: A Practical Guide to Stock Portfolio Optimization and Asset Allocation, Second. ed. Oxford University Press. New York.

Newey, W., West, K., 1987. A simple, positive semi-definite, heteroskedasticity and autocorrelation consistent covariance matrix. Econometrica 55, 703–708.

Newman, M.E.J., 2004. Analysis of weighted networks. Phys. Rev. E.

Onnela, J.P., Chakraborti, A., Kaski, K., Kertész, J., Kanto, A., 2003. Asset trees and asset graphs in financial markets. Phys. Scr. T106, 48–54.

Peralta, G., 2015. Network-based measures as leading indicators of market instability: the case of the Spanish stock market. J. Netw. Theory Financ. 1, 91–122.

Petersen, M., 2009. Estimating Standard Errors in Finance Panel Data Sets: Comparing Approaches. Rev. Financ. Stud. 22, 435–480.

Politis, N., Romano, J., 1994. The Stationary Bootstrap. J. Am. Stat. Assoc. 89, 1303–1313.

Pozzi, F., Di Matteo, T., Aste, T., 2013. Spread of risk across financial markets: better to invest in the peripheries. Sci. Rep. 3, 1665.

Trzcinka, C., 1986. On the Number of Factors in the Arbitrage Pricing Model. J. Finance 41, 374–368.

Tse, C.K., Liu, J., Lau, F.C.M., 2010. A network perspective of the stock market. J. Empir. Financ. 17, 659–667.

Van Mieghem, P., 2011. Graph Spectra for Complex Networks. Cambridge University Press.

Vandewalle, N., Brisbois, F., Tordoir, X., 2001. Non-random topology of stock markets. Quant. Financ. 1, 372–374.

White, H., 1980. A Heteroskedasticity-Consistent Covariance Matrix Estimator and a Direct Test for Heteroskedasticity. Econometrica.

Zareei, A., 2015. Network Centrality, Failure Prediction and Systemic Risk. J. Netw. Theory Financ. 1.

Appendix A: Proof of Proposition 1

Let us consider two symmetric square $n \times n$ matrices Ω^0 and $\Omega^1 = \Omega^0 + a * I$ where $a \in \mathbb{R}$ and I is the identity matrix with their corresponding sets of eigenvectors and eigenvalues denoted by $\{v_1^s, \dots, v_n^s\}$ and $\{\lambda_1^s, \dots, \lambda_n^s\}$ for $s = 1,0$. By definition of eigenvectors $\lambda_k^s v_k^s = \Omega^s v_k^s$, it follows that $\lambda_k^1 v_k^1 = \Omega^1 v_k^1 = (\Omega^0 + a * I)\, v_k^1$. After some simple algebraic manipulations $(\lambda_k^1 - a)v_k^1 = \Omega^0 v_k^1$ that allows us to conclude that $v_k^1 = v_k^0$ and $\lambda_k^1 = \lambda_k^0 + a$. Therefore, as a preliminary result, we show that the eigenvectors of Ω^0 and $\Omega^1$are exactly equal and the corresponding associated eigenvalues are related as follows: $\lambda_k^1 = \lambda_k^0 + a$ for $k = 1 \dots n$.

The proof of Proposition 1 is stated only for the case of the mean-variance strategy given that the minimum-variance rule follows exactly the same steps. We assume that the correlation matrix Ω is a $n \times n$ diagonalizable symmetric matrix with a set of eigenvectors given by $\{v_1, \dots v_n\}$ and a set of eigenvalues given by $\{\lambda_1, \dots \lambda_n\}$, both sets arranged in descendent order. Then, $\Omega = P\Lambda P^T$, where P is an $n \times n$ orthogonal matrix whose columns are $v_1, \dots v_n$. Let us denote by $\Lambda = diag(\lambda_i)$ a diagonal matrix whose ith-main diagonal element is λ_i. Thus the inverse of Ω could be written as

$$\Omega^{-1} = P\Lambda^{-1}P^T = P * diag(1/\lambda_i) * P^T \qquad \text{A.1}$$

$$\Omega^{-1} = \sum_k \left(\frac{1}{\lambda_k} v_k {v_k}^T\right) = \frac{1}{\lambda_1} v_1 {v_1}^T + \frac{1}{\lambda_2} v_2 {v_2}^T + \cdots + \frac{1}{\lambda_n} v_n {v_n}^T \qquad \text{A.2}$$

From equation (7) in section 2.2, we have $\widehat{w}^* = \varphi\Omega^{-1}\hat{\mu}^e$. By adding and subtracting $\varphi\hat{\mu}^e$ from this expression we get

$$\widehat{w}^* = \varphi\hat{\mu}^e + \varphi[\Omega^{-1} - I]\hat{\mu}^e \qquad \text{A.3}$$

Using the preliminary results above-mentioned in this appendix, we know that the matrix $\Omega^{-1} - I$ has the same eigenvectors with eigenvalues equal to $\frac{1}{\lambda_k} - 1$ for $k = 1 \dots n$. Therefore, A.3 is stated as follows:

$$\widehat{w}^* = \varphi\hat{\mu}^e + \varphi\left[\sum_k \left(\frac{1}{\lambda_k} - 1\right) v_k {v_k}^T\right]\hat{\mu}^e \qquad \text{A.4}$$

Given that eigenvector centralities refer to the elements of the eigenvector corresponding to the largest eigenvalue, we define $\Gamma = \varphi\left[\sum_{k=2}^n \left(\frac{1}{\lambda_k} - 1\right) v_k {v_k}^T\right]\hat{\mu}^e$. Then, A.4 is stated as

$$\widehat{w}^* = \varphi\hat{\mu}^e + \varphi\left(\frac{1}{\lambda_1} - 1\right) v_1 {v_1}^T \hat{\mu}^e + \Gamma \quad \text{A.5}$$

$$\widehat{w}^* = \varphi\hat{\mu}^e + \varphi\left(\frac{1}{\lambda_1} - 1\right) ({v_1}^T \hat{\mu}^e) v_1 + \Gamma \quad \text{A.6}$$

$$\widehat{w}^* = \varphi\hat{\mu}^e + \varphi\left(\frac{1}{\lambda_1} - 1\right) \hat{\mu}_M^e v_1 + \Gamma \quad \text{A.7}$$

Appendix B: Descriptive Statistics of Stock Performance in terms of Centrality

Table B.1. Sharpe ratios, excess returns and standard deviations of returns for the stocks included in the d-S&P dataset conditioning on their centralities. The stocks are categorised in terms of the low, middle and high terciles of the centrality distribution.

	Mean	Std	Percentiles					Skew	Kurtosis
Sharpe Ratio			Min	5%	50%	95%	Max		
Low	3.31%	1.57%	-0.22%	1.23%	3.03%	6.16%	7.92%	0.51	0.13
Middle	2.82%	1.13%	-0.07%	0.88%	2.85%	4.35%	5.86%	-0.02	-0.06
High	2.88%	0.92%	1.03%	1.36%	2.86%	4.04%	5.33%	0.00	-0.66
Excess Return									
Low	0.07%	0.05%	-0.01%	0.02%	0.06%	0.18%	0.22%	1.20	0.84
Middle	0.06%	0.03%	0.00%	0.02%	0.06%	0.12%	0.13%	0.58	-0.08
High	0.06%	0.02%	0.02%	0.03%	0.06%	0.09%	0.16%	0.85	2.59
Std									
Low	2.05%	0.70%	1.09%	1.20%	1.95%	3.21%	4.84%	1.30	2.53
Middle	2.09%	0.63%	1.09%	1.15%	2.03%	3.24%	3.82%	0.58	-0.23
High	2.24%	0.50%	1.43%	1.49%	2.23%	3.17%	3.76%	0.60	0.23

Appendix C: Securities' description by their Centrality in the d-S&P dataset

Table C.1. Sharpe ratio, CAPM Beta, Market capitalization and Centrality ranking for each stock in the d-S&P dataset

Ticker	Name	Economic Sector	Sharpe Ratio	CAPM Beta	Market Cap.	Centrality
BEN	FRANKLIN RESOURCES INC	Finance, Insurance, And Real Estate	0.554	1.493	26588.88	0.0892
TROW	PRICE (T. ROWE) GROUP	Finance, Insurance, And Real Estate	0.605	1.628	16593.66	0.0886
DD	DU PONT (E I) DE NEMOURS	Manufacturing	0.290	1.115	41936.60	0.0880
PPG	PPG INDUSTRIES INC	Manufacturing	0.568	1.109	20755.92	0.0872
L	LOEWS CORP	Manufacturing	0.451	1.240	16038.30	0.0868
EMR	EMERSON ELECTRIC CO	Manufacturing	0.475	1.130	35205.53	0.0866
UTX	UNITED TECHNOLOGIES CORP	Manufacturing	0.547	0.976	75165.85	0.0860
PCAR	PACCAR INC	Manufacturing	0.614	1.432	15959.13	0.0856
ITW	ILLINOIS TOOL WORKS	Manufacturing	0.415	1.033	28182.33	0.0854
PX	PRAXAIR INC	Manufacturing	0.648	1.048	32520.54	0.0843
AXP	AMERICAN EXPRESS CO	Finance, Insurance, And Real Estate	0.373	1.488	64492.56	0.0842
APD	AIR PRODUCTS & CHEMICALS INC	Manufacturing	0.403	1.051	17508.17	0.0839
HON	HONEYWELL INTERNATIONAL INC	Mining	0.530	1.098	49720.61	0.0837
ETN	EATON CORP PLC	Manufacturing	0.565	1.149	18307.42	0.0831
DIS	DISNEY (WALT) CO	Services	0.527	1.101	94569.29	0.0826
CVX	CHEVRON CORP	Manufacturing	0.605	0.998	211649.54	0.0826
DHR	DANAHER CORP	Manufacturing	0.593	0.923	38721.26	0.0823
WY	WEYERHAEUSER CO	Manufacturing	0.355	1.262	15041.49	0.0822
CAT	CATERPILLAR INC	Manufacturing	0.638	1.232	58598.03	0.0821
XOM	EXXON MOBIL CORP	Manufacturing	0.530	0.937	394610.88	0.0816
MMM	3M CO	Manufacturing	0.370	0.836	64245.78	0.0816
IR	INGERSOLL-RAND PLC	Manufacturing	0.452	1.320	14512.69	0.0814
UPS	UNITED PARCEL SERVICE INC	Transp., Comm., Elect., Gas, Sant. S	0.217	0.797	140381.93	0.0808
BK	BANK OF NEW YORK MELLON	Finance, Insurance, And Real Estate	0.207	1.575	30033.20	0.0807

	CORP					
GE	GENERAL ELECTRIC CO	Manufacturing	0.163	1.152	220107.37	0.0805
VNO	VORNADO REALTY TRUST	Retail Trade	0.443	1.425	14906.33	0.0804
JPM	JPMORGAN CHASE & CO	Finance, Insurance, And Real Estate	0.433	1.609	167063.15	0.0804
CMI	CUMMINS INC	Manufacturing	0.842	1.619	20423.98	0.0797
BXP	BOSTON PROPERTIES INC	Finance, Insurance, And Real Estate	0.537	1.346	15962.07	0.0797
PRU	PRUDENTIAL FINANCIAL INC	Finance, Insurance, And Real Estate	0.385	1.847	24746.29	0.0796
SCHW	SCHWAB (CHARLES) CORP	Finance, Insurance, And Real Estate	0.323	1.505	18308.84	0.0795
ECL	ECOLAB INC	Manufacturing	0.599	0.845	21060.08	0.0794
MET	METLIFE INC	Finance, Insurance, And Real Estate	0.316	1.690	35003.59	0.0790
SPG	SIMON PROPERTY GROUP INC	Finance, Insurance, And Real Estate	0.607	1.445	48904.96	0.0790
GS	GOLDMAN SACHS GROUP INC	Finance, Insurance, And Real Estate	0.343	1.426	62006.90	0.0789
PLD	PROLOGIS INC	Finance, Insurance, And Real Estate	0.352	1.707	16818.13	0.0787
MS	MORGAN STANLEY	Finance, Insurance, And Real Estate	0.214	2.093	151051.07	0.0787
PSA	PUBLIC STORAGE	Finance, Insurance, And Real Estate	0.628	1.246	49470.50	0.0787
DOW	DOW CHEMICAL	Manufacturing	0.286	1.296	38770.45	0.0787
FDX	FEDEX CORP	Transp., Comm., Elect., Gas, Sant. S	0.308	1.041	30527.15	0.0786
ALL	ALLSTATE CORP	Finance, Insurance, And Real Estate	0.243	1.193	19402.11	0.0785
COP	CONOCOPHILLIPS	Mining	0.574	1.055	70393.77	0.0784
DE	DEERE & CO	Manufacturing	0.548	1.229	33464.03	0.0781
CBS	CBS CORP	Transp., Comm., Elect., Gas, Sant. S	0.272	1.480	48475.70	0.0781
JCI	JOHNSON CONTROLS INC	Manufacturing	0.422	1.226	37478.21	0.0780
MHFI	MCGRAW HILL FINANCIAL	Manufacturing	0.361	1.142	15181.86	0.0780
CSX	CSX CORP	Transp., Comm., Elect., Gas, Sant. S	0.595	1.162	20349.09	0.0778
CCL	CARNIVAL CORP/PLC (USA)	Transp., Comm., Elect., Gas, Sant. S	0.300	1.204	30038.82	0.0775
OXY	OCCIDENTAL PETROLEUM CORP	Mining	0.639	1.257	62068.18	0.0774
MRO	MARATHON OIL CORP	Mining	0.597	1.284	21645.96	0.0773
CB	CHUBB CORP	Finance, Insurance, And Real Estate	0.512	0.981	39459.22	0.0773
IP	INTL PAPER CO	Manufacturing	0.278	1.345	17473.82	0.0771

OKE	ONEOK INC	Mining	0.724	0.943	17493.21	0.0770
UNP	UNION PACIFIC CORP	Mining	0.629	1.002	59230.57	0.0769
HCP	HCP INC	Finance, Insurance, And Real Estate	0.491	1.330	19417.90	0.0766
ADP	AUTOMATIC DATA PROCESSING	Services	0.393	0.794	27234.43	0.0766
BBT	BB&T CORP	Manufacturing	0.209	1.358	20363.64	0.0764
IBM	INTL BUSINESS MACHINES CORP	Manufacturing	0.606	0.795	216438.64	0.0764
AFL	AFLAC INC	Finance, Insurance, And Real Estate	0.348	1.441	24898.61	0.0762
BLK	BLACKROCK INC	Finance, Insurance, And Real Estate	0.604	1.260	35561.77	0.0761
NSC	NORFOLK SOUTHERN CORP	Transp., Comm., Elect., Gas, Sant. S	0.507	1.082	19544.10	0.0761
HD	HOME DEPOT INC	Retail Trade	0.449	1.000	100112.32	0.0761
EQR	EQUITY RESIDENTIAL	Finance, Insurance, And Real Estate	0.477	1.385	17152.58	0.0761
SLB	SCHLUMBERGER LTD	Mining	0.508	1.261	91998.73	0.0756
COF	CAPITAL ONE FINANCIAL CORP	Finance, Insurance, And Real Estate	0.345	1.792	33674.64	0.0754
MSFT	MICROSOFT CORP	Services	0.245	0.948	256956.00	0.0753
USB	U S BANCORP	Finance, Insurance, And Real Estate	0.373	1.274	60049.63	0.0750
STT	STATE STREET CORP	Finance, Insurance, And Real Estate	0.302	1.646	22039.55	0.0749
PCP	PRECISION CASTPARTS CORP	Manufacturing	0.927	1.139	27770.42	0.0749
NBL	NOBLE ENERGY INC	Mining	0.619	1.249	18211.46	0.0749
DTE	DTE ENERGY CO	Transp., Comm., Elect., Gas, Sant. S	0.434	0.678	20665.97	0.0745
NI	NISOURCE INC	Transp., Comm., Elect., Gas, Sant. S	0.410	0.760	15411.73	0.0745
WFC	WELLS FARGO & CO	Finance, Insurance, And Real Estate	0.325	1.553	180799.38	0.0744
INTC	INTEL CORP	Manufacturing	0.298	1.119	102728.84	0.0744
HCN	HEALTH CARE REIT INC	Finance, Insurance, And Real Estate	0.567	0.971	15907.19	0.0741
M	MACY'S INC	Retail Trade	0.431	1.419	15626.20	0.0738
APA	APACHE CORP	Mining	0.427	1.178	30714.85	0.0738
SRE	SEMPRA ENERGY	Transp., Comm., Elect., Gas, Sant. S	0.690	0.761	17167.48	0.0737
ACE	ACE LTD	Finance, Insurance, And Real Estate	0.473	1.058	27110.84	0.0736
BAC	BANK OF AMERICA CORP	Finance, Insurance, And Real Estate	0.134	1.855	125124.05	0.0734
LOW	LOWE'S COMPANIES INC	Wholesale Trade	0.307	1.037	42887.37	0.0734

TWX	TIME WARNER INC	Services	0.344	1.076	45438.50	0.0733
CSCO	CISCO SYSTEMS INC	Manufacturing	0.312	1.118	85858.85	0.0732
TMO	THERMO FISHER SCIENTIFIC INC	Manufacturing	0.556	0.911	22974.50	0.0729
TYC	TYCO INTERNATIONAL LTD	Manufacturing	0.456	0.999	25866.88	0.0728
HAL	HALLIBURTON CO	Mining	0.590	1.323	32192.32	0.0725
APC	ANADARKO PETROLEUM CORP	Mining	0.470	1.289	37132.70	0.0725
COH	COACH INC	Manufacturing	0.683	1.306	16804.75	0.0724
NOV	NATIONAL OILWELL VARCO INC	Manufacturing	0.609	1.541	29177.17	0.0723
GD	GENERAL DYNAMICS CORP	Manufacturing	0.348	0.795	24457.15	0.0723
ORCL	ORACLE CORP	Services	0.555	1.061	159407.81	0.0722
BHI	BAKER HUGHES INC	Mining	0.274	1.275	17932.14	0.0722
T	AT&T INC	Transp., Comm., Elect., Gas, Sant. S	0.468	0.819	192384.94	0.0722
NKE	NIKE INC -CL B	Manufacturing	0.671	0.885	110200.60	0.0720
WM	WASTE MANAGEMENT INC	Transp., Comm., Elect., Gas, Sant. S	0.321	0.753	15650.87	0.0714
PNC	PNC FINANCIAL SVCS GROUP INC	Finance, Insurance, And Real Estate	0.325	1.378	30845.99	0.0713
D	DOMINION RESOURCES INC	Transp., Comm., Elect., Gas, Sant. S	0.554	0.630	29764.79	0.0712
FCX	FREEPORT-MCMORAN COP&GOLD	Mining	0.592	1.608	32455.80	0.0711
EXC	EXELON CORP	Transp., Comm., Elect., Gas, Sant. S	0.297	0.785	25406.38	0.0711
NEE	NEXTERA ENERGY INC	Transp., Comm., Elect., Gas, Sant. S	0.591	0.697	29281.61	0.0709
PG	PROCTER & GAMBLE CO	Manufacturing	0.366	0.547	167831.49	0.0709
RL	RALPH LAUREN CORP	Manufacturing	0.664	1.154	15356.42	0.0709
DVN	DEVON ENERGY CORP	Mining	0.364	1.135	21076.20	0.0708
TGT	TARGET CORP	Retail Trade	0.359	0.994	39538.35	0.0708
HES	HESS CORP	Manufacturing	0.395	1.322	18088.32	0.0707
VFC	VF CORP	Manufacturing	0.652	0.908	16597.19	0.0705
C	CITIGROUP INC	Retail Trade	-0.012	1.901	116010.54	0.0703
ADBE	ADOBE SYSTEMS INC	Services	0.499	1.171	17122.67	0.0703
VZ	VERIZON COMMUNICATIONS INC	Transp., Comm., Elect., Gas, Sant. S	0.484	0.749	123492.58	0.0701
STI	SUNTRUST BANKS INC	Finance, Insurance, And Real Estate	0.133	1.604	15275.57	0.0699

SBUX	STARBUCKS CORP	Retail Trade	0.599	1.048	38529.45	0.0697
PEG	PUBLIC SERVICE ENTRP GRP INC	Transp., Comm., Elect., Gas, Sant. S	0.483	0.780	15480.32	0.0696
PFE	PFIZER INC	Manufacturing	0.155	0.771	184648.21	0.0694
VLO	VALERO ENERGY CORP	Manufacturing	0.577	1.309	18884.29	0.0693
JNJ	JOHNSON & JOHNSON	Manufacturing	0.293	0.530	193655.32	0.0692
LLY	LILLY (ELI) & CO	Manufacturing	0.164	0.737	54636.25	0.0690
EIX	EDISON INTERNATIONAL	Transp., Comm., Elect., Gas, Sant. S	0.720	0.778	14723.39	0.0689
ED	CONSOLIDATED EDISON INC	Transp., Comm., Elect., Gas, Sant. S	0.469	0.496	32532.20	0.0689
EOG	EOG RESOURCES INC	Mining	0.633	1.187	32715.95	0.0688
CTSH	COGNIZANT TECH SOLUTIONS	Services	0.806	1.243	22160.25	0.0682
QCOM	QUALCOMM INC	Manufacturing	0.584	1.050	106948.64	0.0680
MMC	MARSH & MCLENNAN COS	Finance, Insurance, And Real Estate	0.129	0.885	18743.96	0.0679
TJX	TJX COMPANIES INC	Retail Trade	0.669	0.847	32947.65	0.0678
PPL	PPL CORP	Transp., Comm., Elect., Gas, Sant. S	0.446	0.688	16633.17	0.0677
NOC	NORTHROP GRUMMAN CORP	Manufacturing	0.233	0.697	33207.73	0.0675
AGN	ALLERGAN INC	Manufacturing	0.519	0.803	27553.94	0.0675
SYY	SYSCO CORP	Wholesale Trade	0.205	0.673	17447.53	0.0672
FE	FIRSTENERGY CORP	Transp., Comm., Elect., Gas, Sant. S	0.358	0.717	17464.69	0.0672
KMB	KIMBERLY-CLARK CORP	Manufacturing	0.415	0.513	33121.87	0.0666
COST	COSTCO WHOLESALE CORP	Wholesale Trade	0.549	0.751	42401.49	0.0665
KO	COCA-COLA CO	Manufacturing	0.357	0.562	162617.50	0.0664
MSI	MOTOROLA SOLUTIONS INC	Manufacturing	0.292	1.212	31236.48	0.0663
EBAY	EBAY INC	Services	0.492	1.095	65991.02	0.0662
TXN	TEXAS INSTRUMENTS INC	Manufacturing	0.368	1.050	34621.60	0.0659
WMB	WILLIAMS COS INC	Construction	0.825	1.339	20527.98	0.0659
SHW	SHERWIN-WILLIAMS CO	Manufacturing	0.791	0.812	15859.92	0.0658
AEP	AMERICAN ELECTRIC POWER CO	Transp., Comm., Elect., Gas, Sant. S	0.400	0.718	41418.02	0.0657
HPQ	HEWLETT-PACKARD CO	Manufacturing	0.219	1.010	27242.95	0.0656
SYK	STRYKER CORP	Manufacturing	0.334	0.758	20842.62	0.0653

GPS	GAP INC	Retail Trade	0.459	1.000	15686.40	0.0647
RIG	TRANSOCEAN LTD	Mining	0.363	1.161	16051.65	0.0645
ADM	ARCHER-DANIELS-MIDLAND CO	Manufacturing	0.398	0.958	19483.20	0.0643
SO	SOUTHERN CO	Transp., Comm., Elect., Gas, Sant. S	0.476	0.475	37420.48	0.0641
MON	MONSANTO CO	Manufacturing	0.845	1.010	46367.59	0.0635
EMC	EMC CORP/MA	Manufacturing	0.585	1.069	53298.37	0.0634
CTL	CENTURYLINK INC	Construction	0.428	0.729	24377.39	0.0633
PEP	PEPSICO INC	Manufacturing	0.451	0.516	106134.93	0.0632
WMT	WAL-MART STORES INC	Retail Trade	0.261	0.574	234892.09	0.0631
INTU	INTUIT INC	Services	0.407	0.868	17076.96	0.0627
BMY	BRISTOL-MYERS SQUIBB CO	Manufacturing	0.372	0.671	53773.50	0.0627
WAG	WALGREEN CO	Retail Trade	0.187	0.724	30698.70	0.0625
DUK	DUKE ENERGY CORP	Transp., Comm., Elect., Gas, Sant. S	0.534	0.610	89830.40	0.0624
ACN	ACCENTURE PLC	Services	0.625	0.837	39386.24	0.0623
MDT	MEDTRONIC INC	Manufacturing	0.108	0.659	47146.80	0.0622
BRK.B	BERKSHIRE HATHAWAY	Finance, Insurance, And Real Estate	0.296	0.607	666986.40	0.0620
PCG	PG&E CORP	Transp., Comm., Elect., Gas, Sant. S	0.686	0.625	17251.56	0.0618
CI	CIGNA CORP	Finance, Insurance, And Real Estate	0.378	1.109	15319.54	0.0617
EL	LAUDER (ESTEE) COS INC -CL A	Manufacturing	0.585	0.811	42074.07	0.0616
LMT	LOCKHEED MARTIN CORP	Manufacturing	0.298	0.636	29863.84	0.0614
K	KELLOGG CO	Manufacturing	0.431	0.475	19994.30	0.0614
BF.B	BROWN-FORMAN -CL B	Manufacturing	0.682	0.599	30119.15	0.0613
MCD	MCDONALD'S CORP	Retail Trade	0.839	0.608	88562.84	0.0612
CL	COLGATE-PALMOLIVE CO	Manufacturing	0.451	0.516	49393.26	0.0611
SYMC	SYMANTEC CORP	Services	0.355	0.997	17009.18	0.0611
GLW	CORNING INC	Manufacturing	0.639	1.272	18652.36	0.0609
MRK	MERCK & CO	Manufacturing	0.214	0.769	124637.90	0.0609
ESRX	EXPRESS SCRIPTS HOLDING CO	Services	0.716	0.880	43718.39	0.0607
CAH	CARDINAL HEALTH INC	Wholesale Trade	0.101	0.735	14532.00	0.0606

AET	AETNA INC	Finance, Insurance, And Real Estate	0.580	0.961	15490.70	0.0605
MCK	MCKESSON CORP	Wholesale Trade	0.527	0.757	25154.68	0.0604
CCI	CROWN CASTLE INTL CORP	Transp., Comm., Elect., Gas, Sant. S	0.980	1.077	42308.98	0.0602
MDLZ	MONDELEZ INTERNATIONAL INC	Manufacturing	0.210	0.533	45232.57	0.0600
CVS	CVS CAREMARK CORP	Manufacturing	0.579	0.725	60244.10	0.0600
AON	AON PLC	Finance, Insurance, And Real Estate	0.490	0.740	17721.07	0.0599
AAPL	APPLE INC	Manufacturing	1.252	1.019	625254.73	0.0598
BRCM	BROADCOM CORP -CL A	Manufacturing	0.524	1.285	37460.88	0.0595
UNH	UNITEDHEALTH GROUP INC	Finance, Insurance, And Real Estate	0.391	0.894	54890.88	0.0591
BDX	BECTON DICKINSON & CO	Manufacturing	0.568	0.545	15677.04	0.0590
WFM	WHOLE FOODS MARKET INC	Retail Trade	0.533	1.020	17975.56	0.0584
AMGN	AMGEN INC	Manufacturing	0.345	0.686	66210.21	0.0582
ABT	ABBOTT LABORATORIES	Manufacturing	0.413	0.530	103533.75	0.0579
WLP	WELLPOINT INC	Finance, Insurance, And Real Estate	0.313	0.785	19129.61	0.0579
STZ	CONSTELLATION BRANDS -CL A	Manufacturing	0.450	0.771	16242.10	0.0577
HSY	HERSHEY CO	Manufacturing	0.528	0.513	32237.28	0.0568
CELG	CELGENE CORP	Manufacturing	0.884	0.938	33269.00	0.0563
AMT	AMERICAN TOWER CORP	Transp., Comm., Elect., Gas, Sant. S	1.038	1.035	30549.00	0.0556
GIS	GENERAL MILLS INC	Manufacturing	0.489	0.403	30333.64	0.0548
YHOO	YAHOO INC	Services	0.493	1.025	23600.70	0.0547
GILD	GILEAD SCIENCES INC	Manufacturing	0.746	0.794	55670.17	0.0546
AIG	AMERICAN INTERNATIONAL GROUP	Finance, Insurance, And Real Estate	-0.035	1.825	52113.24	0.0542
MO	ALTRIA GROUP INC	Manufacturing	0.813	0.532	63670.15	0.0540
TAP	MOLSON COORS BREWING CO	Manufacturing	0.301	0.581	15507.10	0.0536
BAX	BAXTER INTERNATIONAL INC	Manufacturing	0.443	0.578	36570.27	0.0533
BIIB	BIOGEN IDEC INC	Manufacturing	0.480	0.845	34630.70	0.0517
ISRG	INTUITIVE SURGICAL INC	Manufacturing	0.860	1.118	19516.72	0.0517
RAI	REYNOLDS AMERICAN INC	Manufacturing	0.864	0.528	23157.22	0.0502
PCLN	PRICELINE.COM INC	Transp., Comm., Elect., Gas, Sant. S	0.990	1.161	30936.37	0.0491

ALXN	ALEXION PHARMACEUTICALS INC	Manufacturing	0.958	0.883	18207.68	0.0489
REGN	REGENERON PHARMACEUTICALS	Manufacturing	0.690	1.214	16508.26	0.0468
NEM	NEWMONT MINING CORP	Mining	0.309	0.611	45653.85	0.0392

Appendix D: Regressions of returns from ρ-dependent strategy on the four risk factors, MKT, HML, SMB, MOM without winsorizing.

Table D.1. OLS estimation of Annualized Carhart's Alpha from the four factor model in equation (17).We consider the d-S&P, and d-FTSE, m-NYSE datasets and without winsorising. *t-statistics* are in parentheses and the statistical significance is as follows: * at 5% level, ** at 1% and *** at 0.1% level. Standard errors are corrected following Newey and West (1987). Portfolios of size 10, 20 and 50 are considered with a holding period of one (1d) and twenty (20d) for the daily datasets and one (1m) and twelve (12m) months for the monthly dataset.

Dataset	Obs	Portfolio Setting		α	β_{MKT}	β_{HML}	β_{SMB}	β_{MOM}
		Stocks	Holding Period					
SP500	1580	10	1d/1m	12.87	0.87	-0.15	0.06	0.18
				(2.74)***	(53.93)***	(-3.32)***	(1.49)	(0.76)
			20d/12m	15.06	0.9	-0.17	0.01	0.04
				(3.20)***	(38.60)***	(-3.34)***	(0.16)	(1.72)*
		20	1d/1m	3.5	0.89	-0.19	-0.07	0.03
				(2.60)***	(54.95)***	(-5.28)***	(-2.47)**	(2.02)**
			20d/12m	11.79	0.9	-0.21	-0.1	0.03
				(3.33)***	(33.82)***	(-4.39)***	(-2.39)**	-1.61
		50	1d/1m	8.14	0.92	-0.14	-0.14	0.05
				(3.44)***	(61.96)***	(-5.06)***	(-5.93)***	(3.95)***
			20d/12m	8.27	0.93	-0.17	-0.17	0.04
				(3.47)***	(47.79)***	(-5.60)***	(-5.60)***	(3.57)
FTSE	1000	10	1d/1m	35.45	-0.01	0.19	-0.02	0.01
				(5.37)***	(-0.39)	(0.30)	(-0.39)	(0.14)
			20d/12m	34.03	-0.01	0.03	-0.03	0.02
				(5.07)***	(-0.07)	(0.51)	(-0.54)	(0.55)
		20	1d/1m	31.27	-0.2	0.04	0.01	0.03
				(5.13)***	(-0.61)	(0.73)	(0.18)	(0.85)
			20d/12m	30.49	-0.02	0.03	0.01	0.03
				(5.02)***	(-0.59)	(0.57)	(0.11)	(0.86)
		50	1d/1m	24.77	-0.02	0.02	0.03	0.06
				(3.77)***	(-0.54)	(0.32)	(0.6)	(1.37)
			20d/12m	24.59	-0.02	0.02	0.03	0.05
				(3.73)***	(-0.54)	(0.36)	(0.59)	(1.35)
NYSE	324	10	1d/1m	0.88	0.91	0.32	0.36	-0.07
				(0.38)	(17.16)***	(4.64)***	(4.31)***	(-0.38)
			20d/12m	1.4	0.89	0.41	0.32	-0.1
				(0.62)	(17.55)***	(4.81)***	(4.37)***	(-1.64)
		20	1d/1m	1.69	0.95	0.41	0.29	-0.14
				(0.93)	(23.08)***	(5.79)***	(4.91)	(-2.64)***
			20d/12m	1.11	0.93	0.38	0.27	-0.14
				(0.63)	(21.60)***	(5.63)***	(4.78)***	(-2.99)***
		50	1d/1m	2.01	0.91	0.38	0.23	-0.13
				(1.40)	(26.68)***	(5.59)***	(3.93)***	(-2.77)***
			20d/12m	2.25	0.89	0.38	0.24	-0.12
				(1.59)	(26.04)***	(5.85)***	(3.97)***	(-2.64)***

Appendix E: Annualized risk-adjusted returns for ρ-dependent strategy with 0% and 10% winsorization

Table E.1. Annualized risk-adjusted returns for different settings of ρ-dependent strategy without winsorisation**.** We report annualized risk-adjusted returns for different settings of the ρ-dependent strategy on the four Carhart (1997) factors, MKT, HML, SMB, MOM. The estimation window is considered to be 1000 days (192 months) for daily (monthly) datasets. The t-statistics are reported in the parentheses. ** and * indicate significance at 1% and 5% levels, respectively.

Portfolio Setting		Alpha (no winsorizing)		
Stocks	Holding Period	d-S&P	d-FTSE	m-NYSE
10	1d/1m	12.87	35.45	0.88
		(2.74)**	(5.37)**	(0.38)
	20d/12m	15.06	34.03	1.4
		(3.20)**	(5.07)**	(0.62)
20	1d/1m	3.5	31.27	1.69
		(2.60)**	(5.13)**	(0.93)
	20d/12m	11.79	30.49	1.11
		(3.33)**	(5.02)**	(0.63)
50	1d/1m	8.14	24.77	2.01
		(3.44)**	(3.77)**	(1.4)
	20d/12m	8.27	24.59	2.25
		(3.47)**	(3.73)**	(1.59)

Table E2. Annualized risk-adjusted returns for ρ-dependent Strategy with 10% winsorisation. We report annualized risk-adjusted returns for various settings of ϱ-dependent strategy on the four Carhart (1997) factors, MKT, HML, SMB, MOM with 10% winsorisation. The estimation window is considered to be 1000 days (192 months) for daily (monthly) datasets. The t-statistics are reported in the parentheses. ** and * indicate significance at 1% and 5% levels, respectively.

Portfolio Setting		Alpha (10% winsorizing)		
Stocks	Holding Period	d-S&P	d-FTSE	m-NYSE
10	1d/1m	14.81	35.14	5.16
		(3.82)**	(7.06)**	(2.48)*
	20d/12m	17.85	34.75	5.3
		(4.57)**	(6.88)**	(2.55)*
20	1d/1m	13.83	34.47	9.98
		(4.24)**	(7.77)**	(4.29)**
	20d/12m	15.72	33.7	5.91
		(4.86)**	(7.60)**	(3.39)**
50	1d/1m	12.68	29.51	5.78
		(4.51)**	(6.19)**	(3.70)**
	20d/12m	13.14	29.74	6.45
		(4.70)**	(6.70)**	(4.03)**

Appendix F: The Relationship between Stock Centrality and Stability

We associate the concept of stock stability with the tendency of a particular asset to remain listed in the market through time without any change in its relative centrality status. This appendix analyzes the stability of stocks listed in NYSE from two different perspectives. First, we present results regarding the switching nature of assets in accordance to their different centrality in the stock market network. Second, we investigate whether the period size chosen to compute the correlation matrix influence the ranking of centralities.

We employ an m-NYSE dataset that accounts for all of the NYSE stocks with monthly pricing records in the period starting from April-1968 until April-2012. Thus, we include a full list of companies that have ever existed at some point in this period. We analyze the change in the nature of stocks in terms of centrality by relying on a moving window approach. We specify a 30-year moving window and divide it into two sub-periods, each of 15 years. We use the first and the second period to give an initial and final categorization of stocks in accordance with their centrality. Three exclusive and collectively exhaustive groups of stocks are created: high, medium and low central stocks in accordance to the top, middle and bottom terciles of the centrality distribution. Next, we construct a switching matrix accounting for the distribution of stocks belonging to a particular range of centrality in the initial period, in terms of their centrality in the final period. Since a one-year displacement step is under consideration, 15 individual switching matrices were computed. Figure F1 reports the results for each of those iterations[21].

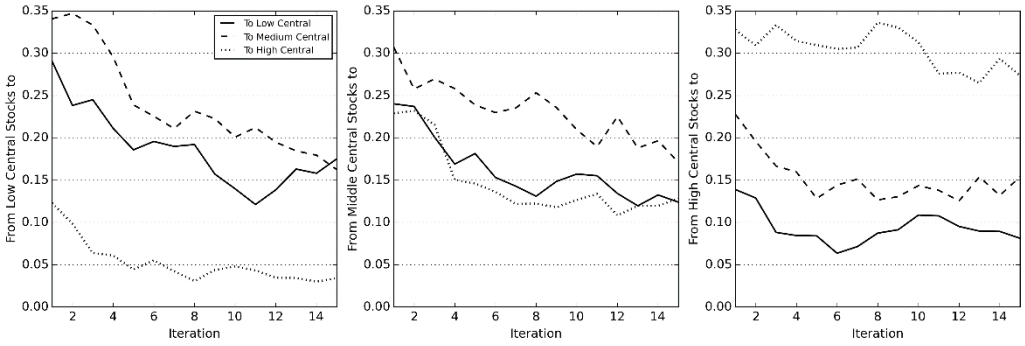

Figure F.1: Change in centrality of securities from an initial tercile of centrality to a final tercile of centrality across 15 iterations in m-NYSE dataset. We specify a 30-year moving window and divide it into two sub-periods, each of 15 years. We use the first and the second period to have an initial and final categorization of stocks securities in accordance with their centrality. Three exclusive and collectively exhaustive groups of stocks are created: high, medium and low central stocks in accordance to the top, middle and bottom terciles of the centrality distribution.

[21] The sum of vertical height for each line does not sum to one since the proportion of the delisted firms is not included in the graph.

In the left-panel of Figure F1, it is obvious that most of low central stocks tend to change their nature to medium central or stay low central. Additionally, we can see that just a small proportion of low central stocks change to become highly central. The middle-panel of Figure F1 depicts the changing nature of medium central stocks. As it can be inferred, medium central stocks mostly stay in the middle range of centrality and lower percentages of them tend to change towards the low or high centrality bucket. Finally, the right-panel of Figure F1 presents the result of the experiment when stocks were initially classified as highly central assets. We can observe that high central stocks tend to stay central across the iterations and only lower percentage of them tend to become low or medium central. As a summary, Figure F2 presents the average of the percentage of switching in centrality over the 15 interactions. In a nutshell, we find that among the stocks that remain listed, there is a tendency to occupy the same position into the stock market network through time providing a sort of stability to the structure.

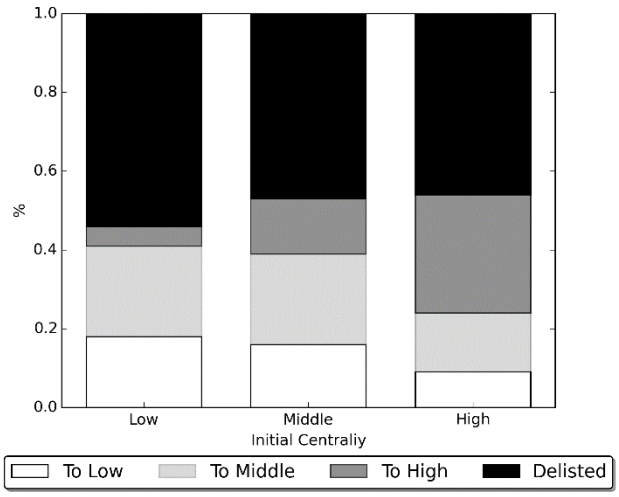

Figure F.2: Average percentage of centrality switching for low, medium and high central securities. A 30-year moving window is specified in m-NYSE dataset and it is divided into two sub-periods, each of 15 years. We use the first and the second period to give an initial and final categorization of securities in accordance to their centrality. Three exclusive and collectively exhaustive groups of assets are created: high, medium and low central stocks, in accordance with the top, middle and bottom terciles of the centrality distribution.

In the second analysis, we investigate the relationship between the ranking of centrality and the size of the period chosen to compute the correlation matrix. We consider the d-S&P dataset for this analysis because several lengths of period can be investigated with a daily frequency.

We split the d-S&P data into several yearly subsamples made of 250 daily returns and compute the centrality rankings for each of these subsamples. In the next step, we further divide the yearly subsamples into shorter datasets accounting for one month (25 daily returns), two month (50

returns) and so on up to the yearly subsamples. Afterward, the mean correlations between the ranking of centralities obtained from these shorter datasets with the initial yearly subsamples are computed and reported in figure F.3. Clearly, the correlation between these centrality rankings is high (on average 0.8) indicating that the ordering it provides is considerably robust to the period size used to estimate the correlation matrix.

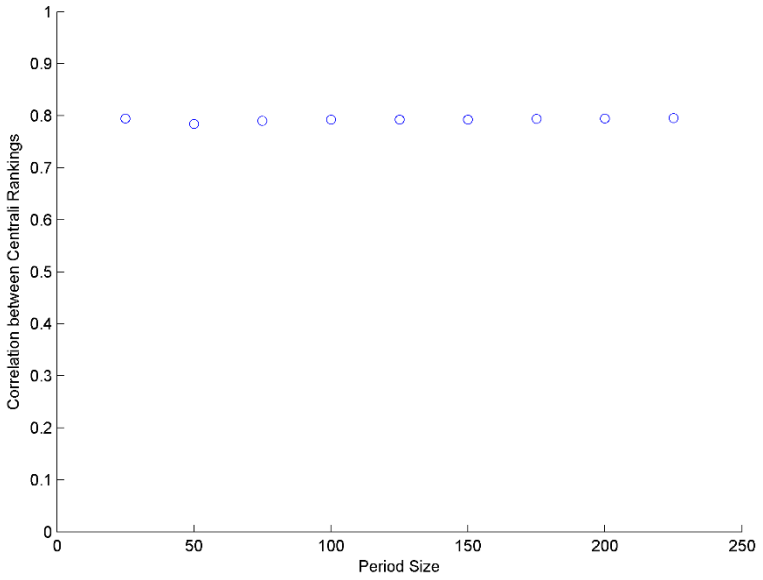

Figure F.3: Average correlation of centrality rankings in the d-S&P500 dataset between yearly subsamples (250 returns) and a set of lower-size subsamples starting with length equal to 25 days and subsequent increments of 25 days up to 250 days (one year).

Appendix G: Turnover-driven Transaction Cost

The analysis in section 6.5 assumes that investor faces a fixed transaction cost without accounting for the magnitude of changes in portfolio weights. However, investors may incur proportional costs that severely undermine the performance of their strategy. In order to take this point into account, we compute another version of the breakeven transaction cost (BETC) by solving the next expression:

$$\sum_{t=M}^{T-1}\left[(1+R_t)\left(1-BETC^{*}\times\sum_{j=1}^{N}\left|w_{j,t+1}^{s}-w_{j,t^{+}}\right|\right)-1\right]=0 \qquad \text{(G.1)}$$

Therefore, the value of $BETC^{*}$represents the corresponding proportional of transaction cost that is required in order to eliminate portfolio return. The results are presented in table G.1 where low values of $BETC^{*}$ are displayed. Nevertheless, considering the low proportional transaction cost that investors face in the current state of the financial markets, we conclude that the ρ–dependent strategy remains profitable even from this perspective.

Table G.1. $BETC^{*}$ for ρ–dependent strategy**.** We report the $BETC^{*}$ for ρ–dependent strategy in various strategy settings across the three datasets of d-S&P, d-FTSE and m-NYSE. The results are reported in basis points.

Portfolio Setting		BETC		
Stocks	Holding Period	d-S&P	d-FTSE	m-NYSE
10	20d/12m	13	20	12
20	20d/12m	12	19	14
50	20d/12m	11	18	13

Since the corresponding $BETC^{*}$s for one day/month holding period are extremely low, table G.1 does not report their values. In these cases, even a small proportional transaction cost might eliminate any benefit which in turn raises the concern derived from the application of the ρ–dependent strategy in a highly frequent rebalancing framework.

Chapter 2: Network-based Measures as Leading Indicators of Market Instability: The case of the Spanish Stock Market†

Abstract

This paper studies the undirected partial-correlation stock network for the Spanish market that considers the constituents of IBEX-35 as nodes and their partial correlations of returns as links. I propose a novel methodology that combines a recently developed variable selection method, Graphical Lasso, with Monte Carlo simulations as fundamental ingredients for the estimation recipe. Three major results come from this study. First, in topological terms, the network shows features that are not consistent with random arrangements and it also presents a high level of stability over time. International comparison between major European stock markets extends that conclusion beyond the Spanish context. Second, the systemic importance of the banking sector, relative to the other sectors in the economy, is quantitatively uncovered by means of its network centrality. Particularly interesting is the case of the two major banks that occupy the places of the most systemic players. Finally, the empirical evidence indicates that some network-based measures are leading indicators of distress for the Spanish stock market.

Keywords: Network Theory, Stock Markets, Systemic Risk Indicators, Leading Indicators

JEL Classification: G01, G12, G17, C45, C58

† I thank Pablo Gasós y Casao and Ricardo Crisóstomo Ayala for their useful feedbacks.

1. Introduction

Our interactions are embedded in different systems that can be thought as networks. Examples include the social network of acquaintance, the Internet, the World Wide Web, the network of academic citation and the list is easily extendable, (see Newman, 2003). As a consequence of the recent financial crisis, the fields of economics and finance have captured the attention of network researchers aiming to revise and extend established theoretical frameworks (Jackson, 2014).

Recently, several papers studying stock markets through the lens of network theory have been published in prestigious academic journals. The current paper contributes to this branch of literature in three directions. First, I propose an enhanced and convenient methodology for estimating a network based on partial correlation for stocks that are listed in a particular market. This methodology is grounded in a high-dimensional setting and allows researchers to control for the statistical significance of the underlying network. Second, since the mainstream literature is centered in the US market, the current paper contributes to this line of research by targeting the Spanish stock market. The aim is to develop new insights into its topological structure and to quantitatively identify its systemic players. Additionally, four other European stock markets are included in the study which allows us to compare their salient characteristics under the same unified framework. Finally, I provide an empirical assessment accounting for the role of some network-based measures as leading indicators of financial distress for the Spanish market.

Specifically, I estimate the Spanish Partial-Correlated Stock Network (PCSN) in which each node corresponds to a stock comprising the market index, IBEX-35, and the links between them account for their return's partial correlation. Since a sparse partial correlation matrix is required in order to detect the skeleton of the market, I estimate such a matrix by applying a recently developed Graphical Lasso algorithm by Friedman, Hastie, and Tibshirani (2008). Methodologically, the paper presents some improvements when it is compared to the mainstream literature solving, or at least attenuating, three of its drawbacks. First, partial correlations of returns are computed instead of direct correlations. This enables us to calculate the co-movements between two stocks while controlling for the effects exerted by the rest of the firms in market. Second, Graphical Lasso is a totally automatic and data-driven technique which is grounded in a high-multivariate setting. Such a technique permits the estimation of sparse partial correlation matrices which in turns allows us to uncover the underlying network structure. Since there is no need to use ad-hoc topological constraints or arbitrarily predefined thresholds, as it is the case with traditional methodologies, the resulting structure is not distorted by artificial

restrictions. Finally, Monte Carlo simulations are implemented in order to determine the statistical significance of the related network.

Three empirical results come from this study. First, the main indicators of the Spanish PCSN show features that are inconsistent with networks made by chance. The evidence supports a fairly stable structure with high levels of transitivity and smaller connected components.[22] In addition, four large European markets, namely the UK, France, Germany and Italy, are included in the analysis for comparison purposes. Following the exact same approach for all of them, the evidence shows an astonishing similarity in terms of their topological organization.

Second, an in-depth study of the systemic importance of different economic sectors is presented for the abovementioned stock markets. The quantification of the systemic importance of sectors and stocks is based on the notion of network centrality. In general terms, the data shows a positive and statistically significant relationship between market capitalization and stock centrality after controlling for the effects of economic sectors. Moreover, the importance of economic sectors varies across stock markets since the PCSN of Spain, France and Italy are characterized by a greater centrality of the banking industry. The cases of Germany and UK are different since for those structures it is the utilities and industrial sector, respectively, the most influential ones. For specific case of the Spanish network, it is particularly interesting to mention the disproportionally large centrality scores shown by two financial firms, Banco Santander and BBVA. This observation is consistent with the conventional wisdom and previous empirical findings and allows us to consider them as the most systemic players in the Spanish market.

Third, I investigate the extent to which network-based measures are leading indicators of market distress by means of two complementary approaches. As a first approach I estimate a Probit model where the dependent variable assumes value one when the IBEX-35 drops by more than 3 standard deviations and zero otherwise. The set of independent variables includes lagged values of some network measures; say density, transitivity and the centrality of the banking sector. The result shows that the probability that the Spanish market suffers from large negative movement increases when the lagged network becomes denser or when the banking industry scores high in centrality. In the second approach it is assumed that the return process of the market index follows an ARCH model. In this model the specification of the conditional market volatility includes as independent variables the same set of lagged network measures as in the previous approach. The estimation shows that the market variance increases with network density and with the centrality of the banking sector while it reduces with the level of transitivity.

[22] A list with definitions of network-related concepts is provided in the Appendix H of the paper.

Physics literature has been shown to be very productive in using network concepts to describe stock markets. Mantegna (1999) and Bonanno, Lillo, and Mantegna (2001) were among the first in this endeavor, applying a particular correlation-based filtering procedure, the so-called Minimum Spanning Tree (MST), for the US market in order to study its skeleton.[23] In similar vein, Vandewalle, Brisbois, and Tordoir (2001) estimate the MST also for the US stock market providing evidence for power-law degree distributions and connectivity patterns that are inconsistent with random networks. For applications of this approach to markets other than the US or with broader datasets, see Jung et al. (2006), Garas and Argyrakis (2007) and Huang, Zhuang, and Yao (2009). Two variations of this baseline framework are noted. On the one hand, Onnela et al. (2003) introduces the so-called Dynamic Asset Trees while Onnela et al. (2003) proposes a threshold approach. More recently and closely related to the current paper, Kenett et al. (2010) study the US market by mean of directed stocks networks based on partial correlations. They uncover the importance of financials stocks, a result consistent with the empirical evidence in this manuscript. For authoritative summaries of this research line see Tumminello, Lillo, and Mantegna (2010).

The last years have witnessed increased interest in network theory among the financial and econometric research communities with the aim to get new insights about systemic risk issues. In Billio et al. (2012) the authors build a directed Granger-causality network where links account for statistically significant lead-lag relationships between returns. Diebold and Yılmaz (2014) proposes a network in which connections between financial institutions are assigned according to the variance decomposition of the volatility forecast error giving rise to a volatility weighted-directed network. The correlation in the tails of the return's distributions in considered in Hautsch, Schaumburg, and Schienle (2014) by estimating a tail-risk network, a weighted-directed network in which the links between institutions are given by the interconnectedness of firms' Value-at-Risk. Finally, it is worth mentioning the important methodological contributions made by Brownlees, Nualart, and Sun (2014) and Barigozzi and Brownlees (2014) to estimated correlation-based networks. Barigozzi and Brownlees (2014) develops an algorithm named NETS which implements LASSO regressions to compute three different networks: the long run partial correlation network, the Granger network and the contemporaneous network. Brownlees, Nualart, and Sun (2014) also uses LASSO to obtain a sparse estimation of the realized precision matrix (high frequency data) in order to quantify the so-called Realized Network.

[23] MST is a filtering technique that allows us to build a connected network of N stocks by joining together pairs of them according to their pair correlation (in decreasing order) as long as no loops are formed in the structure. The resulting network is a tree network.

The remainder of the paper is organized as follows. Section 2 defines the Partial-Correlated Stock Network. Section 3 describes the dataset used and the estimation methodology. Section 4 establishes the main results from the estimation procedure distinguishing between a static and dynamic analysis. Section 5 provides the statistical assessment of some network-based measures acting as leading indicators of market distress. Finally, section 6 concludes and outlines future research lines.

2. Networks in the Context of Stock Markets

Let us assume $\boldsymbol{r} = (r_1, \dots, r_n)^T$ to be a random vector following a multivariate normal distribution with mean vector μ and covariance matrix Σ. The partial correlation between r_i and r_j, denoted by ρ_{ij}, quantifies the correlation between these two variables conditional on the rest. In this Gaussian environment, it is well known that $\rho_{ij} = 0$ implies conditional independency between i and j. The inverse of the covariance matrix (commonly named as the precision matrix), denoted by $\Omega = \Sigma^{-1} = [\omega_{i,j}]$, contains the fundamental information regarding the partial correlations matrix ρ as follows.

$$\rho = [\rho_{ij}] = -\Delta\Omega\Delta \qquad (1)$$

where $[\Delta]_{ij} = 1/\sqrt{\omega_{ii}}\ for\ i = j\ and\ [\Delta]_{ij} = 0\ for\ i \neq j$. Simple calculations show that the elements of the main diagonal of ρ are (-1) which is meaningless in our framework and therefore I set them equal to zero. It is also important to mention the close connection between ρ and regression analysis as it is in Stevens (1998). The reader is referred to Appendix A for the formal mathematical treatment of this association.

Grounded on the Gaussian Graphical Models literature Whittaker (1990), I define two types of undirected PCSN depending on whether the focus is on the weighted or on the unweighted version. The weighted PCSN, $\varphi^w = \{N, \rho\}$, with N as the set of stock under study and the partial correlation matrix of stock's returns taking the place of its adjacency matrix.[24] Therefore, for $\rho_{ij} \neq 0$, there is a link connecting stock i and j with intensity ρ_{ij}. The unweighted PCSN, $\varphi^u = \{N, \varrho\}$ consists of the same set of stocks while its corresponding adjacency matrix $\varrho = [\varrho_{ij}]$ is given by the following rules:

[24] As it was commented, for both φ^w and φ^u I discard the information in the main diagonal of the corresponding adjacency matrix to prevent uninformative self-loops.

$$\varrho_{ij} = \begin{cases} 1, & \rho_{ij} \neq 0 \\ 0, & \rho_{ij} = 0 \end{cases} \quad (2)$$

The need to include zeros outside the main diagonal of ρ (sparsity) is evident since a fully connected network comprises too much information to be analyzed. Then, sparsity in the partial correlation matrix is an essential feature to be investigated for construction of a valuable and informative PCSN, an aspect that is considered in the estimation methodology below.

3. Database Description and Estimation Methodology

The period of study covers almost 10 years of daily data starting from Nov 1, 2004 until Sep 30, 2014. I rely on Datastream for the information about dividends-and-split adjusted stock prices and returns. Additionally, market value and industrial sectors for the selected companies were also used throughout the analysis. The set of firms included into the sample comprises the constituents of the index IBEX-35 at September 2014. Table 1 reports the sample of firms including the corresponding ticker, their market value for the last day in the sample, the inception date in the index and descriptive statistics for their return distribution.

A dense partial correlation matrix would lead to a fully connected PCSN (a network in which each pair of nodes is connected) thus obscuring its salient features. The most popular filtering procedures in the relevant literature are the Minimum Spanning Tree (MST) (Bonanno, Lillo, and Mantegna, 2001), Planar Maximally Filtered Graph (PMFG) (Tumminello et al., 2005) and the Threshold Method (TM) (Onnela et al., 2003). All of them present severe drawbacks. Considering MST and PMFG, these methods retain the highest correlations in accordance with strong artificial topological restrictions. For example, MST only considers the largest correlations as links between stocks as long as the network becomes connected and no loops of order three are formed. Then, if a large association between two nodes exists but taking it into consideration implies a triangle in the network, it is discarded. The TM just consists of discarding as links in the network the correlations below a given threshold, possibly resulting in a disconnected structure. However, the determination of such a threshold represents its major weakness since it is usually pre-specified without any theoretical or statistical support. In other words, the lack of any objective function driving the elimination of links from the structure is the most important drawback of this method. A final comment regards to the application of these approaches to the direct correlation matrix of return instead of the partial correlation matrix as it is usually done in

the literature. This is another inconvenience since a direct correlation between pairs of stocks could be due to the effect of a third one affecting both simultaneously and thus distorting the resulting pattern of interconnections.

Descriptive statistics

Industry / Name	Ticker	Inception Date	Market Value* $	Market Value* %	Mean ** (1)	Median **	Std ** (2)	(1)/(2)
Industrial								
ABENGOA B SHARES	ABS	25/10/2012	3,159	1%	33.2%	0.0%	46.3%	71.7%
ABERTIS INFRAESTRUCTURAS	ACE		14,049	2%	8.4%	0.0%	24.8%	33.9%
ACCIONA	ANA		3,393	1%	7.5%	0.0%	37.0%	20.3%
ACS ACTIV.CONSTR.Y SERV.	ACS		9,690	2%	12.4%	18.7%	28.7%	43.1%
AMADEUS IT HOLDING	AMS	29/04/2010	13,257	2%	22.5%	18.5%	23.5%	96.1%
ARCELORMITTAL (MAD)	MITT	28/07/2006	18,153	3%	1.4%	0.0%	46.8%	3.0%
DIST. INTNAC.DE ALIM	DIA	05/07/2011	3,701	1%	21.1%	0.0%	28.8%	73.2%
FERROVIAL	FERC		11,354	2%	11.8%	0.0%	35.0%	33.7%
FOMENTO CONSTR.Y CNTR.	FCC		1,940	0%	-0.1%	0.0%	36.0%	-0.2%
GAMESA CORPN.TEGC.	GAM		2,437	0%	8.6%	0.0%	45.1%	19.1%
GRIFOLS ORD CL A	PROB	17/05/2006	6,912	1%	27.1%	0.0%	30.7%	88.4%
INDITEX	IND		68,177	12%	20.2%	0.0%	27.5%	73.5%
INDRA SISTEMAS	IDR		1,822	0%	3.2%	0.0%	26.9%	11.8%
JAZZTEL	JAZ		3,287	1%	22.1%	0.0%	49.4%	44.7%
MEDIASET	TL5		4,009	1%	3.8%	0.0%	37.2%	10.3%
OBRASCON HUARTE LAIN	OHL		2,642	0%	21.8%	0.0%	36.9%	59.1%
REPSOL YPF	REP		25,385	4%	6.9%	0.0%	29.7%	23.1%
SACYR	SCYR		2,141	0%	4.6%	0.0%	49.1%	9.4%
TECNICAS REUNIDAS	TECN	21/06/2006	2,347	0%	16.8%	5.2%	36.1%	46.6%
VISCOFAN	VIS		2,023	0%	20.2%	0.0%	25.4%	79.7%
Utility								
ENAGAS	ENAG		6,095	1%	12.1%	5.5%	24.3%	49.9%
GAS NATURAL SDG	CTG		23,326	4%	7.1%	0.0%	27.9%	25.5%
IBERDROLA	IBE		35,762	6%	9.8%	0.0%	29.7%	33.1%
RED ELECTRICA CORPN.	REE		9,274	2%	17.9%	11.6%	24.5%	73.2%
TELEFONICA	TEF		55,773	10%	2.9%	0.0%	23.4%	12.2%
Transportation								
INTL.CONS.AIRL.GP.	IAG	24/01/2011	9,611	2%	15.3%	0.0%	35.0%	43.8%
Bank/Savings & Loan								
BANCO DE SABADELL	BSAB		9,407	2%	1.4%	0.0%	29.3%	4.9%
BANCO POPULAR ESPANOL	POP		10,186	2%	-7.7%	0.0%	36.6%	-20.9%
BANCO SANTANDER	SCH		91,241	16%	8.5%	0.0%	34.2%	24.9%
BANKIA	BKIA	20/07/2011	17,023	3%	-28.5%	-6.9%	141.1%	-20.2%
BANKINTER 'R'	BKT		6,037	1%	11.2%	0.0%	36.7%	30.7%
BBV.ARGENTARIA	BBVA		56,697	10%	5.1%	0.0%	34.0%	14.9%
CAIXABANK	CABK	10/10/2007	27,243	5%	6.9%	0.0%	32.8%	20.9%
Insurance								
MAPFRE	MAP		8,635	2%	9.4%	0.0%	34.5%	27.3%
Other Financial								
BOLSAS Y MERCADOS ESP	BOLS	14/07/2006	2,524	0%	4.9%	0.0%	30.7%	15.9%

* In Millons, ** Annualized return and volatility

Table 1

In order to overcome these drawbacks and with the goal of obtaining a statistically validated sparse partial correlation matrix that translates into a clearer PCSN, a 2-Step procedure is proposed. In the first step, I rely on the Graphical Lasso (GL) algorithm developed by Friedman, Hastie, and Tibshirani (2008). This approach maximizes the penalized log-likelihood of a multivariate normal distribution with respect to the precision matrix, Ω.

$$\Omega_{G-Lasso} = \arg\max log|\Omega| - tr(S\Omega) - \gamma\|\Omega\|_1 \qquad (3)$$

where S is the sample covariance matrix, tr is the trace operator and $\|\Omega\|_1$ is the L1-norm - the sum of the absolute values of the elements of Ω. The reader should note that the elimination of links in in GL is driven by the maximization of the likelihood function, thus overcoming the major shortcoming of TM.

The penalty or regularization parameter γ controls for the amount of shrinkage in the values of the components of Ω. When $\gamma = 0$, the estimation of Ω is just its maximum likelihood estimator, S^{-1}. When the amount of regularization increases, $\gamma > 0$, more parameters are pushed toward zero resulting in sparser solutions. Due to the particular form of the restriction in (3), exact zeros are found in the results of the algorithm. It is important to determine the value of the shrinking parameter in an optimal way. A tradeoff in determining γ exists since lower values of γ fit better to the data, at the cost of denser Ω. In the current setting γ is determined by 10-fold cross validation as it is proposed in Friedman, Hastie, and Tibshirani (2008).[25]

The statistical significance of the previous estimation is provided in the second step of the procedure by implementing Monte Carlo simulations as follows. Once $\Omega_{G-Lasso}$ is estimated, I move on to compute ρ in accordance to equation (1). Next, I check whether the elements of ρ are statistically different from zero for a pre-specified level of confidence α. To quantitatively determine the significance of each ρ_{ij}, a non-parametric kernel density of returns for each stock in the sample is adjusted.[26] Then, a sample of size 1.000 is independently drawn from each one of those densities. With this artificial and non-correlated sample of returns, a new partial covariance matrix is computed serving as a null hypothesis for the inference. I do this many times in order to obtain an empirical distribution for each ρ_{ij}. Finally, I calculate the percentiles for each of those distributions in accordance with a specified confidence level equal to α. When the original estimation of ρ_{ij} is larger than the percentile just mentioned, such ρ_{ij} is stated as statistically significant and retained as a link between node i and j, otherwise the connection between those nodes is discarded.

This second step attempts to eliminate from the network those partial correlations that are non-statistically different from zero. The null hypothesis to which to compare the estimated ρ_{ij} come from partial correlations calculated by randomly selected returns from the non-parametric

[25] The optimization is implemented through Coordinate Descent algorithm

[26] A Gaussian kernel with smoothing parameter equal to 0.2 is assumed. In non-tabulated analysis, this value was optimally selected by cross-validation using a pooled version of the daily return's dataset.

marginal distributions of stocks i and j. Therefore, zero partial correlation assumption is not intended to represent the real return process but only to take the place of the null hypotheses in the statistical tests.

This 2-step estimation algorithm posits several benefits compared to more traditional applications. Among them it worth mentioning that it is a totally data-driven procedure without any a-priori topological constraints. Moreover, since it is rooted on the optimization of the likelihood function, ad-hoc parameters (like thresholds) are not imposed to the algorithm except for α. In a closely related paper, Kenett et al. (2010) estimates the so-called Partial Correlation Planar Graph and Partial Correlation Threshold Network for the US market. As commented previously, the former imposes severe restriction on the structure while the latter is computed assuming a threshold selected without empirical justification. The 2-step estimation algorithm overcomes these drawbacks while keeping its tractability. In what follows, the PCSNs are constructed in accordance with this methodology. Appendix B provides evidence that supports its benefits by proving the result of its implementation with an artificially created dataset.

4. Empirical Results

The subsequent analysis is divided in two parts. The first one accounts for a static study by considering only the 250 most recent trading days (approximately one year). The aim is to describe the current state of the Spanish PCSN. The second part considers a dynamic perspective of the PCSN and therefore larger time series are required. In order to fulfill this data requirement, those firms whose inception date falls after the beginning of the dataset are excluded from the analysis. The parameters for the 2-step estimation algorithm are set as follows: 500 repetitions in order to obtain the an empirical distribution for each ρ_{ij}, a significance level of 1% and 10 fold Cross-Validation.

4.1 Static analysis

The results from the estimation reveal an optimal regularization parameter γ equal to 0.042. Figure 1 plots the non-parametric distribution and key descriptive statistics for the non-zero partial correlations for this optimal γ. In addition, the distribution of direct correlations estimated by means of optimal shrinkage (Ledoit and Wolf, 2004) is included for comparison.

The direct correlation is a symmetric bell-shaped curve that resembles a normal density function. Relative to the non-zero partial correlation distribution, it shows fatter tails with a significantly

lower mean value (0.412 vs 0.122).[27] Such a difference in mean's levels might be partially explained by the shrinkage-toward-zero effect generated by GL. Note that the direct correlation distribution lies only on the positive quadrant while the partial correlation distribution shows negative values as well. The full partial correlation matrix and the direct correlation matrix are provided in appendix C. From the full matrix of partial correlation, it worth highlighting the extremely large value assumed by some of its components related to the banking and utilities sectors (for the pair (BBVA, SCH) is 0.6. for (BSAB, POP) is 0.3 and (ENAG, CTG) is 0.3).

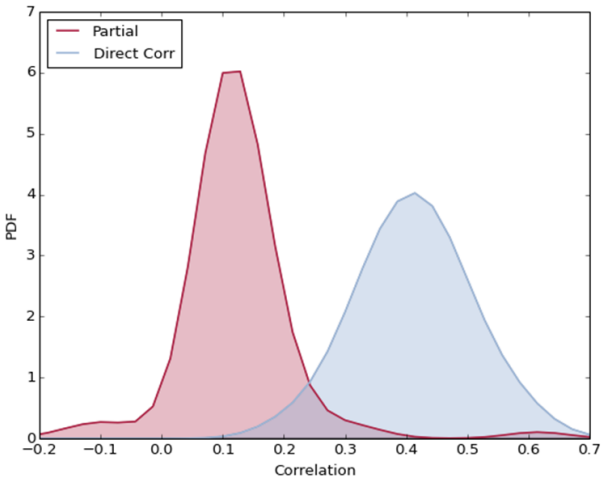

	Non Zero Partial Corr	Direct Corr
Size		
Count	77	595
Position		
Mean	0.122	0.412
Median	0.111	0.413
Dispersion		
Std	0.084	0.089
Min	-0.141	0.165
5%	0.076	0.265
95%	0.211	0.566
Max	0.615	0.774
Shape		
Skewness	2.16	0.07
Kurtosis	15.08	0.26

Figure 1: Non-parametric density of partial and direct correlation

Figure 2 shows the density d and the size of the largest connected component S of networks corresponding to different levels of the regularization parameter γ. There are three aspects that deserve some attention. First, S remains positive even for large values of γ evidencing an extremely persistent group of stocks intensively interrelated. This cluster of stocks belongs to the banking sector as it is clearly seen in figure 3 below. Since S is a proportion, it cannot be negative, however, it could be zero representing a situation of a totally disconnected structure. Second, there is a non-linear and decreasing relationship between the γ and d. More interestingly, the optimal γ (vertical red line) roughly coincides with a turning point of d at around 0.15 evidencing a sharp transition between regimes with different slopes. Finally, note that PCSN never becomes connected unless γ is set to zero. Therefore, there exists a group of companies that tends to be disconnected from the structure.

[27] A proper comparison between the means of the direct and partial correlation implies a degree of caution given the different nature of the estimation methodologies used in each case.

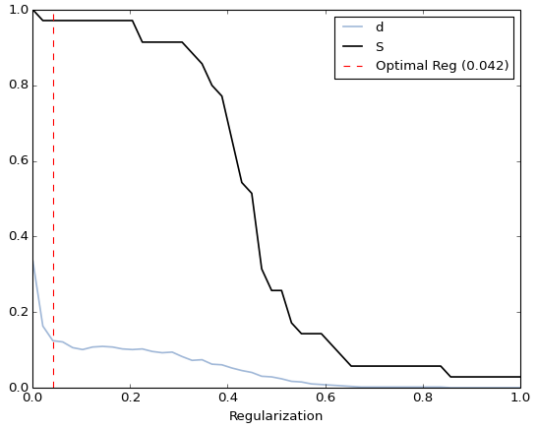

Figure 2: Network's measures for different levels of regularization

The PCSN's for selected values of γ are depicted in figure 3 where the first one corresponds to the optimal PCSN, defined as the one associated with the optimal γ. The size of the nodes/stocks in the networks accounts for their (rescaled) market value for the last day in the sample. Their colors account for different industries (see figure caption for more details).

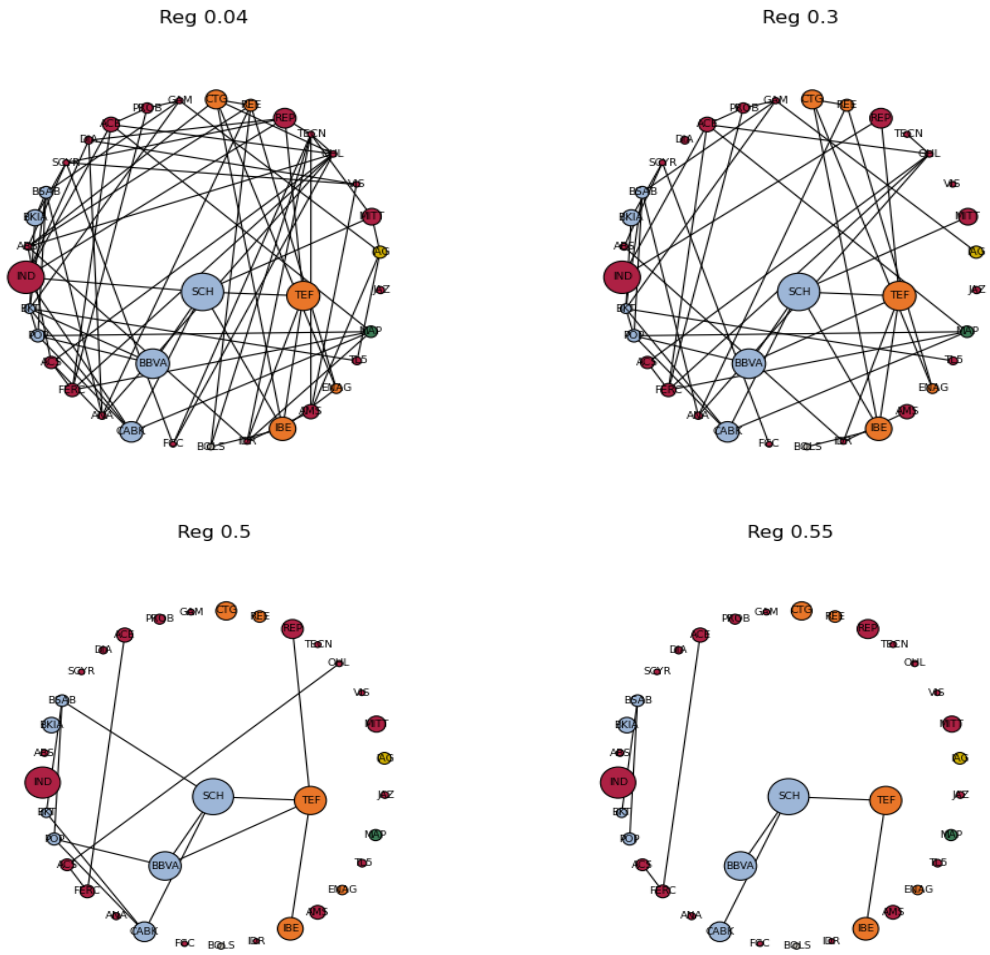

Figure 3: Networks for selected levels of regularization. The colors of the nodes correspond to sectors: Industrial (Red), Bank/Savings & Loan (Blue), Utility (Orange), Insurance (Green), Other Financial (Grey) and Transportation (Yellow). The size of each node corresponds to its (rescaled) market value at Sep30, 2014.

The importance of the banking sector is noticeable in figure 3. An artificial increase in γ eliminates less significant partial correlations. However, the cluster of nodes belonging to such sectors remains connected (e.g. SCH, BBVA, CABK, BSAB, POP) giving us some insights about their systemic importance, a results that is consistent with the findings in Kenett et al. (2010). Following the same reasoning, stocks from the utilities sector also assume prominent positions in the structure (see the cases of TEL and IBE). On the other hand, the more peripheral role of the industrial stocks stems from their earlier disconnection from the network, as long as γ increases. This happens in spite of the large market capitalization shown by some of them (e.g. Inditex). A plausible explanation comes from the logic behind the functioning of the banking sector. Its business is based on the interaction with other companies by providing financing and thus can take root in almost any segment of the economy. The next subsection is devoted to deeper analysis of the centrality of different economic sectors.

Network's measures for different levels of regularization

	Networks for different regularization*				
	Optimal	0.30	0.5	0.55	Random Network
Basics					
Nodes	35	35	35	35	35
Links	77	48	15	8	76.9
Density	0.13	0.08	0.03	0.01	0.13
Mean Degree	4.40	2.74	0.86	0.46	4.40
Distance					
Diameter	5 (0.21)	7	4	3	4.989
Mean Distance	2.50 (0.43)	3.41	2.00	1.80	2.49
Components					
Largest Comp	0.97 (0.06)	0.91	0.26	0.14	0.99
Isolates	0.03 (0.05)	0.09	0.63	0.69	0.01
Patterns of Connectivity					
Transitivity	0.21 (0.00)	0.25	0.11	0.00	0.13
Assortativity	-0.17 (0.15)	-0.07	0.10	-0.56	-0.06

* Measures corresponding to the weigthed version of the PCSN
Specific definitions and unit of measures for each network statistics are provided in Appendix H
In parenthesis the p-values of the measures relative to the random counterpart
Table 2

Key network measures are reported in table 2. The first four columns account for the networks from figure 3. The last column reports the average of the same set of measures over 1.000 realizations of networks made at random (Erdös-Rényi network) matched to the density of the optimal one. The evidence supports significant differences between the optimal Spanish PCSN

and its random counterpart in several dimensions. Despite the fact that the largest connected component is barely smaller for the Spanish PCSN (97% vs 99%), such difference is statistically significant at conventional levels. As a consequence, its disconnected component is significantly larger than a random arrangement (3% vs 1%). This feature confers a sort of protection since the cluster of connected nodes is reduced preventing broader propagation of an initial shock. The large and significant value of transitivity for the Spanish PCSN relative to a random network (21% vs 13%) constitutes another potential source of strength. This is the case since conditioning on the network density, producing a large number of triangles, prevents local shocks becoming global by containing the former inside a group of tightly interrelated stock. Finally, it is worth mentioning that the Spanish PCSN seems to be disassortative (-0.17); highly connected stocks tend to be linked to poorly connected ones. This could be interpreted as a sign of weakness since any negative shock in poorly connected stock might be transmitted to rest of the market throughout its path toward the hub of the network. However, this effect is not statistically significant at conventional levels.

4.1.1 Systemic Stocks in the Spanish Market

The systemic importance of a firm assesses its potential to greatly affect the performance of the entire market. In what follows I measure the systemic importance of stocks by means of the eigenvector centralities, see appendix H. Therefore, those central stocks in the PCSN rank high as systemic firms and as a consequence they could potentially cause large market movements.

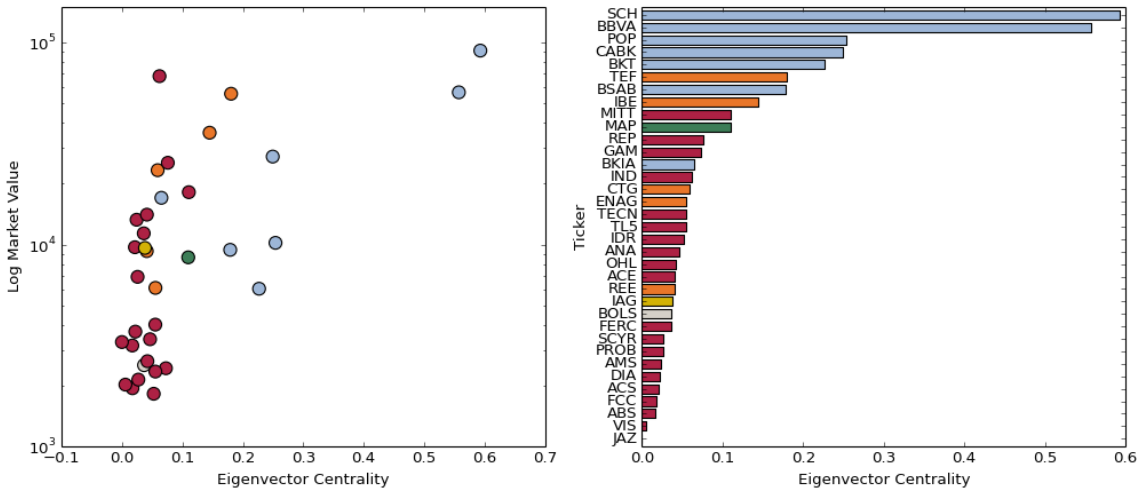

Figure 4: Relationship between centrality, market capitalization and economic sectors. The colors of the nodes correspond to sectors: Industrial (Red), Bank/Savings & Loan (Blue), Utility (Orange), Insurance (Green), Other Financial (Grey) and Transportation

The left-hand panel of figure 4 shows a scatter plot between a firm's centrality and its market capitalization (logarithmic scale) for the last day in the sample. The colors of the dots correspond

to different industrial sectors (see the legend's figure for more details). The right-hand panel of the same figure depicts the centrality of each stock with their corresponding tickers (see table 1).

From figure 4, the positive relationship between market capitalization and stock centrality is evident. Additionally, note that the banking sector is by far the most systemic one. It is particular interesting to note the case of the two most central firms in the market, Banco Santander and BBVA, showing a clear distinct pattern from the rest. This evidence is consistent with the findings in Kenett et al. (2010) in terms of the dominating role played by the financial stocks. Appendix D provides the full list of firms with their corresponding centrality score.

In order to investigate deeply the relationship between market capitalization and centrality, the cross-sectional regression (4) is estimated by OLS with the aim of separating the market capitalization effect from effects of economic sectors. In this expression, $Centrality_i$ and MV_i corresponds to the eigenvector centrality and market value of firm i, respectively. D_j represents dummy variables for economic sectors where Ind={Insurance (Ins), Utility (Ut), Industrial (Ind), Transportation (Tra), Other Financial (OF)}. Note that significant and negative (positive) coefficients indicate lower (higher) centrality relative to the banking sector.

$$Centrality_i = \beta_0 + \beta_1 \ln(MV_i) + \sum_{j \in Ind} D_j + e_i \qquad (4)$$

Table 3 reports the results of the estimation. A positive and statistically significant coefficient for β_1 is found evidencing that firms with large market capitalization tends to present high centrality scores which is consistent with the left-hand panel of figure 4. Further, the coefficients for the economic sector dummy variables are all negative and statistically significant at conventional levels. This indicates that large centrality score of the banking sector is in part explained by its high market capitalization but it is also inherent to its business.

Regression of centrality on market capitalization and economic sectors

β_0	β_1	β_{Ins}	β_{Ut}	β_{Ind}	β_{Tra}	β_{OF}	R^2 Adj	F (pvalue)
-0.156	0.047	-0.156	-0.205	-0.203	-0.248	-0.180	0.670	0.000
(-1.086)	(3.305)***	(-1.881)*	(-4.569)***	(-5.286)***	(-2.997)***	(-2.062)**		

Significance * p<0.10,** p<0.05,*** p<0.01

Table 3

4.1.2 International evidence

In order to compare the Spanish PCSN with other structures, the same methodology is applied to the set of stocks constituting the market indexes FTSE-100, CAC-40, DAX-30 and FTSE-MIB as representatives of the UK, French, German and Italian market, respectively. I rely on

Datastream to construct similar datasets as for the Spanish case covering the exact same time period. In table 4 a comparison between the network topologies of theses stock markets is provided.

Network's measures - International comparison

	Spain	UK	France	Germany	Italy
Basics					
Nodes	35	101	40	30	37
Links	77	136	70	58	66
Density	0.13	0.03	0.09	0.13	0.10
Mean Degree	4.40	2.69	3.50	3.87	3.57
Distance					
Diameter	5	11	6	7	7
Mean Distance	2.50	5.00	2.84	2.86	3.02
Components					
Largest Comp	0.97	0.82	0.93	1.00	0.97
Isolates	0.03	0.03	0.03	0.00	0.03
Patterns of Connectivity					
Transitivity	0.21	0.19	0.09	0.21	0.15
Assortativity	-0.17	0.04	-0.07	0.07	0.12

* Measures corresponding to the weigthed version of the PCSN
Specific definitions and unit of measures for each network statistics are provided in Appendix H
Table 4

Notice that each of the network presents a sizable largest connected component and also a high value of transitivity. The largest connected component of the UK network is somehow smaller 82% which could be interpreted as a source of strength as it was commented before. In terms of connectivity, the Spanish and German structured show the largest density (13%) while the UK network is the less connected one (3%). This feature is also evident in the mean distance where it is 2.50 for the case of Spanish PCSN while it is 5.00 for the British network. Note, moreover, that the only market showing a strong disassortative arrangement is Spain (-0.17) which could comprise a source of weakness, as was commented before.

The association between market capitalization and centrality is quantified in table 5. This table reports the estimation of equation 4 for each of the markets under analysis. The coefficient β_1 is positive and significant for all PCSN except the French case which is non-statistically significant. In general terms, the sectorial dummies tend to be negative and statistically significant for French, German and Italian PCSN as they are for the Spanish case evidencing the prominent role of the banking system. However, a distinctive feature in the French PCSN is that its Insurance sector is on average more central than the Banking sector in accordance to the positive and significant coefficient β_{Ins}. This result should be taken with caution since there is only one stock representing that sector. Interestingly, the UK market behaves in a totally different way since

none of the sectorial dummy variables are statistically different from zero. Therefore, for the UK market, members of the banking sector do not necessarily take central positions in the network. This result could be driven by the low connectivity level found in the UK PCSN (3%).

Regression of centrality on market capitalization and economic sectors - International Comparison

	Spain	UK	France	Germany	Italy
β0	-0.156	-0.156	0.153	-0.247	-0.038
	(-1.086)	(-1.755)*	(1.307)	(-1.538)	(-0.417)
β1	0.047	0.020	0.000	0.048	0.021
	(3.305)***	(1.836)*	(0.005)	(2.516)**	(1.682)*
βIns	-0.156	-0.025	0.181	-0.022	-0.050
	(-1.881)*	(-0.814)	(3.011)***	(-0.321)	(-1.003)
βUt	-0.205	-0.040	-0.133	0.066	-0.080
	(-4.569)***	(-1.045)	(-3.099)***	(1.141)	(-2.224)**
βInd	-0.203	0.006	-0.079	-0.110	-0.107
	(-5.286)***	(0.286)	(-3.162)***	(-2.837)***	(-4.469)***
βTra	-0.248	-0.019		-0.124	
	(-2.997)***	(-0.385)		(-2.151)**	
βOF	-0.180	-0.018	-0.101		0.028
	(-2.062)**	(-0.551)	(-1.825)*		(0.628)
R^2 Adj	0.670	0.007	0.743	0.384	0.702
F (pvalue)	0.000	0.354	0.000	0.004	0.000

Significance * p<0.10,** p<0.05,*** p<0.01

Table 5

In order to facilitate the comparison, figure 5 plots the mean eigenvector centrality at sector level for each of the countries in the sample. I normalize the eigenvector centralities by requiring that the sum of its components equals the number of stock in each market, thus accounting for different network sizes. The banking sector assumes a critical role in Spain, France and Italy.[28] For the German case, companies from the utilities sector show on average the highest central position. Consistent with the evidence in table 5, the UK network presents a distinctive behavior. In particular, note how the centrality is distributed only inside the industrial sector. A plausible explanation might be found in term of the degree of market internationalization[29;] however, this is an empirical question not addressed in the manuscript. Appendix F provides descriptive tables

[28] In this calculation, the increased centrality of the Insurance sector in France does not capture the evidence presented in table 6. Probably, this is due to the fact that this sector is represented by only one firm.

[29] It might be the case that constituents of the UK market index are more partially correlated with firms not included that index.

of centrality and market capitalization for each country in the study. These structural differences among the PCSN could shed some light on the differential response of European stock markets when facing the same shock. Further analysis is required in this regards.

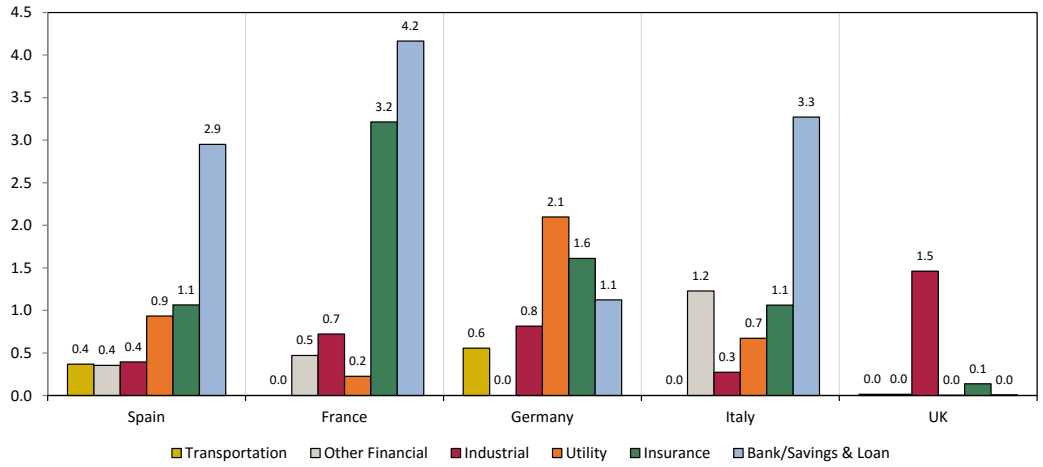

Figure 5: Centrality by economic sectors – International comparison

4.2 Dynamic analysis

This section studies the dynamical properties of the Spanish PCSN and discusses its stability through time by relying on a moving window approach. The 2-step estimation algorithm (see section 3) is implemented upon moving windows of returns of 250 trading days of length. Since a one-day displacement step is considered, 2.336 PCSN are estimated with their corresponding network measures and firm's centrality scores. Given that large time series of data are required in the section, those firms with inception dates later than Nov 1, 2004 (10 firms) are discarded for this analysis. I also define (negative) market events when the return of market index is lower than three standard deviations computed for the entire sample period. The dates for such market events are plotted in the following figures as vertical black lines.

The time series of three selected network measures, Density, Mean Distance and Transitivity, are depicted in figure 6. Light-red lines accounts for the exact quantities while the dark-red line corresponds to the 60-days centered moving average. Visual inspection does not allow us to conclude about any clear pattern in the data regarding the performance of those network measures around market events. Nevertheless, section 5 provides rigorous statistical assessment in this respect.

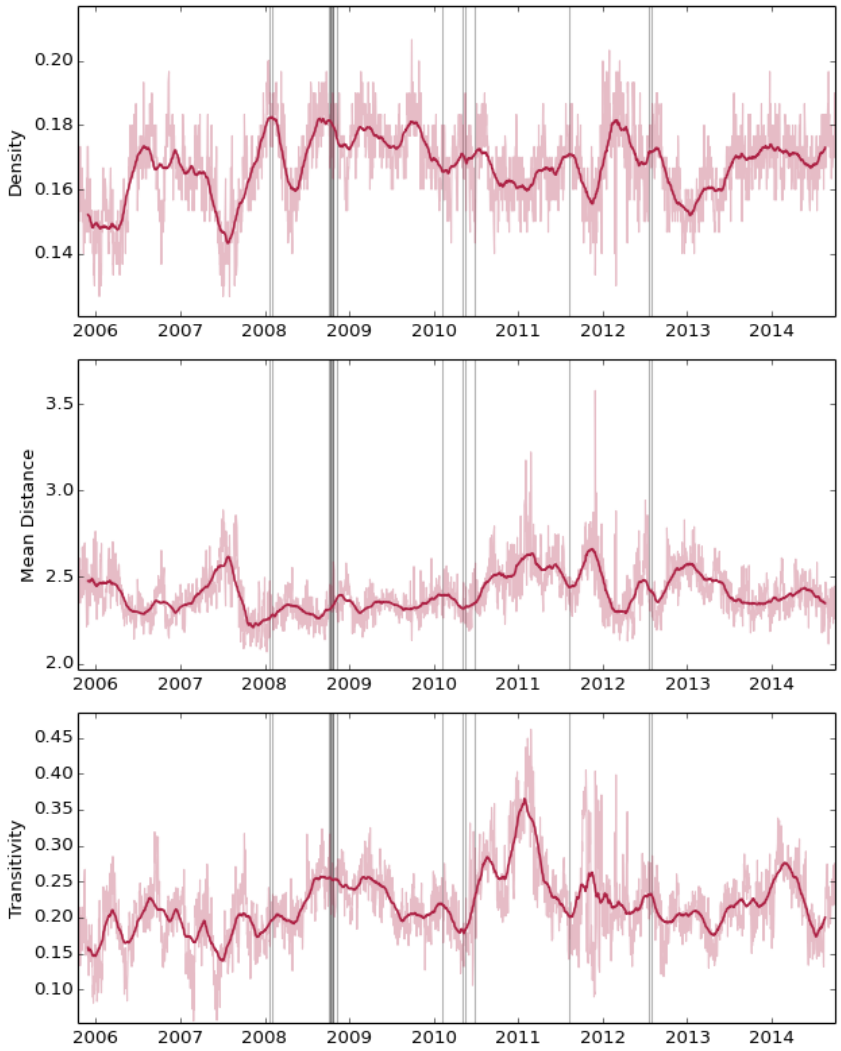

Figure 6: Time series of selected network's measures

Despites the comments already mentioned about figure 6, a quite clear pattern arises when the centrality of the banking industry (mean of the centrality of the firms belonging to this sector) is under analysis. Figure 7 plots the time series of the mean centrality of the banking sector in light-red and its 60-days center moving average in dark-red. Note that negative market shocks tend to occur when the centrality of the banking sectors presents a downward slope. In other words, before a market event, the centrality of the banking sectors reaches a peak and starts to decline afterwards. In fact, there is just one episode in mid-2010 for which this observation does not come true. As it was mentioned, section 5 investigates this phenomenon further.

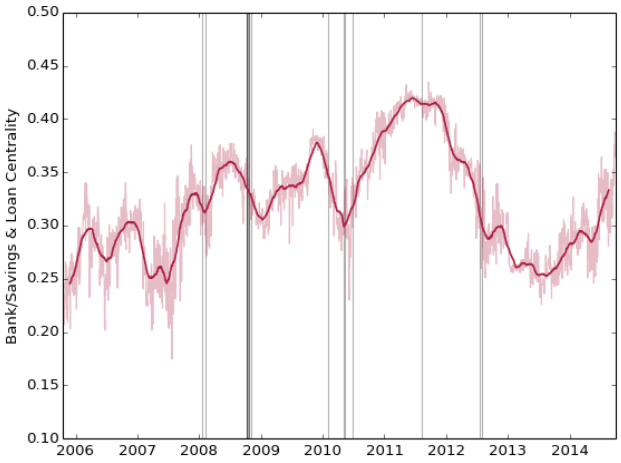

Figure 7: Banking sector centrality through time

A final comment regards to the stability of the PCSN through time. Since each of the PCSN is composed of exactly the same set of stocks/nodes, the only elements that change from period t-1 to t are the links in subsequent networks. Therefore, I will measure the stability of the Spanish PCSN as the proportion of significat links in period t-1 that remains significat in t. To be more concrete, let us define the set of PCSN indexed by time as $\Psi = \{\varphi_1^u, \varphi_2^u, \dots, \varphi_{2337}^u\}$ and their corresponding set of links as $\Phi = \{\varrho_1, \varrho_2, \dots, \varrho_{2337}\}$. The intersection network in period t, $\tilde{\varphi}_t^u$, is built upon the intersection of two subsequent set of links as $\tilde{\varrho}_t = \varrho_{t-1} \cap \varrho_t$. Then the stability ratio in period t SR_t is given by formula (5) and its time series is plotted in figure 8.

$$SR_t = \frac{\#\ of\ elements\ in\ \tilde{\varrho}_t}{\#\ of\ elements\ in\ \varrho_{t-1}} \qquad (5)$$

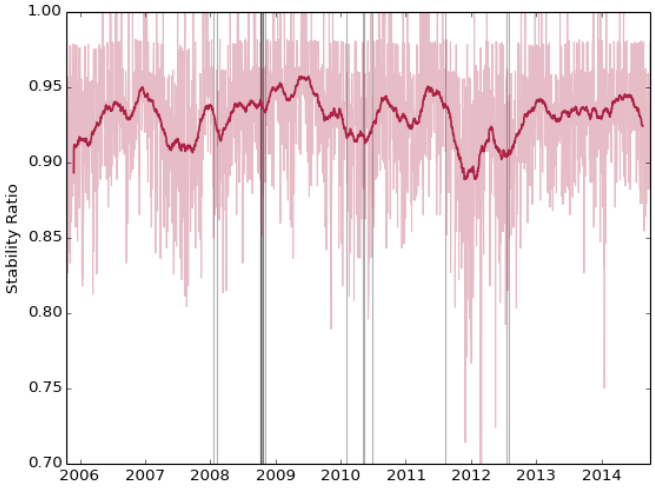

Figure 8: Stability ratio through time

As before, the light-red lines correspond to the exact stability ratio in period t while the dark-red line accounts for its 60-days centered moving average. The mean and standard deviation of the centered SR is 93% and 4%, respectively. The fact that more than 90% of the links remains significat from subsequent networks confers a sort of structural stability through time to the Spanish PCSN. Note also that the minimum values of SR are reached in the periods following the inclusion of Bankia as a new constituent of the IBEX-35, say after Ago-2011. In fact, the centered SR shows a negative trend starting in Ago-2011 that reverts by the end of that year (values of this variable below 90% corresponds to the period Oct-2011 until Feb-2012). In this regard it could be said that the market required approximately 6 months to digest such network reconfiguration. The time series of the stability ratio does not show any other observable patters in relation to others firms' entries or exists. However, a systematic study in this regards is an interesting research line to pursue.

5. Network measures as leading indicators of market instability

The extent to which a set of network measures might be used as leading indicators of market distress is investigated in this section. The behavior of three network-based measures, Density, Mean Distance and Transitivity, around negative market events is depicted in figure 9.

In this figure market events are aligned at day zero and 100 trading days before and after such an event are considered. This alignment is plotted in the x-axis. The y-axis shows the mean of each network-based measure in dark-red, the mean of its corresponding 60-days length moving average in blue and the region comprising +/- one standard deviation away from mean in light-red. In order to account for different levels of the network measure when a market event takes place, I normalize such measures to 1 in such dates.

From figure 9 there is no identifiable pattern for the transitivity. However, this is not the case for the density and the mean distance. Considering the network density, let us note that it tends to be above its mean value at the moment of the negative shock for at least 30 trading days before such event. For the mean distance, the reverse is true since about 30 trading days before a large and negative market movement this measure tends to be below its mean value at the moment of the negative shock. Therefore, the Spanish PCSN presents particular features that seem to anticipate market distress episodes. In particular it could be said that just before a negative event, the stock network becomes densely connected while shortening its mean distance. This behavior is expected since these two variables show a strong negative correlation (-0.72), see appendix E.

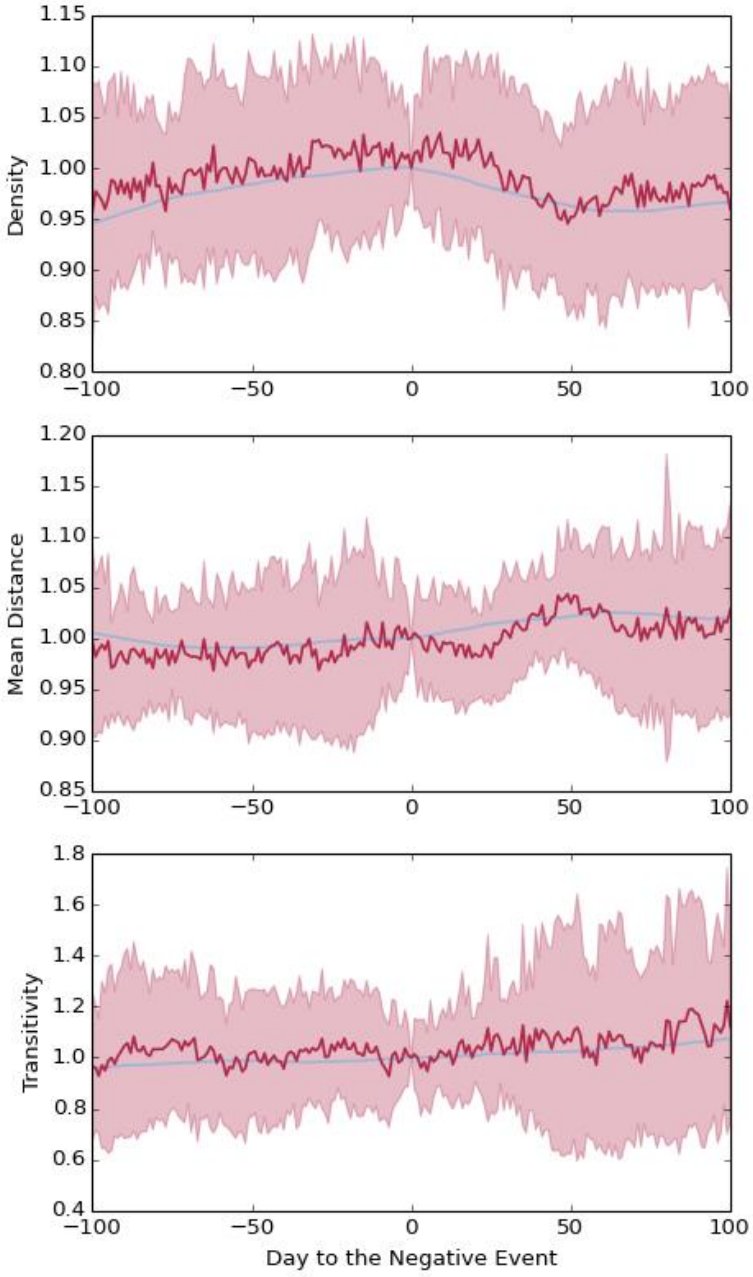

Figure 9: Behavior of network's measures around a market event

In order to better understand this phenomenon two alternative and complementary approaches are pursued. Subsection 6.1 relies on Probit models while subsection 6.2 estimates ARCH models. Both of them use lagged network measures as explanatory variables.

5.1 A Probit model for negative market movement with network measures as independent variables

I estimate a Probit model to quantitatively assess the extent to which lagged network-based measures can predict large and negative market movements. The dependent variable is dichotomous assuming value one if the market suffers from a negative return larger than three

standard deviations (computed from the entire dataset) and zero otherwise. As explanatory variables I include the two of the network measures depicted in figure 9, Density and Transitivity.[30] Additionally, the centrality of the banking sector is also introduced as an independent variable. Since predictability is at the center of the analysis, I consider lags at 10 and 30 trading days in setting the explanatory variables. Given that the set of regressors shows a significant level of autocorrelation (see appendix E), standard errors tend to be downward biased leading to incorrect t-statistics. In order to account for the correction in the standard errors due to heteroskedasticity and autocorrelation, I implement bootstrap methods as suggested by Berg and Coke (2004).

Results of Probit model's estimations

Dependent Variable Prob that Ibex Ret <-3 Std

Density	***Model 1***	***Model 2***	***Model 3***
Lag 10	21.23	18.32	18.81
	(2.2)**	(1.77)*	(1.83)*
Lag 30	21.94	25.14	24.93
	(2.37)**	(2.27)**	(2.28)**
Banks Centrality			
Lag 10		-6.52	-6.17
		(-1.22)	(-1.12)
Lag 30		10.27	10.00
		(2.02)**	(1.85)*
Transitivity			
Lag 10			-1.22
			(-0.53)
Lag 30			0.57
			(0.22)
Likelihood Ratio Index	0.099	0.127	0.129
LLR p-value	0.000	0.000	0.000

SE estimated by Bootstrapping. Significance * p<0.10,** p<0.05,*** p<0.01
Specific definitions and unit of measures for each network statistics are provided in Appendix H
Table 6

Table 6 reports the results of the estimation of three different models that progressively include the independent variables. Model 1 presents positive and significant effects of network density on the probability of a large and negative market movement. Therefore, a dense PCSN shows a higher probability to suffer a large negative return, an observation consistent with the evidence presented in figure 9. The inclusion of the banking centrality as an additional independent variable in model 2 also shows a positive and significant effect at lag 30 while retaining the

[30] I discard the mean distance as an additional independent variable given the high negative correlation between this variable and density (see appendix E).

significance of network density. Therefore, a network more densely connected in which the banking sector assumes a central position is consistent with an increased probability for a large and negative shock in the market. Finally, in model 3, all of the considered network measures are included in the estimation. However, transitivity does not show any significant coefficient for any of its lags, an observation which is also consistent with figure 9. In any case, the conclusions regarding the signs of the coefficients and their significance for the case of density and banks centrality remain valid. The rest of the possible Probit models arising from different combination of independent variables are presented in appendix G where the abovementioned conclusions remain valid.

In summary it could be said that there is some evidence that network-based measures are a leading indicator of large market distress events. In particular, the statistical results show that the probability for a large negative movement increases when Spanish PCSN becomes more densely connected. In cases where the banking sector assumes more central position in the structure, the effect is reinforced by increasing further the probability of this type of episodes. In Kenett et al. (2010), the authors find a prominent role of financial firms affecting the correlation structure of the market. The results from this section contribute to this line by presenting evidence showing how the dominant position of financial stocks is related to the instability of the market.

5.2 ARCH models for the Spanish Market with network measures as independent variables

The heteroskedasticity of the return process is a well-documented phenomenon in the econometric literature, (Engle, 1982 and Hamilton, 1994). Following Bollerslev (1987) and Hamilton (1994), I assume that return process is described by an ARCH model specified in equations (6) to (8) where the error term η_t comes from a t-student distribution with ν degrees of freedom. The novelty of this specification arises from the inclusion in the equation of the conditional variance σ_t^2 (expression 8) lagged network measures as explanatory variables. As in the previous subsection, the set of lagged network measures considered for the experiment is N={Density, Transitivity, Centrality of the Banking Sector}.

$$r_t = c_r + \varepsilon_t \tag{6}$$

$$\varepsilon_t = \sigma_t \eta_t \tag{7}$$

$$\sigma_t^2 = c_\sigma + \sum_{i}^{q} \alpha_i \varepsilon_{t-i}^2 + \sum_{n \in N} \sum_{j \in \{10,30\}} \alpha_j^n \, n_{t-j} \tag{8}$$

The model (6)-to-(8) is estimated by maximizing the log likelihood where ν is considered as an additional parameter. The order of the process is set to 5 since in non-tabulated results, the coefficients α_i beyond that period are not statistically significant. Table 7 shows the estimated parameter for three models with the sequential inclusion of Density, Centrality of the Banking Sector and Transitivity as independent variables.

Results of ARCH model's estimations

Density	***Model 1***	***Model 2***	***Model 3***
Lag 10	14.67	9.64	12.83
	(4.12)***	(2.76)***	(3.21)***
Lag 30	2.91	-1.21	-0.85
	(0.71)	(-0.29)	(-0.22)
Banks Centrality			
Lag 10		0.40	1.24
		(0.33)	(0.89)
Lag 30		3.73	3.82
		(3.12)***	(2.92)***
Transitivity			
Lag 10			0.23
			(0.23)
Lag 30			-2.33
			(-2.51)**
Squared Residuals			
Lag 1	0.08	0.07	0.07
	(2.77)***	(2.51)**	(2.45)**
Lag 2	0.14	0.13	0.12
	(4.17)***	(3.94)***	(3.91)***
Lag 3	0.16	0.15	0.14
	(4.82)***	(4.63)***	(4.55)***
Lag 4	0.21	0.19	0.18
	(5.77)***	(5.6)***	(5.38)***
Lag 5	0.16	0.16	0.15
	(4.51)***	(4.51)***	(4.51)***
Others Parameter			
T-Student df	6.33	6.64	6.69
	(6.51)***	(6.39)***	(6.28)***
Akaike criterion	3.427	3.422	3.421
Schwarz criterion	3.452	3.452	3.456
Log Likelihood	- 3,893.7	- 3,885.5	- 3,882.7

Significance * p<0.10,** p<0.05,*** p<0.01

Specific definitions and unit of measures for each network statistics are provided in Appendix H

Table 7

Model 1 considers the lags of density as the only network-based independent variables. In this model, lag 10 shows a positive and statistically significant coefficient which means that denser networks increased the conditional market volatility. In model 2, the centrality of the banking sector is considered as an additional independent variable. A positive and statistically significant coefficient is found for its lag 30. Moreover, the sign and significance of the density at lag 10 remains. The comparison between model 1 and 2 from table 6 with those models from table 7 confers some robustness on the results. Therefore, denser networks where the centrality of the banking sector is high show larger probabilities of a strong negative movement. This could be explained by their positive effect of those variables on the conditional market volatility.

Model 3 in table 7 presents the major difference its equivalent in table 6. In the former table, the transitivity level at lag 30 shows a negative and significant effect on market variance. As discussed in Newman and Park (2003), large transitivity is consistent with networks arranged in communities. Then, an increase in the number of triangles in the network, controlling by its density, leads to an internal organization of the structure characterized by groups of stocks tightly interrelated. This would undermine the possibility of macro effect as a consequence of shocks at micro level and thus reducing the conditional market variance.

The rest of the possible ARCH models considering different combination of independent variables are presented in appendix G. The abovementioned conclusions remain valid except for the case when transitivity enters as the only independent variables showing a positive coefficient.

6. Conclusion and Future Research Lines

Network theory as a general analytic framework has been considered extremely useful in several branches of sciences. Recently, the financial research community has started to adopt it in order to get new and valuable insights in the context of stock markets. The current paper proposes a 2-step algorithm to estimate the Spanish Partial Correlated Stock Network. This algorithm is designed to overcome or at least to attenuate the shortcomings of standard techniques. The estimated network is formed by the constituents of IBEX-35 as nodes and statistically significant partial correlations as links connecting pairs of them. Once the network is in place, different network-based measures are computed.

Three major results come from the empirical study. First, consistent with previous finding in the literature, the banking sector assumes a central position in the network and thus could severely affect the performance of the market. Second, the investigated network is found to be quite

stable over time and presents properties that are inconsistent with a random arrangement. It is worth mentioning that the largest connected component is smaller, and the transitivity level is larger in comparison with those features coming from Erdös-Rényi networks. International comparability is also addressed by identifying common traits between the PCSN from Spain, UK, France, Germany and Italy. All of such networks present sizable values for the largest connected component and transitivity. The central positions occupied by different economic sectors in those structures reveal a distinctive organization of such networks which prevents simple comparisons. Finally, there is also evidence that the current state of the Spanish PCSN, captured by key network measures, could be used as leading indicators of market distress. Therefore, including a set of network-based measures as part of the early-warning tool box for market regulators seems to be a suitable choice in order to properly assess systemic risk.

Two main research lines are left for future studies. The first one consists of an in-depth analysis of the similarities and differences between the largest stock markets around the world based on this unified framework. Such methodology could shed some light on the heterogeneous performances of different countries across the recent financial crisis. Another promising research line relates to the consideration of a directed stock network instead of the undirected one which is analyzed in the current paper. The possibility of including directed links in the structure would allow us to enrich the framework and to complement the conclusions already provided in this paper.

References

Barigozzi, M., and C. Brownlees, 2014, Nets: Network Estimation for Time Series, SSRN - Working Paper, 1–43.

Berg, A., and R. N. Coke, 2004, Autocorrelation-Corrected Standard Errors in Panel Probits: An Application to Currency Crisis Prediction, IMF Working Papers 4, 1–18.

Billio, M., M. Getmansky, A. W. Lo, and L. Pelizzon, 2012, Econometric measures of connectedness and systemic risk in the finance and insurance sectors, Journal of Financial Economics 104, 535–559.

Bollerslev, T., 1987, A Conditionally Heteroskedastic Time Series Model for Speculative Prices and Rates of Return, The Review of Economics and Statistics 3, 542–547.

Bonanno, G., F. Lillo, and R.N. Mantegna, 2001, High-frequency cross-correlation in a set of stocks, Quantitative Finance 1, 96–104.

Brownlees, C., E. Nualart, and Y. Sun, 2014, Realized Networks, SSRN - Working Paper, 1–63.

Diebold, F. X., and K. Yılmaz, 2014, On the network topology of variance decompositions: Measuring the connectedness of financial firms, Journal of Econometrics 182, 119–134.

Engle, R., 1982, Autoregressive conditional heteroscedasticity with estimates of the variance of United Kingdom inflation, Econometrica 50, 987–1006.

Friedman, J., T. Hastie, and R. Tibshirani, 2008, Sparse inverse covariance estimation with the graphical lasso., Biostatistics (Oxford, England) 9, 432–41.

Garas, A., and P. Argyrakis, 2007, Correlation study of the Athens Stock Exchange, Physica A: Statistical Mechanics and its Applications 380, 399–410.

Hamilton, J. D., 1994, Time Series Analysis (Princeton University Press).

Hamilton, J. D., 1994, Autoregressive conditional heteroskedasticity and changes in regime, Journal of Econometrics 64, 307–333.

Hautsch, N., J. Schaumburg, and M. Schienle, 2014, Financial Network Systemic Risk Contributions, Review of Finance.

Huang, W. Q., X. T. Zhuang, and S. Yao, 2009, A network analysis of the Chinese stock market, Physica A: Statistical Mechanics and its Applications 388, 2956–2964.

Jackson, M. O., 2014, Networks in the Understanding of Economic Behaviors, Journal of Economic Perspectives, 1–23.

Jung, W., S. Chae, J. S. Yang, and H. Moon, 2006, Characteristics of the Korean stock market correlations, Physica A: Statistical Mechanics and its Applications 361, 263–271.

Kenett, D. Y., M. Tumminello, A. Madi, G. Gur-Gershgoren, R. N. Mantegna, and E. Ben-Jacob, 2010, Dominating clasp of the financial sector revealed by partial correlation analysis of the stock market., PloS one 5, e15032.

Ledoit, O., and M. Wolf, 2004, Honey, I Shrunk the Sample Covariance Matrix, The Journal of Portfolio Management 30, 110–119.

Mantegna, R. N., 1999, Hierarchical structure in financial markets, The European Physical Journal B - Condensed Matter 11, 193–197.

Newman, M. E. J., 2003, The structure and function of complex networks, SIAM review 45, 167–256.

Newman, M. E. J., and J. Park, 2003, Why social networks are different from other types of networks, Physical Review E 68.

Onnela, J. P., A. Chakraborti, K. Kaski, J. Kertész, and A. Kanto, 2003, Asset trees and asset graphs in financial markets, Physica Scripta, 48–54.

Onnela, J. P., A. Chakraborti, K. Kaski, J. Kertész, and A. Kanto, 2003, Dynamics of market correlations: Taxonomy and portfolio analysis, Physical Review E 68, 056110.

Stevens, G., 1998, On the Inverse of the Covariance in Portfolio Analysis, The Journal of Finance 53, 1821–1827.

Tumminello, M., T. Aste, T. Di Matteo, and R. N. Mantegna, 2005, A tool for filtering information in complex systems., Proceedings of the National Academy of Sciences of the United States of America 102, 10421–6.

Tumminello, M., F. Lillo, and R. N. Mantegna, 2010, Correlation, hierarchies, and networks in financial markets, Journal of Economic Behavior & Organization 75, 40–58.

Vandewalle, N., F. Brisbois, and X. Tordoir, 2001, Non-random topology of stock markets, Quantitative Finance 1, 372–374.

Whittaker, J., 1990, Graphical Models in Applied Multivariate Statistics (John Wiley & Sons, Inc.).

Appendix A: Relation between Partial Correlation and Regression Analysis

In this appendix I follow Stevens (1998) to show the connection between the partial correlations of returns and the regression coefficients resulting from regressing the return of a particular stock with the rest of them.

Let us assume that the correlation matrix of returns is given by the $n \times n$ matrix $\Sigma = [\sigma_{ij}]$ which could be partitioned as follows:

$$\Sigma = \begin{bmatrix} \sigma_{11} & \sigma_{1j} \\ \sigma_{j1} & \Sigma_{n-1} \end{bmatrix} \tag{A.1}$$

where $\sigma_{11}$is the variance of returns for asset 1, σ_{1j} is a $1 \times n-1$ vector of covariance between stock 1 and the other $n-1$ stocks in the sample and Σ_{n-1} corresponds to the sub-matrix of Σ resulting from the elimination of its first row and column. Defining the inverse of the covariance matrix as $\Omega = [\omega_{ij}] \equiv \Sigma^{-1}$, its partitioned form is written as

$$\Omega = \begin{bmatrix} \omega_{11} & \omega_{1j} \\ \omega_{j1} & \Omega_{n-1} \end{bmatrix} \tag{A.2}$$

Since $\Omega * \Sigma = I$, the next two expressions could be derived (first row of Ω with the columns of Σ)

$$\omega_{1j} = -\omega_{11}\sigma_{1j}\Sigma_{n-1}^{-1} = -\omega_{11}\sigma_{1j}\Omega_{n-1} \tag{A.3}$$

$$\omega_{11} = \left[\sigma_{11} - \sigma_{1j}\Sigma_{n-1}^{-1}\sigma_{j1}\right]^{-1} = \left[\sigma_{11} - \sigma_{1j}\Omega_{n-1}\sigma_{j1}\right]^{-1} \tag{A.4}$$

Note that the term $\sigma_{1j}\Sigma_{n-1}^{-1}$ in A.3 corresponds to the row vector of the regression coefficients that result from regressing stock 1 returns on the rest of the stocks. We call this vector β_1'. Additionally, by definition R^2 in such regression is given by

$$R_1^2 \equiv \frac{\sigma_{1j}\Sigma_{n-1}^{-1}\sigma_{j1}}{\sigma_{11}} \tag{A.5}$$

Therefore, equation (A.4) is restated as

$$\omega_{11} = [\sigma_{11}(1 - R_1^2)]^{-1} = \frac{1}{\sigma_{e1}^2} \tag{A.6}$$

where σ_{e1}^2accounts for the proportion of the total return's variance of stock 1 that is not explained by the regression or the variance of the residual. Finally, introducing expression A.6 into A.3

$$\omega_{1j} = -\frac{\beta_1'}{\sigma_{e1}^2} \tag{A.7}$$

Although A.6 and A.7 assumes the dependent variable in the regression is the return of stock 1, a convenient permutation of row and columns allows us to fully characterize Ω as follows:

$$\Omega = \begin{bmatrix} \frac{1}{\sigma_{e1}^2} & -\frac{\beta_{12}}{\sigma_{e1}^2} & \cdots & -\frac{\beta_{1n}}{\sigma_{e1}^2} \\ -\frac{\beta_{21}}{\sigma_{e2}^2} & \frac{1}{\sigma_{e2}^2} & & -\frac{\beta_{2n}}{\sigma_{e2}^2} \\ \vdots & & \ddots & \vdots \\ -\frac{\beta_{n1}}{\sigma_{en}^2} & -\frac{\beta_{n2}}{\sigma_{en}^2} & \cdots & \frac{1}{\sigma_{en}^2} \end{bmatrix} \tag{A.8}$$

On the other hand, we have defined the matrix of partial correlation coefficients between stocks as

$$\rho = [\rho_{ij}] = -\Delta\Omega\Delta \tag{A.9}$$

where $\Delta = diag(1/\sqrt{\omega_{ii}})$. Simple calculations show that

$$\rho = \begin{bmatrix} -1 & \beta_{12}\frac{\sigma_{e2}}{\sigma_{e1}} & \cdots & \beta_{1n}\frac{\sigma_{en}}{\sigma_{e1}} \\ \beta_{21}\frac{\sigma_{e1}}{\sigma_{e2}} & -1 & & \beta_{2n}\frac{\sigma_{en}}{\sigma_{e2}} \\ \vdots & & \ddots & \vdots \\ \beta_{n1}\frac{\sigma_{e1}}{\sigma_{en}} & \beta_{n2}\frac{\sigma_{e2}}{\sigma_{en}} & \cdots & -1 \end{bmatrix} \tag{A.10}$$

Appendix B: Test for the 2-Step Estimation Methodology

This appendix is devoted to testing the estimation methodology explained in section 4 by means of a toy example. I proceed as follows. The "skeleton" of the market is given by a structure of a balance tree with branching and height equal to 3 and 4 respectively, as in figure B.1. Therefore, the network is composed of 40 stocks and 39 links. Starting from the center of that network, the links corresponding to the first, second, and third step away from it are given values 0.5, 0.3 and 0.15, respectively (see black letters in figure B.1). These numbers are going to take the role of the partial correlations between pair of the stocks. The weight for the rest of the links not considered in figure B.1 are assumed equal to zero.

With this structure at hand and the weighed adjacency matrix recovered using the expression (1), I compute the associated real covariance matrix.[31] Additionally, I assume a mean vector with components equal to 0.08 for the central node and 0.06, 0.04 and 0.02 for nodes located one, two, and three steps away from the center (see red figures in figure B.1). Using this covariance matrix and the commented mean vector as the real parameter of the process, I draw a sample of size 1.000 from a multivariate normal distribution. Next, I implement the 2-step estimation methodology explained at the beginning of this section assuming a confidence level of 1% upon this artificial dataset in order to estimate the PCSN.

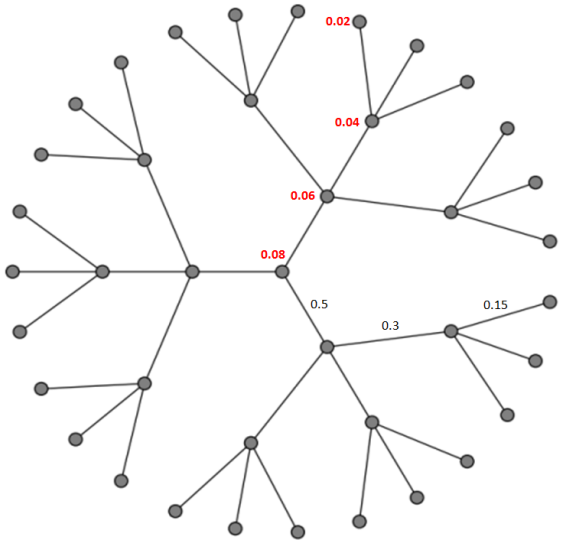

Figure B.1: Artificial partial correlation network

Table B.1 provides a general assessment of the estimation performance by presenting the number of links correctly and incorrectly detected by the algorithm. Panel A shows the result of the

[31] Since the matrix Δ only takes the role of normalization in equation (1), I consider as the relevant covariance just $-\rho^{-1}$ which is equivalent to saying that $\rho_{ij} = \beta_{ij}$

estimation before filtering out the non-significant partial correlations. Panel B presents the same information after implementation of Monte Carlo Simulations.

Initial Estimates (Panel A)

	Real Structure		
Estimated Structure	Non Null	Null	**Total**
Non Null	39	316	355
Null	0	425	425
Total	39	741	780

Final Estimates - Montecarlo Simulation (Panel B)

	Real Structure		
Estimated Structure	Non Null	Null	**Total**
Non Null	37	21	58
Null	2	720	722
Total	39	741	780

B.1Estimation algorithm's performance

From panel A in table B.1, the first thing to notice is that the initial estimation does a good job of identifying the true network, although it is not perfect. Out of the 39 links that actually exist, all of them were initially captured. Its major problem is due to the number of links that the algorithm erroneously identified, say 316, leading to a network density of 45.5%. In general terms, the initial estimation provides good results in selecting the links that actually exist and discarding those not included in the real structure. The hit ratio of this estimation is (39+425)/780=59.5%.

Panel B from table B.1 shows the benefits of using Monte Carlo Simulation for uncovering the real network structure. The major change from panel A to panel B is due to the reduction of erroneously detected links. Such a reduction reaches 93%, from 316 to 21 leading to a higher hit ratio (37+720)/780=97.1%. Unfortunately, the algorithm discards two links that actually exist in the structure. Overall, the 2-step estimation methodology performs well and seems to be a suitable tool to uncover the hidden stock network.

Appendix C: Direct and Partial Correlation Matrix

	ABS	AMS	ACE	BBVA	BKIA	BKT	POP	BSAB	SCH	BOLS	CTG	IDR	FERC	FCC	MAP	ANA	DIA	ENAC	CABK	OHL	GAM	IBE	IND	TL5	ACS	PROB	REE	REP	IAG	TECN	TEF	SCYR	VIS	JAZ	MITT
ABS																																			
AMS	-																																		
ACE	-	0.1																																	
BBVA	-	-	-																																
BKIA	-	-	-	-																															
BKT	-	-	-	0.1	0.1																														
POP	-	-	-	0.1	-	0.1																													
BSAB	-	-	-	-	0.1	0.1	0.3																												
SCH	-	-	-	0.6	-	-	-	-																											
BOLS	-	-	-	-	-	-	-	-	-																										
CTG	-	0.1	-	-	-	-	-	-	-	-																									
IDR	0.1	0.1	-	-	-	-	-	-	-	-	-																								
FERC	-	-	0.1	-	-	-	-	-	-	-	-	-																							
FCC	-	-	-	-	-	-	-	-	-	-	-	-	-																						
MAP	-	-	0.1	-	-	-	0.1	-	-	-	-	0.1	0.1	-																					
ANA	-	-	-	-	-	-	-	0.1	-	-	-	-	-	-	-																				
DIA	-	-	-	-	-	-	-	-	-	-	-	-	-	-	-	-																			
ENAG	-	-	-	-	-	-	-	-	-	-	0.3	-	-	-	-	-	-																		
CABK	-	-	-	-	0.1	0.2	0.2	-	0.2	-	-	-	-	-	0.2	-	-	-																	
OHL	0.1	-	0.1	-	-	-	-	-	-	-	-	-	0.1	0.1	-	0.1	-	-	-																
GAM	-	-	-	-	-	0.1	-	0.1	-	-	-	-	-	-	-	-	-	-	-	-															
IBE	-	-	-	-	-	-	-	-	0.1	0.1	0.1	-	-	-	-	-	-	0.1	-	-	-														
IND	-	-	0.1	0.1	-	-	-	-	-	-	-	-	-	-	-	-	0.1	-	- 0.1	-	-	-													
TL5	-	-	-	-	-	0.2	-	-	-	-	-	-	-	-	-	-	-	-	-	-	-	-	-												
ACS	-	-	-	-	-	-	-	-	-	-	-	-	0.2	-	-	0.1	-	-	-	0.1	-	-	-	-											
PROB	-	-	0.1	-	-	-	-	-	-	-	-	-	0.1	-	-	-	-	-	-	-	0.2	-	-	-	-										
REE	-	-	-	-	-	-	-	-	-	0.1	0.1	-	-	-	-	0.1	-	0.2	-	-	-	-	-	-	-	-									
REP	-	-	-	-	-	-	-	-	-	-	-	-	-	-	-	-	0.1	-	-	-	-	-	0.1	-	-	-	-								
IAG	-	0.1	-	-	-	-	-	-	-	-	-	-	-	-	-	-	-	-	-	-	0.1	-	-	0.1	-	-	-	-							
TECN	-	0.1	-	-	-	-	-	-	-	0.1	-	0.1	-	0.1	-	-	-	-	-	0.1	-	-	-	-	-	-	-	0.1	-						
TEF	-	-	-	-	-	-	-	-	0.1	-	-	0.1	-	-	-	-	-	-	-	-	-	0.2	-	-	-	-	-	0.2	-	-					
SCYR	0.2	-	-	-	0.1	-	0.1	0.1	-	-	-	-	-	0.2	-	-	-	-	-	-	-	-	-	-	-	-	-	0.1	-	-	-				
VIS	-	0.1	-	-	-	-	-	-	-	-	-	-	-	-	-	-	0.2	-	-	-	-	-	-	-	-	-	-	-	-	-	-	-			
JAZ	-	-	-	-	-	-	-	-	-	-	-	-	-	-	-	-	-	-	-	-	-	-	-	-	-	-	-	-	-	-	-	-	-		
MITT	-	-	-	-	-	-	-	-	0.1	-	-	-	-	-	-	-	-	-	-	-	-	-	-	-	-	-	-	-	-	0.1	-	-	-	-	

C.1 Partial Correlation Matrix with optimal regularization parameter

	ABS	AMS	ACE	BBVA	BKIA	BKT	POP	BSAB	SCH	BOLS	CTG	IDR	FERC	FCC	MAP	ANA	DIA	ENAG	CABK	OHL	GAM	IBE	IND	TL5	ACS	PROB	REE	REP	IAG	TECN	TEF	SCYR	VIS	JAZ	MITT
ABS																																				
AMS	0.34																																		
ACE	0.42	0.43																																	
BBVA	0.42	0.36	0.55																																
BKIA	0.42	0.37	0.46	0.55																															
BKT	0.43	0.30	0.51	0.60	0.54																														
POP	0.38	0.34	0.46	0.60	0.50	0.57																													
BSAB	0.43	0.35	0.52	0.61	0.54	0.60	0.64																												
SCH	0.40	0.35	0.55	0.77	0.55	0.59	0.58	0.61																											
BOLS	0.30	0.33	0.46	0.44	0.34	0.39	0.40	0.39	0.45																										
CTG	0.22	0.23	0.45	0.42	0.35	0.41	0.34	0.38	0.42	0.31																									
IDR	0.44	0.43	0.50	0.48	0.44	0.43	0.47	0.44	0.46	0.39	0.32																								
FERC	0.43	0.37	0.58	0.57	0.44	0.51	0.48	0.54	0.57	0.41	0.42	0.44																							
FCC	0.36	0.33	0.44	0.39	0.38	0.38	0.39	0.39	0.40	0.38	0.39	0.41	0.45																						
MAP	0.35	0.39	0.54	0.57	0.43	0.50	0.54	0.51	0.58	0.43	0.41	0.49	0.55	0.40																					
ANA	0.39	0.27	0.45	0.49	0.44	0.40	0.44	0.51	0.49	0.34	0.37	0.40	0.46	0.41	0.39																				
DIA	0.33	0.33	0.45	0.46	0.34	0.40	0.35	0.36	0.45	0.31	0.40	0.39	0.46	0.31	0.44	0.41																			
ENAG	0.19	0.21	0.34	0.28	0.26	0.27	0.20	0.28	0.27	0.26	0.50	0.28	0.33	0.29	0.30	0.30	0.27																		
CABK	0.38	0.28	0.48	0.59	0.52	0.58	0.58	0.57	0.61	0.41	0.37	0.39	0.47	0.42	0.55	0.42	0.39	0.23																	
OHL	0.44	0.38	0.55	0.50	0.42	0.46	0.47	0.53	0.50	0.41	0.46	0.44	0.55	0.46	0.49	0.51	0.41	0.33	0.48																
GAM	0.41	0.35	0.46	0.51	0.46	0.52	0.48	0.53	0.49	0.39	0.41	0.37	0.46	0.39	0.45	0.44	0.33	0.31	0.47	0.41															
IBE	0.32	0.33	0.55	0.58	0.43	0.51	0.43	0.52	0.60	0.47	0.52	0.42	0.55	0.40	0.51	0.49	0.45	0.42	0.47	0.48	0.45														
IND	0.32	0.34	0.49	0.52	0.37	0.39	0.36	0.36	0.52	0.33	0.40	0.39	0.48	0.33	0.45	0.34	0.42	0.26	0.33	0.42	0.37	0.45													
TL5	0.40	0.35	0.42	0.49	0.45	0.51	0.44	0.48	0.47	0.38	0.36	0.41	0.48	0.34	0.42	0.38	0.38	0.27	0.42	0.41	0.44	0.43	0.39												
ACS	0.45	0.39	0.57	0.59	0.50	0.52	0.47	0.54	0.59	0.42	0.48	0.49	0.60	0.43	0.52	0.51	0.45	0.38	0.47	0.56	0.48	0.57	0.44	0.47											
PROB	0.39	0.35	0.48	0.43	0.39	0.41	0.41	0.44	0.43	0.31	0.36	0.42	0.48	0.30	0.39	0.42	0.37	0.29	0.37	0.41	0.46	0.43	0.36	0.38	0.46										
REE	0.38	0.29	0.47	0.40	0.37	0.37	0.33	0.41	0.39	0.41	0.48	0.38	0.38	0.35	0.35	0.46	0.32	0.45	0.35	0.45	0.42	0.49	0.30	0.35	0.48	0.39									
REP	0.33	0.34	0.46	0.55	0.42	0.42	0.41	0.43	0.57	0.38	0.43	0.43	0.50	0.38	0.47	0.42	0.45	0.27	0.46	0.46	0.42	0.53	0.49	0.37	0.50	0.36	0.39								
IAG	0.39	0.39	0.47	0.48	0.39	0.45	0.41	0.43	0.45	0.34	0.31	0.41	0.46	0.35	0.39	0.39	0.37	0.25	0.42	0.40	0.46	0.41	0.34	0.44	0.46	0.39	0.33	0.33							
TECN	0.34	0.40	0.47	0.45	0.38	0.36	0.36	0.42	0.46	0.44	0.43	0.45	0.48	0.43	0.45	0.40	0.39	0.35	0.33	0.49	0.40	0.47	0.42	0.35	0.47	0.35	0.39	0.47	0.32						
TEF	0.37	0.37	0.55	0.63	0.47	0.50	0.48	0.52	0.64	0.44	0.45	0.50	0.54	0.43	0.54	0.45	0.46	0.30	0.49	0.51	0.41	0.61	0.47	0.44	0.57	0.40	0.38	0.58	0.45	0.47					
SCYR	0.47	0.39	0.45	0.53	0.51	0.48	0.51	0.54	0.52	0.39	0.42	0.46	0.51	0.47	0.46	0.46	0.40	0.26	0.46	0.49	0.46	0.47	0.38	0.39	0.51	0.43	0.43	0.48	0.41	0.45	0.47				
VIS	0.16	0.31	0.30	0.31	0.18	0.24	0.21	0.29	0.31	0.26	0.29	0.29	0.35	0.28	0.34	0.22	0.38	0.21	0.26	0.34	0.21	0.35	0.31	0.31	0.29	0.20	0.20	0.33	0.21	0.34	0.33	0.19			
JAZ	0.31	0.29	0.33	0.39	0.38	0.36	0.34	0.35	0.38	0.31	0.28	0.34	0.38	0.31	0.34	0.31	0.26	0.25	0.38	0.32	0.37	0.38	0.34	0.35	0.39	0.34	0.27	0.33	0.33	0.30	0.35	0.36	0.20		
MITT	0.31	0.31	0.43	0.47	0.39	0.37	0.41	0.42	0.49	0.33	0.30	0.35	0.41	0.36	0.42	0.35	0.33	0.19	0.41	0.38	0.36	0.38	0.36	0.34	0.40	0.36	0.26	0.35	0.39	0.42	0.43	0.37	0.26	0.30	

C.2 Direct Correlation Matrix

Appendix D: Eigenvector Centrality for the constituent of the IBEX-35

Centrality for each of the firms in IBEX-35 considering the most recent 250 trading days in the sample

Ticker	NAME	Industry	Centrality
SCH	BANCO SANTANDER	Bank/Savings & Loan	0,593
BBVA	BBV.ARGENTARIA	Bank/Savings & Loan	0,557
CABK	CAIXABANK	Bank/Savings & Loan	0,249
POP	BANCO POPULAR ESPANOL	Bank/Savings & Loan	0,254
BKT	BANKINTER 'R'	Bank/Savings & Loan	0,227
BSAB	BANCO DE SABADELL	Bank/Savings & Loan	0,179
TEF	TELEFONICA	Utility	0,181
MAP	MAPFRE	Insurance	0,110
MITT	ARCELORMITTAL (MAD)	Industrial	0,111
IND	INDITEX	Industrial	0,062
BKIA	BANKIA	Bank/Savings & Loan	0,065
GAM	GAMESA CORPN.TEGC.	Industrial	0,073
REP	REPSOL YPF	Industrial	0,076
IBE	IBERDROLA	Utility	0,145
TL5	MEDIASET ESPANA COMUNICACION	Industrial	0,055
ACE	ABERTIS INFRAESTRUCTURAS	Industrial	0,041
IDR	INDRA SISTEMAS	Industrial	0,053
TECN	TECNICAS REUNIDAS	Industrial	0,055
FERC	FERROVIAL	Industrial	0,036
OHL	OBRASCON HUARTE LAIN	Industrial	0,042
ANA	ACCIONA	Industrial	0,047
SCYR	SACYR	Industrial	0,027
PROB	GRIFOLS ORD CL A	Industrial	0,026
AMS	AMADEUS IT HOLDING	Industrial	0,024
IAG	INTL.CONS.AIRL.GP. (MAD) (CDI)	Transportation	0,038
CTG	GAS NATURAL SDG	Utility	0,059
ENAG	ENAGAS	Utility	0,055
ABS	ABENGOA B SHARES	Industrial	0,017
REE	RED ELECTRICA CORPN.	Utility	0,041
ACS	ACS ACTIV.CONSTR.Y SERV.	Industrial	0,021
BOLS	BOLSAS Y MERCADOS ESPANOLES	Other Financial	0,037
FCC	FOMENTO CONSTR.Y CNTR.	Industrial	0,017
DIA	DISTRIBUIDORA INTNAC.DE ALIMENTACION	Industrial	0,022
VIS	VISCOFAN	Industrial	0,006
JAZ	JAZZTEL	Industrial	0,000

D.1 Centrality by firm

Appendix E: Cross-Correlation and Autocorrelation of Regressors

	Density	Mean Distance	Transitivity	CentralityBank
Density				
Mean Distance	-0.702			
Transitivity	0.145	0.236		
CentralityBank	0.112	0.177	0.344	

E.1 Correlation matrix between regressors

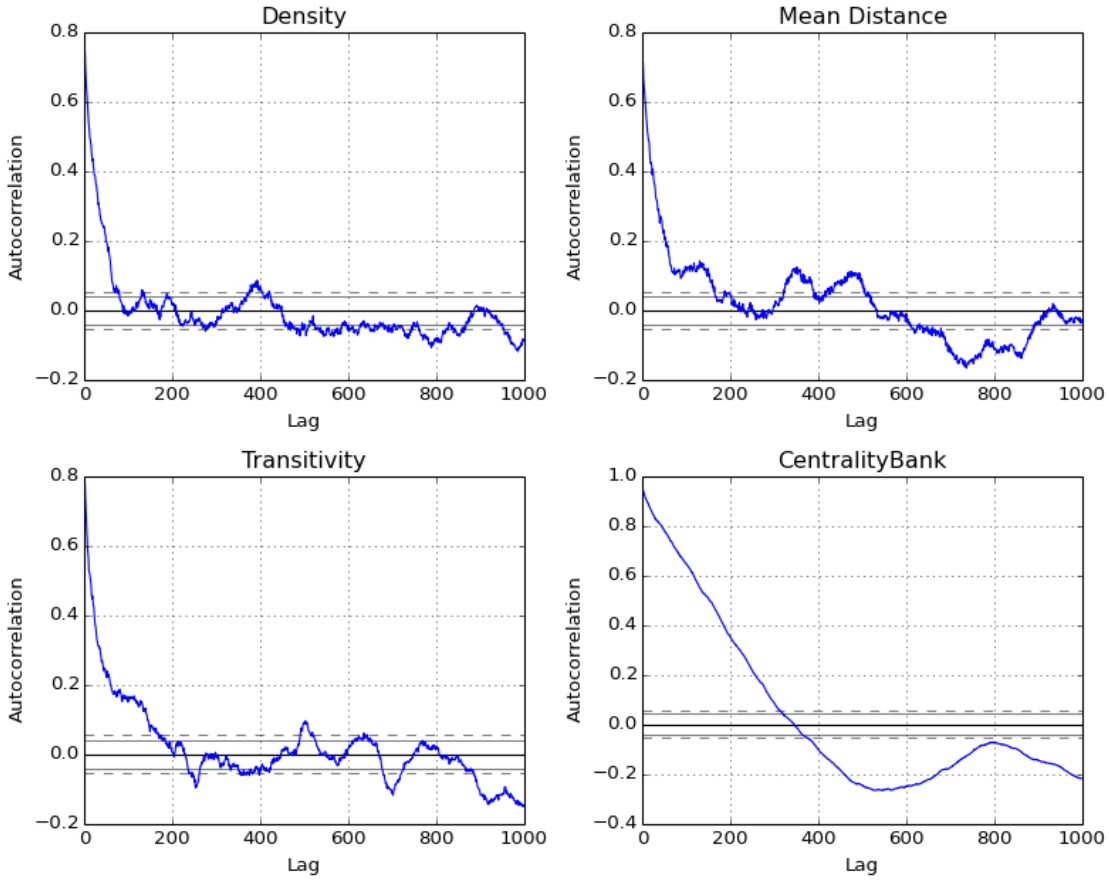

Figure E.1: Autocorrelation function of regressors

Appendix F: Mean and total centrality by economic sectors

Spain	Number of Firms	Eigenvector Centrality		Market Value*	
		Total	Mean	Total	Mean
Other Financial	1	0.037	0.037	2,524.4	2,524.4
Transportation	1	0.038	0.038	9,611.1	9,611.1
Insurance	1	0.110	0.110	8,635.1	8,635.1
Utility	5	0.481	0.096	130,229.9	26,046.0
Industrial	20	0.812	0.041	199,877.9	9,993.9
Bank/Savings & Loan	7	2.125	0.304	217,833.3	31,119.0
Total	***35***	***3.602***	***0.103***	***568,711.5***	

* In Millons of €

Table F.1

France	Number of Firms	Eigenvector Centrality		Market Value*	
		Total	Mean	Total	Mean
Other Financial	1	0.049	0.049	19,969.1	19,969.1
Transportation					
Insurance	1	0.335	0.335	47,251.2	47,251.2
Utility	3	0.071	0.024	127,758.0	42,586.0
Industrial	32	2.413	0.075	863,541.5	26,985.7
Bank/Savings & Loan	3	1.302	0.434	128,771.3	42,923.8
Total	***40***	***4.171***	***0.104***	***1,187,291.0***	

* In Millons of €

Table F.2

Germany	Number of Firms	Eigenvector Centrality		Market Value*	
		Total	Mean	Total	Mean
Other Financial					
Transportation	2	0.162	0.081	36,468.0	18,234.0
Insurance	2	0.468	0.234	85,546.1	42,773.0
Utility	3	0.915	0.305	100,876.6	33,625.5
Industrial	21	2.487	0.118	654,366.7	31,160.3
Bank/Savings & Loan	2	0.327	0.163	51,514.2	25,757.1
Total	***30***	***4.359***	***0.145***	***928,771.7***	

* In Millons of €

Table F.3

Italy	Number of Firms	Eigenvector Centrality		Market Value*	
		Total	Mean	Total	Mean
Other Financial	2	0.243	0.122	7,011.4	3,505.7
Transportation					
Insurance	2	0.210	0.105	31,034.9	15,517.4
Utility	6	0.399	0.067	87,142.5	14,523.7
Industrial	20	0.543	0.027	194,897.5	9,744.9
Bank/Savings & Loan	7	2.266	0.324	95,289.8	13,612.8
Total	***37***	***3.662***	***0.099***	***415,376.0***	

* In Millons of €

Table F.4

UK	Number of Firms	Eigenvector Centrality		Market Value*	
		Total	Mean	Total	Mean
Other Financial	8	0.0033	0.0004	44,977.0	5,622.1
Transportation	3	0.0013	0.0004	17,665.3	5,888.4
Insurance	10	0.0371	0.0037	104,199.3	10,419.9
Utility	7	0.0003	0.0000	159,222.0	22,746.0
Industrial	68	2.6636	0.0392	1,219,609.4	17,935.4
Bank/Savings & Loan	5	0.0012	0.0002	263,657.1	52,731.4
Total	***101***	***2.7068***	***0.027***	***1,809,330.2***	

* In Millons of £

Table F.5

Appendix G: Probit and ARCH Alternative Models

Results of Probit model's estimations (alternative specifications)

Dependent Variable Prob that Ibex Ret <-3 Std

Density	***Model 1***	***Model 2***	***Model 3***	***Model 4***
Lag 10			22.24	
			(2.18)**	
Lag 30			21.43	
			(2.21)**	
Banks Centrality				
Lag 10	-5.10			-5.12
	(-1.19)			(-1.23)
Lag 30	8.59			8.51
	(2.02)**			(2.02)**
Transitivity				
Lag 10		-0.26	-1.56	-0.58
		(-0.2)	(-0.67)	(-0.46)
Lag 30		1.54	1.12	0.79
		(0.93)	(0.45)	(0.45)
Likelihood Ratio Index	0.031	0.004	0.101	0.033
LLR p-value	0.050	0.674	0.001	0.185

SE estimated by Bootstrapping. Significance * p<0.10,** p<0.05,*** p<0.01

Specific definitions and unit of measures for each network statistics are provided in Appendix H

Table G.1

Results of ARCH model's estimations (alternative specifications)

Density	*Model 1*	*Model 2*	*Model 3*	*Model 4*
Lag 10			15.07	
			(3.92)***	
Lag 30			3.41	
			(0.87)	
Banks Centrality				
Lag 10	0.73			0.73
	(0.56)			(0.5)
Lag 30	4.51			4.77
	(3.82)***			(3.52)***
Transitivity				
Lag 10		2.27	1.33	1.34
		(1.65)*	(1.4)	(1.3)
Lag 30		0.00	-1.15	-1.65
		(0.00)	(-1.41)	(-1.58)
Squared Residuals				
Lag 1	0.08	0.09	0.09	0.08
	(2.55)**	(2.99)***	(2.78)***	(2.57)***
Lag 2	0.13	0.15	0.14	0.13
	(3.93)***	(4.25)***	(4.17)***	(3.96)***
Lag 3	0.15	0.16	0.15	0.15
	(4.63)***	(4.72)***	(4.74)***	(4.55)***
Lag 4	0.19	0.21	0.20	0.19
	(5.63)***	(5.77)***	(5.62)***	(5.5)***
Lag 5	0.16	0.17	0.16	0.16
	(4.55)***	(4.72)***	(4.5)***	(4.6)***
Others Parameter				
T-Student df	6.44	5.99	6.34	6.48
	(6.53)***	(6.85)***	(6.46)***	(6.48)***
Akaike criterion	3.423	3.433	3.428	3.424
Schwarz criterion	3.449	3.458	3.458	3.454
Log Likelihood	- 3,889.2	- 3,900.3	- 3,892.3	- 3,887.5

Significance * p<0.10,** p<0.05,*** p<0.01

Specific definitions and unit of measures for each network statistics are provided in Appendix H

Table G.2

Appendix H: Network-based Measures

In general terms, a network is a pair of sets $\varphi = \{N, a\}$, with $N = \{1,2, \dots, n\}$ the set of nodes and a the set of links connecting pair of them. Then, if there is a link from node i to node j, $(i,j) \in a$. A convenient way to arrange the information contained in a is by means of the so-called adjacency matrix $A = [A_{ij}]$. A is a $n \times n$ matrix in which $A_{ij} \neq 0$ captures the existence of a relationship between node i and node j. The network is said to be undirected when $(i,j) \in a$ also implies that $(j,i) \in a$ and therefore, $A = A^T$. Note that for an undirected network, no directed relationship is attached to links and they are visually represented as a line, $(j - i)$. On the other hand, the network is said to be directed when it contains directed links pointing from one node to another. Note that the existence of a links from node i to node j, $(j,i) \in a$, does not necessarily imply the reverse and thus A is usually different from A^T. In this case, the links are visually represented as arrows, $(j \to i)$. Further, if $A_{ij} \in \{0,1\}$, φ is said to be unweighted. However, when $A_{ij} \in \mathbb{R}$, such a link also carries information about the intensity in the interaction between nodes leading to a weighted network. The reader is referred to Newman (2010) and Jackson (2010) for a comprehensive treatment of the field.

It has been empirically proved that different sort of networks, ranging from biological to engineering networks, show astonishing similarity when some of their traits are compared. The cases of small world property, fat-tail degree distribution and high clustering are particularly popular in the network literature. Below I comment about those properties while providing a list of fundamental network measures that are going to be used through the paper. This list is by no mean complete and it should be considered as an attempt to enumerate the salient quantities describing any type of network.

Among the most basic network's concepts, node-size and link-size, called n and m respectively, account for the number of nodes and the number of links in the network. The density d measures the fraction of links that actually exist relative to the maximum possible links in the structure. In mathematical terms, $d = m/\binom{n}{2}$.

The degree of node i, k_i, is defined as the number of links attached to that node and the mean degree of the network, c, captures the average number per node in the structure. Formally, $c = 2m/N$. A closely related and fundamental concept describing any network is its degree distribution, $P(k)$, representing the empirical distribution of node degrees. That is, $P(k)$ is the fraction of nodes

in the network showing degree k. When $P(k)$ is bell-shaped most of the nodes in that network show approximately the same degree or connectivity. However it is surprisingly common to observe fat-tailed degree distributions in real-world networks, Barabási and Albert (1999). This evidence highlights the increased probability of observing nodes that are relatively poorly connected co-existing with extremely well connected nodes, the hubs. It is typically to model such fat-tail degree distribution by assuming a power law form $P(k) = \gamma_0 k^{-\gamma_1}$.

A path between nodes i and j is a sequence of successive links $(i_1 i_2), (i_2 i_3), \dots, (i_{t-1} i_t)$ such that each $(i_s i_{s+1}) \in a$ for $s \in \{1, \dots, t-1\}$ with $i_1 = i$ and $i_t = j$. The length of such a path is the number of links traversed along that path. The geodesic path between nodes i and j is the shortest path between those nodes. The diameter of the network is the longest geodesic distance between any two nodes and the mean distance is the average over geodesic paths (note that the average distance is bounded above by the diameter). An interesting regularity observed in real-world networks is the so-called Small Worlds property. This property embodies the idea that the average distance and diameter is surprisingly small in comparison to its node's size. Technically, it is said that the mean distance scales logarithmically (or slower) with the node-size. For example, in the social network literature, the seminal paper Milgram (1967) give rise to the idea of 6 degrees of separation among any two persons in the world. This result also remains valid for Facebook since 5 degrees of separation was found in Ugander et al. (2011).

A network is said to be connected if there is a path connecting any two nodes in the structure, otherwise it is disconnected. When the network is disconnected, each subset of nodes forming a connected sub-network is called a component. In other words, a component is a subset of nodes where for each pair of nodes in that subset there exists at least one path connecting them. The typical network configuration corresponds to several components with just one of them fulfilling a large proportion of the structure. This large component is called the largest component and its size relative to the total number of nodes in the network is denoted by L. For Facebook, L attains a value of 99.91% which basically means that almost any two persons in this virtual world are reachable by following the correct path, Ugander et al. (2011).

Another measure worth defining is the degree of assortativity Q. If the correlation between the degrees of connected nodes is positive, high (low)-degree nodes tends to be connected with other

high (low)-degree nodes. This tendency is called positive assortativeness or just assortative for short. An assortative network is expected to be arranged as a core/periphery structure where the core is composed by highly connected nodes and the periphery by poorly connected ones surrounding the core. For the case in which high-degree nodes tends to be connected with low-degree ones, the correlation between the degrees of connected nodes is negative and we called this tendency as negative assortativeness or disassortative. In this case, the general configuration of the network presents star-like features.

In mathematics, a relationship is said to be transitive when $A \rightarrow B$ and $B \rightarrow C$, then $A \rightarrow C$. In a network context, this relationship means that if node i is connected to j and j is connected to k, then i is connected to k. The level of network transitivity T captures the likelihood that any given pair of nodes shares another common neighbor. Mathematically, T is calculated as the ratio between the number of triangles in the network divided by the total number of connected triples of nodes. In social networks, such a measure tends to be quite high since the probability that a pair of friends shows another friend in common is usually large. Particular interesting to mention is the fact that some researchers associate large values of T with a network structured in communities, Newman and Park (2003).

Most of the measures discussed so far are predominantly macroscopic in nature. However, there exist several measures capturing node's position in a given network. These sorts of measures, commonly referred to as centrality measures, are grounded in the sociological literature and their main goal is to account for the power or influence of each node in a given structure, Freeman (1978). Given the extension of this literature, I just comment about two of them that have become the standard in network analysis. The simplest node's centrality measure is degree centrality which accounts for the degree of a given node. Therefore, the importance of a node in a network is given by the number of links attached to it. This is a local measure that discards the information about the network structure beyond the "first friends" of a give node. A natural extension to the degree centrality is given by the eigenvector centrality due to Bonacich (1972) and Bonacich (2007). Its version for a weighed networks is discussed in Newman (2004). In formal terms, the eigenvector centrality of node i, v_i, is proportional the weighted sum of the centralities of its neighboring nodes. Assuming the adjacency matrix of the network is ρ, the eigenvector centrality of node i is given by

$$v_i = \lambda^{-1} \sum_j \rho_{ij} v_j \qquad \text{(g.1)}$$

Note that equation (g.1) shows that a highly central node becomes central either by being connected with many other nodes (degree centrality) or by being connected with highly central ones. By restating equation (g.1) in matrix terms, it can be seen that the vector of centrality scores, v, is given by the eigenvector of the adjacency matrix corresponding to the eigenvalue λ, where the largest eigenvalue is the preferred choice.[32]

$$\lambda v = \rho v \qquad \text{(g.2)}$$

[32] It is usual to report the vector of centrality normalized to one, this is also the case for the current paper

Chapter 3: The Nature of Volatility Spillovers across the International Network of Capital Markets†

Abstract

This paper studies the nature of volatility spillovers across countries from the perspective of network theory and by relying on data of US-listed ETFs. I use Lasso-related techniques to estimate the short-run, Granger and long-run International Volatility Networks (IVNs) where the nodes correspond large-cap international markets while the links account for significant volatility interactions with different time horizons. Additionally, the International Trade Network (ITN) is included in the analysis where its links measure bilateral export-import flows, thus capturing fundamental interconnections between countries. I find that: (i) the long run IVN and the ITN resemble each other closely indicating that volatility tends to spread across economically related economies and (ii) the Granger IVN is organized in communities where volatility lead-lags are more frequent between countries located in the same continent than across them. Since the community structure of the Granger IVN is consistent with the notion of slow diffusion of news across specialized investors, I formally test this hypothesis by estimating a gradual diffusion of information model where the instantaneous diffusion of information hypothesis is rejected at any sensible level of significance.

Keywords: Network Theory, Spillover of Volatility, International Financial Contagion

JEL Classification: C00, C32, C45, C51, C55, C58, G01, G10, G15, G17

† I would like to thank Guillermo Carlomagno and Ramiro Lozada for helpful comments and suggestions. All mistakes are mine.

1. Introduction

The materialization of recent financial events with negatives and widespread consequences has renewed the interest on the timeless debate about international spillovers. To stimulate the discussion, figure 1 plots the closing prices (left panel) and return's volatilities (right panel) for three US-listed ETFs tracking the European, US and Japanese MSCI market indices during the period Aug-2015 to Jan-2016. Note that the effects of the so-called Chinese's Black Monday on August 24, 2015 were immediately evident worldwide with negative log returns of -2.4%, -4.3% and -3.6% for the European, US and Japanese markets, respectively. The case of market volatility is particularly striking since return variances achieved levels more than 15 times larger than average (over the analyzed period) for the European and Japanese ETFs and more than 20 times larger for the US case.

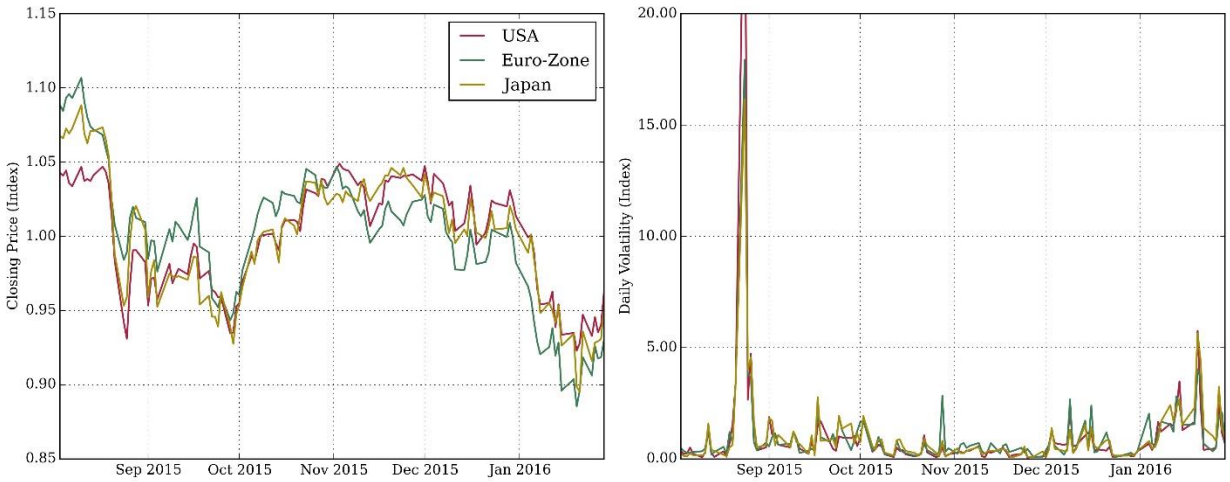

Figure 1: Daily closing price and range-based volatility estimator (see equation 4) for the iShare ETF's tracking the corresponding MSCI indices of the European, US and Japanese markets. The series are scaled by their mean value during the period Aug-2015 to Jan-2016.

An appropriate evaluation of the risks of financial contagion and a soundness international diversification crucially depends on our understanding on the shock-transmission mechanisms across economies. Academic papers have devoted substantial efforts to identify the fundamental drivers behind returns' spillovers among major financial centers (e.g. King and Wadhwani (1990), Hamao, Masulis, and Ng (1990), Lin, Engle, and Ito (1994)). Despite its fundamental relevance, studies specifically concerned on the transmission of volatility among a large panel of countries has not received as much attention until recently (Jung and Maderitsch (2014), Diebold and Yilmaz

(2014), Diebold and Yilmaz (2009), Diebold and Yilmaz (2012)). The current study contributes to this latter branch of literature by uncovering the detailed patterns of volatility spillovers among a panel of countries that jointly represent more than 80% of the worldwide market capitalization. I undertake this task by estimating International Volatility Network (IVN) in which the nodes correspond to a set of large-cap stock markets while the links account for significant volatility interactions. Since cross-sectional dependencies in a time series setting do not only arise contemporaneously but also with lead-lags, three different versions of that network are estimated, each of them corresponding to the short run, Granger and long IVN as defined in Barigozzi and Brownlees (2016).

As discussed by Strohsal and Weber (2012), the concept of market volatility has been ambiguously used in the financial literature as a proxy of the flow of fundamental information arriving to the market and as a measure of investor's uncertainty. Consequently, volatility spillovers across countries can be associated either to the transmission of valuable information across fundamentally interrelated economies or to the transfer of pure uncertainty. I explore this intuition by comparing the long run IVN with another network built upon data on international trades. This International Trade Network (ITN) is formed by the same set of nodes than in the IVNs while the weights of the links account for the value of bilateral export-import flows. Assuming that international trades are sufficient statistics of the "fundamental" interconnections between pairs of economies and in the case that market volatilities carry only economical relevant information, the IVN and the ITN should resemble each other closely. Otherwise, the ITN would be a sub-structure embedded into IVN where the excess interconnections in the latter represent channel through which fear-related shocks flow.

To estimate the IVNs, I implement a combination of Lasso related techniques (Zou (2006), Friedman, Hastie, and Tibshirani (2008), Barigozzi and Brownlees (2016)) upon daily data of US-listed ETFs. This sample covers the period Jun-2013 to Jan-2016 and includes 17 international ETFs where most of them belong to the MSCI iShare family. The main benefit of using ETFs instead of market indices is that it allows to encompass a large panel of countries without the need of cumbersome adjustments due to non-overlapping trading hours. Therefore, I exploit the informational efficiency property of ETFs that has been previously discussed in the literature (Khorana, Nelling, and Tester (1998), Tse and Martinez (2007)). To identify the ITN, I gather data

from the DOT database maintained by the International Monetary Fund regarding the value of bilateral exports and imports for the same period and countries than in ETF dataset.

The first set of results stem from the comparison between the long run IVN and ITN. I find evidence indicating that the correlation between the rankings of *centrality* of countries across these structures is positive and statistically significant. Therefore, highly influential economies in the IVN tends to be highly influential in the ITN, in accordance with the notion of volatility spillovers across fundamentally connected markets. I also report two additional empirical results that provide further support to the hypothesis of informational content of volatility transfers: first, the amount of link's overlapping between the IVN and ITN is unlikely to be generated by random arrangements of connections and second, the slope coefficient that results by regressing the weights of the links form the IVN on the weights of the same links from the ITN is positive and statistically significant. Furthermore, the evidence also indicates that Asian markets, say Hong Kong, China and Japan, are systematically more central as volatility spreaders than as trade partners. A rolling-window analysis confirms this trend and shows that this disproportional influence of Asian markets in the IVN is a relatively new feature that became evident since the Chinese's Black Monday.

The second results come from a detailed analysis on the patterns of lead-lags interactions among markets as contained in the Granger IVN. I find that the magnitude and frequency of volatility lead-lags is larger for pairs of economies located in the same continent than across them. To quantify this tendency, the assortativity coefficient proposed by Newman (2003) is computed indicating the existence of *communities* in the Granger IVN. These communities are formed by tightly interconnected countries that are located in the same continent but weakly interconnected across them. As a plausible explanation for this pattern, the gradual diffusion of information hypothesis discussed in Menzly and Ozbas (2010) is proposed. More precisely, I theorize that specialized investors focused on a particular group of markets are able to incorporate rapidly the innovation arising in those target markets while processing the news from other fundamentally interrelated economies with some delay. I formally test this hypothesis conforming the third result of this study. To do that, an econometric gradual information diffusion model is estimated as in Rapach, Strauss, and Zhou (2013) where the hypothesis of instantaneous diffusion is rejected at any sensible level of significance.

This study is built upon the growing literature of networks based on financial time series (Billio et al. (2012), Diebold and Yilmaz (2014), Hautsch, Schaumburg, and Schienle (2015), Tse, Liu, and Lau (2010), Peralta (2015), Barigozzi and Brownlees (2016)). The closest papers to this manuscript are Diebold and Yilmaz (2014), Diebold and Yilmaz (2015), however, the former is particular concerned on US domestic securities while the latter only considers American and European financial firms. To the extent of my knowledge, this is the only study combining ETFs data with network theory in order to shed some light on process of volatility spillovers across countries.

The remainder of this paper is organized as follows. Section 2 discusses salient features of the ETF market highlighting the informational efficiency of this asset class. Section 3 introduces the International Volatility Network and provides fundamental definitions of network measures. Section 4 describes the datasets and the empirical framework. Section 5 reports the main empirical results. Section 6 formally tests the gradual diffusion of information hypothesis as a plausible explanation of volatility lead-lags. Finally, section 7 concludes and outlines directions for future research.

2. The Informational Efficiency of ETFs

In a nutshell, Exchange-Traded Funds (ETFs) are pool investment vehicles designed to passively track the performance of a benchmark index, thus allowing investors to benefit from diversification with just one trade. The first ETF was launched in 1993 with the goal of replicating the S&P-500 index, since then, this class of financial assets has shown a striking growth. In accordance to Investment Company Institute (2015), the assets under management of ETFs reached to nearly $2 trillion at year-end 2014 for the US market representing 11% of the total Net Asset Value (NAV) managed by the investment companies industry (see figure 2). The remarkable acceptance of this asset class is evident by noting that its mean annual growth rate for the period 2004-2014 was 24.1%, more than three times larger than for the traditional mutual fund industry (7.0%).

As stated in Gastineau (2010), there are many differences between the shares of ETFs and the ones of Equity Index Mutual Funds (MF). Among them it is worth mentioning that: *(i)* ETFs shares are continuously traded during a trading day at a market-determined price similarly as with any other common stock. In contrast, MFs shares are not listed securities and they are bought and sold at the end-of-day NAV's rule, *(ii)* ETFs can be purchased on margin or sold short, characteristics not shown by the equivalent MFs, *(iii)* despite tracking errors in both asset classes, the intra-day

divergence between the NAVs and market prices for ETFs is constraint and short-lived in practice given the internal mechanism of *in-kind creation and redemption of shares* (see below). Since there are not market price for an open-end MFs this comparison is meaningless while for close-end MFs such difference can be substantial.

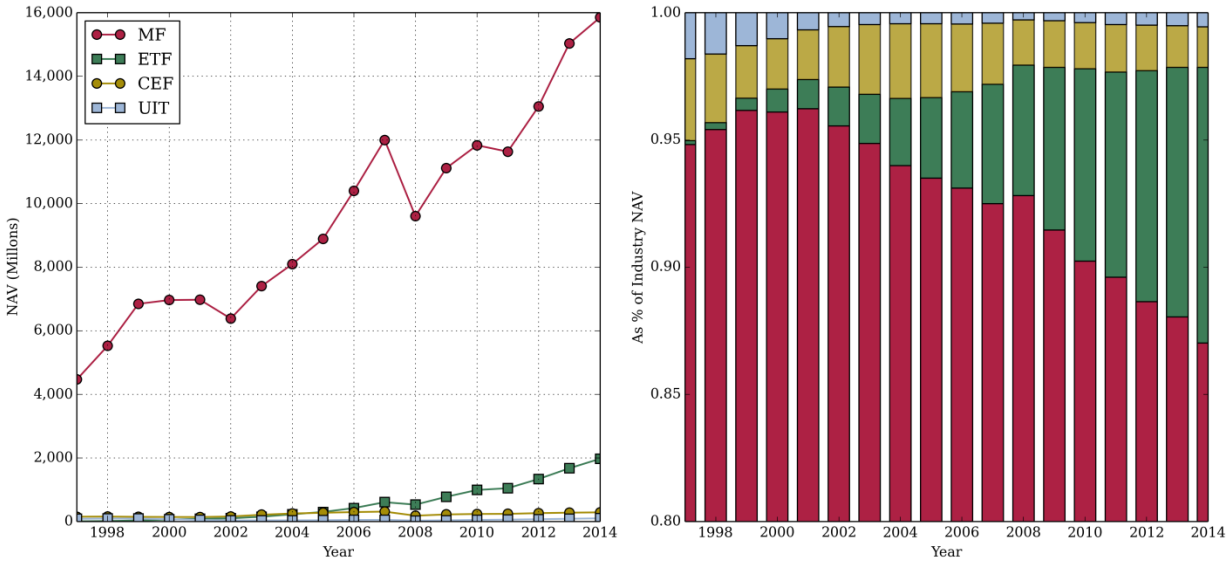

Figure 2: Total Net Asset Value by categories of investment firms in terms Millions of US dollars (left panel) and as a percentage of the total (right panel). The references are as follows: Open-end Mutual Fund (MF), Exchange-Traded Funds (ETF), Closed-end Mutual Fund (CEF) and Unit Investment Trust (UIT).Source: Investment Company Institute (2015)

The informational efficiency of ETFs is ensured through the *in-kind creation and redemption* of shares that prevents large differences between market prices and NAVs. ETF's shares are created when an Authorized Participant (AP), usually a large financial firm, deposits in the fund the creation basket in exchange of ETF's shares. These newly created shares are subsequently traded in the market similarly as with any other ordinary stock (see figure 3). ETF's shares are redeemed when the AP returns to the fund some of its shares in exchange to the redemption basket. The creation and redemption of ETFs shares are referred to as primary market operations while the subsequent trades of outstanding shares correspond to secondary market operations.

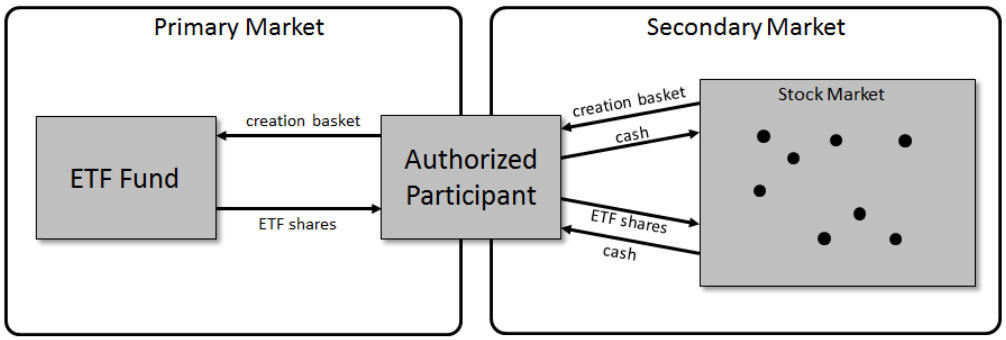

Figure 3: Schematic representation of the ETF shares creation process. The redemption process follows the same steps but reversing the direction of the arrows

Note that any divergence between NAVs and market prices must be short-lived; otherwise, free-lunch profit can be traded by the AP through the mechanism of creation and redemption of shares. If the price of ETFs shares is below NAV, the AP can buy those securities in the market and redeem them to the fund in exchange to the redemption basket, thus obtaining the benefit from the difference between them. In the contrary, if the market price of the ETF is above NAV, the AP could buy the creation basket and deposit it to the fun in exchange to new ETF shares. Again, this provides the AP with the profit from the difference.[33]

The notion of ETFs as highly efficient assets is not just a theoretical argument since it is also supported by substantial empirical evidence. Khorana, Nelling, and Tester (1998) and Tse and Martinez (2007) highlight the good performance of international ETFs in tracking the corresponding indices. In the same line of arguments, Hughen and Mathew (2009) points out the relative efficiency of ETFs versus closed-end MF by incorporating in their price the changes in foreign NAVs in a more accurate and faster way. The subsequent empirical analysis relies on ETF data to analyze volatility spillovers across countries instead of using broad market indices. [34] This is mainly explained as a way to avoid adjustments for non-overlapping trading hours whereas it is justified by the informational efficiency property of this asset class juts commented.

[33] In addition, since ETFs funds are obliged to disclose the creation and redemption baskets of securities on a daily basis, the gap between NAVs and market prices is further discourage.

[34] In accordance to Investment Company Institute (2015), country-specific ETFs represents the second largest category accounting for almost 21% in terms of industry's NAV.

3. The International Volatility Network

In general terms, a network $K = \{N, \omega\}$ is composed by the set of nodes $N = \{1,2, \dots, n\}$ and the set of links ω connecting pairs of them. If there is a link between nodes i and j, it is indicated as $(i,j) \in \omega$. A convenient rearrangement of the information contained in ω is provided by the $n \times n$ adjacency matrix $\pi = [\pi_{ij}]$ whose element $\pi_{\mathrm{ij}} \neq 0$ whenever $(i,j) \in \omega$. Accordingly, the sets $\{N, \omega\}$ and $\{N, \pi\}$ are two different ways to represent the same structure. The network K is said to be undirected if no-causal relationships are attached to the links which in turns implies that $\pi = \pi'$ since $(i,j) \in \omega \Leftrightarrow (j,i) \in \omega$. When π_{ij} entails a causal association from node j to node i, K is said to be directed. In this case, it is likely that $\pi \neq \pi'$ since $(i,j) \in \omega$ does not necessarily imply $(j,i) \in \omega$. For unweighted networks, $\pi_{ij} \in \{0,1\}$ and therefore only on/off relationships exist. On the contrary, when $\pi_{ij} \in \mathbb{R}$, the links track the intensity of the interactions between nodes giving rise to weighted networks.[35]

The International Volatility Network (IVN) is a structure capturing the cross sectional dependency among the time series of market volatilities from a set of countries. Let us consider the n-dimensional vector of returns volatilities indicated as $\sigma_t = [\sigma_{i,t}]$ where each element $\sigma_{i,t}$ accounts for the volatility of the capital market in country i at period t. Let us assume that σ_t follows an n-dimensional and stationary vector autoregression model of order 1, $VAR(1)$, as stated in equation (1)[36]. It is assumed that the vector σ_t is centered thus discarding the constant term in (1).

$$\sigma_t = B\, \sigma_{t-1} + u_t, \qquad u_t \sim w.n.(0, \Theta_s) \tag{1}$$

The elements b_{ij} from the $n \times n$ coefficient matrix B represent the impact of country's *j* volatility in period $t-1$ on country's *i* volatility in period t while $\Theta_s = [\theta_{ij,s}]$ is the covariance matrix of residuals. Two versions of the IVN can be defined from equation (1). Let us first introduce the *Granger IVN* accounting for lead-lag volatility relationships among countries as follows:

35 The reader is referred to Jackson (2010) or Newman (2010) for a comprehensive treatment of the network literature.
36 As discussed by Andersen et al. (2003), there are some benefits for modeling a panel of volatilities as a VAR process instead of more complicated ARCH specifications.

Definition 1. *The Granger International Volatility Network is a weighted and directed network denoted by* $K^G = (N, B)$ *where* N *is the set of country-specific capital markets and* B *from equation (1) is the corresponding adjacency matrix.*

The second network derived from equation (1) is named s*hort run IVN* and captures the contemporaneous interactions as determined by the partial correlations of the VAR residuals. Given Θ_s, the corresponding concentration matrix is denoted by $\Psi_s[\psi_{ij,s}] \equiv \Theta_s^{-1}$. Then, the partial correlation matrix is $\rho_s \equiv -\Delta_s \Psi_s \Delta_s$ where Δ_s is a $n \times n$ diagonal matrix whose *ith*-main diagonal element is $(\psi_{ii,s})^{-1/2}$. Then, the *short run IVN* is defined as follows.

Definition 2. *The short run International Volatility Network is a weighted and undirected network denoted by* $K_s = (N, \rho_s)$ *where* N *is the set of country-specific capital markets and* ρ_s *is the corresponding adjacency matrix representing the partial correlation matrix of residuals.*

The partial correlation matrix of residuals is not a sufficient statistic for the conditional dependency structure of σ_t when serial correlations take place. Barigozzi and Brownlees (2016) proposes to measure the cross-sectional conditional dependency in the long run by means of the long run partial correlation matrix ρ_L encompassing not only contemporaneous interactions but lead-lags as well. To formally introduce ρ_L, let us first define the long run concentration matrix as[37]

$$\Psi_L = (I_n - B)' \Psi_s (I_n - B) \tag{2}$$

where I_n is an n-dimensional identity matrix. Accordingly, the long run partial correlation matrix could be written as $\rho_L \equiv -\Delta_L \Psi_L \Delta_L$ where Δ_L is a $n \times n$ diagonal matrix whose *ith*-main diagonal element is $(\psi_{ii,L})^{-1/2}$. Then, the *long run IVN* results from a non-trivial combination of the short run IVN and the Granger IVN and it is formally stated as follows.

Definition 3. *The long run International Volatility Network is a weighted and undirected network denoted by* $K_L = (N, \rho_L)$ *where* N *is the set of country-specific capital markets and* ρ_L *is the corresponding adjacency matrix representing the long run partial correlation of the* σ_t.

[37] If the second moment of the process (1) is denoted by $\Gamma_\sigma(h) = E(\sigma_t \sigma_{t-h})$, the long run covariance matrix is $\Theta_L = \sum_{h=-\infty}^{\infty} \Gamma_\sigma(h) = (I - B)^{-1} \Theta_s (I - B')^{-1}$. See Barigozzi and Brownlees (2016) for a detailed explanation.

3.1 Network statistics

Since several network statistics are reported throughout the empirical analysis, I collect and define them in this subsection to enhance readability. *Node-size* and *link-size* account for the number of nodes and links in the network $K = (N, [\pi_{ij}])$. The *density* of K measures the fraction of links that actually exist relative to the maximum possible number links in the structure.

For undirected networks, the *degree of node i* (l_i) is the number of links attached to it while the *mean degree* of K captures the average number of links per node. The *degree distribution* of K is denoted by $P(l)$ and represents the empirical distribution of nodes' degrees. For directed networks, the *in-degree of node i* (l_i^{in}) is the number of incoming links attached to it while the *out-degree of node i* (l_i^{out}) accounts for the number of its outgoing links. Similarly to the case of undirected network, for directed structure there is an *in-degree distribution* $P_{in}(l)$ and an *out-degree distribution* $P_{out}(l)$ with similar interpretation as for $P(l)$. Since an outgoing-link from node i corresponds to an incoming-link to node j, the *mean in-degree* of K must be equal to its *mean out-degree*.

An important part of the network literature is devoted to quantify the importance/influence of nodes in a given structure. The most basic centrality measure is *degree centrality* simply accounting for the degrees of the nodes. Therefore, node i is relatively more central than j if $l_i > l_j$. An extension to the degree centrality is provided by the *eigenvector centrality* studied in Bonacich (1972), Bonacich (1987), Bonacich (2007) and extended to weighted network by Newman (2004). The eigenvector centrality of node i, denoted by v_i, corresponds to the weighted sum of its neighbors' eigenvector centrality where π_{ij} are the weighting factors as in equation (3). Therefore, node i is central as long as it is connected to many other central nodes.

$$v_i = \lambda^{-1} \sum_j \pi_{ij} \, v_j \tag{3}$$

By restating expression (3) in matrix terms, we obtain $\lambda v = \rho v$ indicating that the centrality vector v is given by the eigenvector of the adjacency matrix ρ corresponding to largest eigenvalue λ.[38]

38 In principle each eigenvectors of Ω is a solution to equation to (3). However, the centrality vector corresponding to the largest component in the network is given by the eigenvector corresponding to the largest eigenvalue (Bonacich, 1972).

Finally, the assortativity coefficient r (Newman (2003)) quantifying the extent to which a particular network is organized in communities. Assume that the nodes of K are grouped into a set of exclusive and exhaustive categories. Then, r quantifies how likely is to observe the amount of links connecting nodes from same category relative to what it would be expected from a random arrangement. The coefficient $r \in [\underline{r}, 1]$ where 1, 0 and $\underline{r}$ correspond to perfect positive assortativity (nodes belonging to a particular category are only connected to other nodes from the same category), pure random mixing and perfect disassortativity (nodes belonging to a particular category are only connected to nodes from a different category).

4. Data and Empirical Framework

4.1 Data

To circumvent the data adjustments due to non-overlapping trading hours across markets, I exploit the informational efficiency of ETF as discussed in section 2 (see Appendix B for a detail description of open and closing times for the countries in the current sample). Therefore, I collect daily data for a panel of US-listed ETFs replicating the Morgan Stanly Capital International (MSCI) indices corresponding to major financial centers.[39] The sample comprises 16 developed economies as determined by MCSI plus China as an additional emerging market. For the particular case of the US market, I consider SPDR (ticker SPY) instead of the corresponding iShare's ETF since this security is more representative of this industry. I gather this information from Datastream including Open, Close, High and Low prices for the period Jun-2013 to Jan-2016. The final selection of countries in the sample results by discarding iShare ETFs from the set of developed economies when missing data is detected or when the daily average turnover during the last month of the sample is below 100.000 trades.[40]

Table 1 reports the list of countries included in the sample, their total market capitalization as reported by the Bloomberg and some variables characterizing the corresponding ETFs. Note that set of selected economies represents more than 80% of the worldwide market capitalization providing a global perspective on the matter.

[39] MSCI indices are cap-weighted indices commonly used for tracking the performances of particular international capital markets or sectors where broad coverage and comparability are major concerns.

[40] Except for Austria with average daily turnover of 97.000 in the last month of the sample, nearly close to the predefined threshold.

Countries	Market Capitalization (1) Bill $	%	Benchmark Index	Ticker	Short Name	Total NAV (Millons $) (2)	Avr Daily Turover (Thousand) (3)
America							
Canada	1,576	2.7%	MSCI Canada	EWC	CAN	1,639.70	3,286
United States	21,520	37.0%	S&P 500	SPY	USA	169,154.66	195,418
Europe							
Austria	88	0.2%	MSCI Austria IMI 25/50	EWO	AUT	50.63	97
Belgium	376	0.6%	MSCI Belgium IMI 25/50	EWK	BEL	203.94	321
France	1,759	3.0%	MSCI France	EWQ	FRA	358.88	2,058
Germany	1,626	2.8%	MSCI Germany	EWG	DEU	5,517.67	8,521
Italy	494	0.8%	MSCI Italy 25/50	EWI	ITA	809.99	3,200
Netherlands	371	0.6%	MSCI Netherlands Investable	EWN	NLD	143.05	353
Spain	568	1.0%	MSCI Spain 25/50	EWP	ESP	958.61	2,435
Sweden	619	1.1%	MSCI Sweden	EWD	SWE	296.36	453
Switzerland	1,377	2.4%	MSCI Switzerland 25/50	EWL	CHE	1,144.60	1,763
United Kingdom	2,996	5.1%	MSCI United Kingdom	EWU	GBR	2,177.16	5,819
Asia-Pacific							
Australia	964	1.7%	MSCI Australia	EWA	AUS	1,159.50	4,374
China	5,772	9.9%	MSCI China Index	MCHI	CHN	1,750.65	1,438
Hong Kong	3,573	6.1%	MSCI Hong Kong	EWH	HK	1,913.06	6,894
Japan	4,511	7.7%	MSCI Japan	EWJ	JPN	18,942.19	66,016
Singapore	442	0.8%	MSCI Singapore	EWS	SGP	460.88	2,196

Table 1: international ETFs included in the sample.

(1) Retrived from Bloomberg for Feb 24, 2016 and % corresponds to the proportion relative to the worlwide market capitalization

(2) Retrived from in www.ishares.com for Dec 31, 2015 and from www.spdrs.com for Feb 08, 2016.

(3) Retrived from Datastream. Avergae Turnover are in thousand and correspond to January 2016

From each of the countries included in the sample, I also obtain monthly records on the U.S. dollar value of bilateral total exports and imports from the Direction of Trade Statistics (DOTS) database maintained by the International Monetary Fund.[41] Therefore, this dataset allows the computation of trade links between pairs of countries. To maintain consistency with the ETF dataset, I consider the cumulative values of exports and imports from Jan-2013 until Sep-2015 where the latter date corresponds to most recent published period.

4.2 Empirical framework

As far as the volatility process is concerned, I assume that σ_t follows a VAR model as indicated in equation (1). This volatility modelling is not new in the financial literature since similar approaches have been previously considered (see Diebold and Yilmaz (2014), Diebold and Yilmaz (2012), Diebold and Yilmaz (2009), Diebold and Yilmaz (2015), Barigozzi and Brownlees (2016), Jung and Maderitsch (2014), Andersen et al. (2003)).

[41] Available in https://www.imf.org/en/data

I measure the volatility of country i in period t, σ_{it}, by means of range-based volatility estimators as in Garman and Klass (1980) due to their relatively efficiency and robustness to microstructure noise (bid-ask bounce) as argued by Alizadeh, Brandt, and Diebold (2002). Assume that $p_{t,i}^{H}$, $p_{t,i}^{L}$, $p_{t,i}^{O}$ and $p_{t,i}^{C}$ account for the logarithm of the high, low, opening and closing price of country's i ETF in period t, respectively. By introducing the next three auxiliary variables $u = \left(p_{t,i}^{H} - p_{t,i}^{O}\right)$, $d = \left(p_{t,i}^{L} - p_{t,i}^{O}\right)$, $c = \left(p_{t,i}^{C} - p_{t,i}^{O}\right)$ to simplify notation, a relatively efficient volatility estimators of σ_{it} is stated in equation (4) following Garman and Klass (1980, p. 74)

$$\hat{\sigma}_{t,i}^{2} = 0.511(u-d)^{2} - 0.019[c(u+d) - 2ud] - 0.383c^{2} \tag{4}$$

There are convincing evidence showing the existence of a systematic factor leading the auto and cross-correlations of volatilities across countries (Alizadeh, Brandt, and Diebold (2002), Bekaert, Hodrick, and Zhang (2012), Dimpfl and Jung (2012)). Since this observation is inconsistent with the identification of sparse IVNs, I control for systematic components by applying the network estimation approach (described below) upon the series of residuals $\varepsilon_{t,i}$ coming from the regressions (5).

$$\log\left(\hat{\sigma}_{t,i}^{2}\right) = \beta_0 + \beta_d \gamma_{t,i} + \beta_w \gamma_{t,i}^{w} + \beta_m \gamma_{t,i}^{m} + \varepsilon_{t,i} \quad for\ i = 1,2,\dots,n \tag{5}$$

The variable $\gamma_{t,i}$ in (5) is the contemporaneous value of the first principal component of the panel of log volatilities while $\gamma_{t,i}^{w}$ and $\gamma_{t,i}^{m}$ correspond to its mean value over the weekly and monthly time horizon, respectively. There are two aspects that deserve some attention from expression (5). First, since volatility distributions tend to be positively skew, Andersen et al. (2003) suggests to take logarithm to obtain approximately normality which explains the left-hand side term in equation (5). Second, given that the estimated log volatilities present strong persistence with large autocorrelation coefficients even for 20 lags (see table 2 for descriptive statistics), I follow the approach of Jung and Maderitsch (2014) by including $\gamma_{t,i}^{w}$ and $\gamma_{t,i}^{m}$ to properly control for common factors with the most descriptive yet parsimonious model.

The strategy to estimate the IVNs is divided in two stages. In the first stage of the procedure I estimate the matrix B from model (1) by implementing Adaptive Lasso proposed by Zou (2006). The Least Absolute Shrinkage and Selection Operator method (Lasso) proposed by Tibshirani

(1996) is specifically designed to improve OLS results by performing continues shrinkage on regression coefficients and automatic variable selection. Zou (2006) shows that $l1$ regularized models must satisfy non trivial conditions to be an oracle procedure (consistency in selecting and asymptotic normality). This leads the author to propose the Adaptive Lasso to overcome such deficiency. I implement this technique by estimating equation (1) on a row-by-row basis by solving the next expressions

$$\hat{\beta}_i = \arg\min_{\beta_i \in \mathbb{R}^n_+} \left(\sum_{t=1}^{T} \left(\hat{\varepsilon}_{t,i} - \beta_i' \hat{\varepsilon}_{t-1} \right)^2 + \lambda_1 \sum_{j=1}^{n} w_{ij} |\beta_{i,j}| \right) \quad for\ i = 1,2, \dots, n \tag{6}$$

The weighting loadings $w = (w_1 \dots w_n)'$ in (6) are computed as $w_{ij} = \left(|\tilde{\beta}_{ij}| \right)^{-\gamma} for\ j = 1 \dots n$ where $\tilde{\beta}_{ij}$ denotes initial OLS estimations from a regression of $\hat{\varepsilon}_{t,i}$ on $\hat{\varepsilon}_{t-1}$ and $|a|$ is the absolute value of a. Following the convention in the literature, explanatory variables are standardized before computing $\hat{\beta}_i$ and (λ_1, γ) is selected by 3-fold cross validation. See Appendix A for detailed steps of the estimation methodology.

In the second stage of the procedure, Graphical Lasso (GL) algorithm developed by Friedman, Hastie, and Tibshirani (2008) is implemented to get an sparse estimation of the precision matrix Ψ_s where the series of residuals come from solving equation (6). This approach maximizes the penalized log-likelihood of a multivariate normal distribution with respect to the precision matrix by means of Lasso regressions as follows.

$$\widehat{\Psi}_s = \arg\max_{\Psi_s} \left(\log(\det(\Psi_s)) - tr\left(\widehat{\Theta}_s \Psi_s \right) - \lambda_2 \|\Psi_s\|_1 \right) \tag{7}$$

where, $det(A)$, $tr(A)$ and $\|\mathrm{A}\|_1$ denotes the determinant, trace and L_1 norm (sum of absolute values of the elements) of matrix A while $\widehat{\Theta}_s$ is the sample covariance matrix of the series residuals coming from (6). As before, variables are standardized before computing $\widehat{\Psi}_s$ and λ_2 is selected by 3-fold cross validation. The estimated long run partial correlation matrix, say the adjacency matrix of the long run IVN, results from plugging the estimated matrices $\hat{B}$ and $\widehat{\Psi}_s$ into equation (2). In order to focus on large volatility spillovers across countries, the absolute values of $\rho_{ij,L}$ are considered across the study while discarding meaningless self-loops from the long run IVN.

5. Empirical Results

5.1 Descriptive statistics

The descriptive statistics for the log volatilities' series of the sampled ETFs are reported in table 2 where the first principal component is also included for comparison. Note that the means and percentiles assume negative values due to logarithmization. Most of the characteristics exhibited in table 2 like positively skew distributions, excess kurtosis, large autocorrelations and strong persistence, have been previously reported in the literature (see Andersen et al. (2003), Jung and Maderitsch (2014)). Tables C1 and C2 in Appendix C present the same descriptive statistics as in table 2 considering the time series of annualized volatilities and volatility residuals, respectively. From the inspection of tables 2 and C1 it worth noting how the logarithmic transformation effectively encourages normality in terms of both, skewness and kurtosis.

Countries	Mean	Median	Min	Max	Std	Skewness	Kurtosis	Autocorrelation			
								Lag 1	Lag 5	Lag 10	Lag 20
Noth America											
Canada	-10.18	-10.20	-13.43	-6.14	0.96	0.29	0.44	0.50	0.43	0.30	0.27
United States	-10.56	-10.55	-13.30	-5.77	1.03	0.33	0.53	0.53	0.32	0.16	0.11
Europe											
Austria	-10.57	-10.61	-13.51	-6.95	0.90	0.20	0.66	0.28	0.15	0.17	0.06
Belgium	-10.75	-10.75	-13.95	-7.06	0.89	0.18	0.50	0.30	0.24	0.12	0.09
France	-10.43	-10.43	-13.18	-6.75	0.95	0.15	0.26	0.36	0.29	0.12	0.16
Germany	-10.37	-10.35	-12.60	-6.74	0.94	0.14	-0.13	0.44	0.32	0.18	0.22
Italy	-9.89	-9.93	-12.15	-7.05	0.82	0.40	0.30	0.35	0.26	0.12	0.10
Netherlands	-10.76	-10.76	-13.58	-6.42	0.98	0.07	0.41	0.42	0.32	0.17	0.19
Spain	-10.10	-10.09	-12.66	-6.92	0.90	0.18	0.13	0.34	0.22	0.08	0.12
Sweden	-10.40	-10.44	-12.80	-6.95	0.86	0.33	0.48	0.36	0.25	0.11	0.13
Switzerland	-10.86	-10.89	-13.59	-6.91	0.90	0.32	0.66	0.40	0.26	0.18	0.18
United Kingdom	-10.61	-10.61	-13.51	-7.12	0.88	0.31	0.70	0.47	0.34	0.20	0.17
Asia-Pacific											
Australia	-10.50	-10.54	-14.40	-7.06	0.97	0.12	0.69	0.47	0.39	0.29	0.25
China	-10.19	-10.24	-12.95	-5.58	0.96	0.32	0.87	0.49	0.33	0.19	0.19
Hong Kong	-10.73	-10.79	-13.23	-5.94	0.91	0.53	1.21	0.47	0.27	0.17	0.11
Japan	-10.72	-10.76	-13.04	-6.97	0.95	0.27	-0.03	0.53	0.36	0.20	0.17
Singapore	-10.98	-11.00	-13.92	-6.78	0.94	0.40	1.06	0.41	0.31	0.20	0.20
Global											
First PC	-43.09	-43.35	-50.07	-27.55	3.10	0.69	1.07	0.52	0.36	0.19	0.19

Table 2: Descriptive statistics log Volatility for period 2013-6 to 2016-1

For ease of comparison, the boxplots of the annualized volatility distributions by countries are depicted in figure 4 where the largest mean variance are shown by Italy (12.3%) and Spain (11.3%) while the lowest corresponds to Singapore (7.4%) and Switzerland (7.7%).

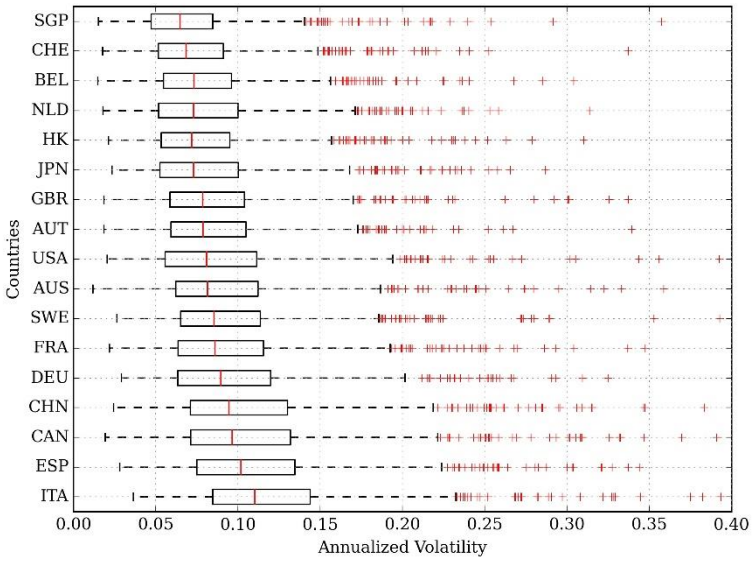

Figure 4: Distribution of Annualized Volatility by country-specific ETFs during the period Jun-2013 to Jan-2016.

5.2 The relation between the IVN and ITN

As suggested by Strohsal and Weber (2012), market volatility has been ambiguously used in the literature involving the arrival of valuable news to the market as well as capturing pure uncertainty. Accordingly, volatility spillovers across markets can indicate the spread of valuable information among fundamentally interrelated economies or the transfer of uncertainly across them. The subsequent analysis attempts to discriminate between these two notions of volatility spillovers by relying on the approach of network theory.

Let us introduce the International Trade Network (ITN) build upon the DOTS dataset (see section 4.1) and entailing the fundamental interconnections among countries as determined by their trade patterns. More specifically, the ITN denoted by $K_T = (N, \rho_T)$ is an undirected and weighted network where N is the set of countries included in the ETF sample while the element $\rho_{ij,T}$ from its adjacency matrix quantifies the logarithm of the sum of the US dollar values of exports and imports between countries i and j.[42] In the case that volatilities carry valuable information and assuming that trade patterns are sufficient statistics of fundamental interactions across countries, the IVN and ITN

[42] For reporting issues, the value of exports reported by country i to country j presents small differences with the value of the imports reported by county j from country i. To solve this inconsistency, the mean between this to quantities is considered.

should resemble each other closely. Otherwise, ITN should be a sort of subnetwork embedded into IVN where the excess interconnectivity from the latter structure indicates uncertainty-related links.

A first glance on the comparison between these two networks is provided by plotting pruned versions of the IVN and of the ITN in the right and left panel of figure 5, respectively. Since these two structures are fully connected networks, a pruning procedure is in place by discarding the least weighted links until the networks remain connected.

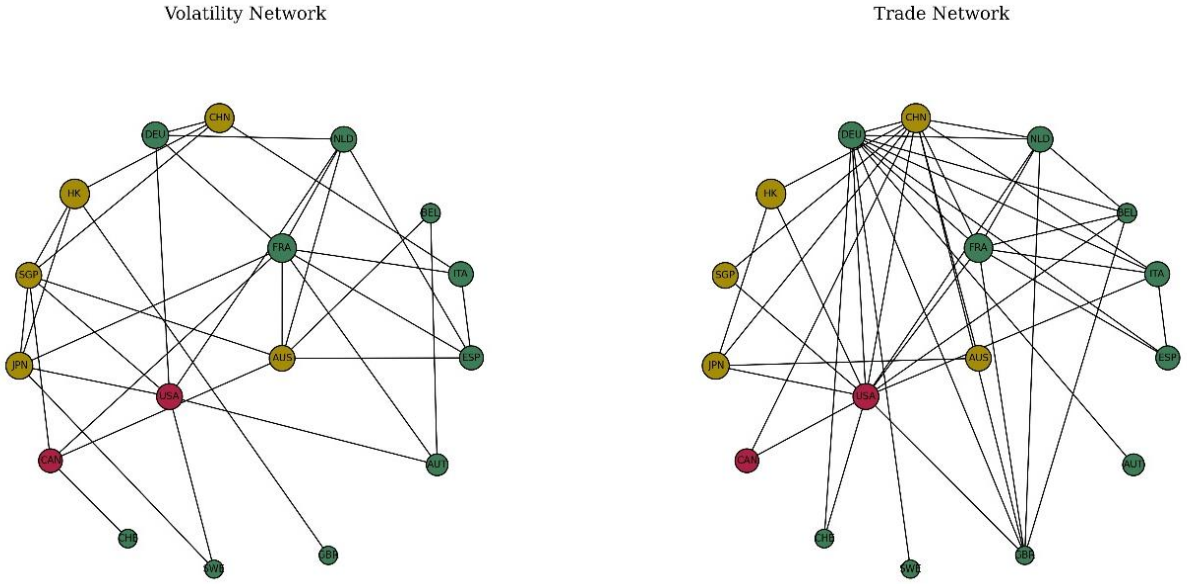

Figure 5: Pruned versions of the long run IVN and the ITN. The colors of the nodes correspond to the geographical region of the particular country as follows: North America (red), Europe (green) and Asia-Pacific (yellow).

Assuming that the fundament information spillover hypothesis holds, it should be observed a similar degree of countries' influence across the networks. The left panel of figure 6 depicts the eigenvector centrality in IVN noting that Hong Kong, China, France and Japan are the most central economies. The right panel from the same figure shows the scatterplot between the rankings of centralities in the IVN and ITN where a positive association is quantified by means of a significant Kendall rank correlation equal to 0.28. [43] Therefore, markets tend to show similar ranking of centralities across the network thus providing some support to the notion of fundamental spillovers. Interestingly, the extreme cases of United Kingdom and Hong Kong severely reduces the reported correlation and deserve further attention.

[43] The p-value of this coefficient is 5.1% and corresponds to a one-tailed test where $H_0: \tau \leq 0$ against $H_0: \tau > 0$ where τ denotes the Kendall correlation.

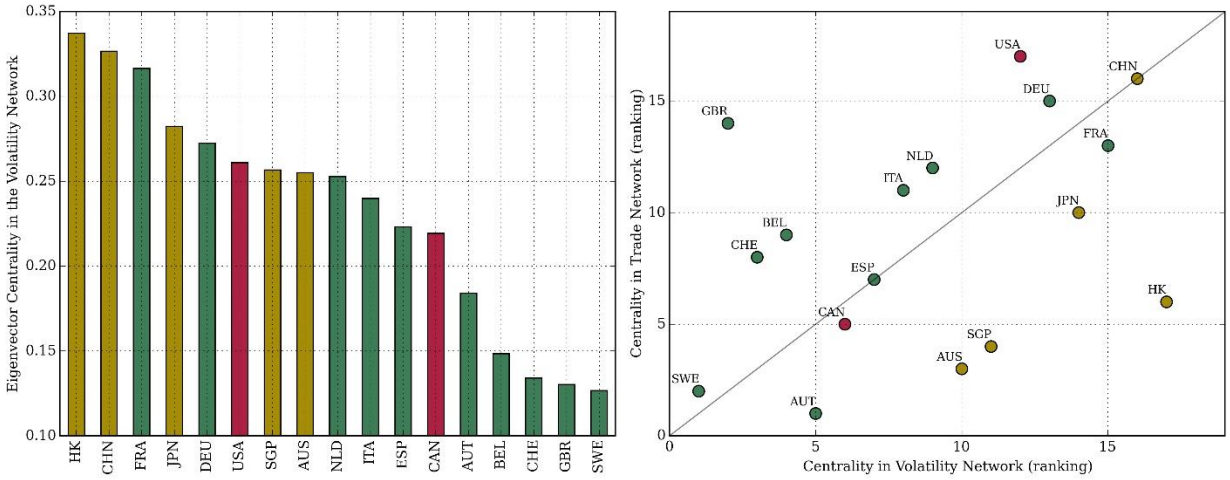

Figure 6: Eigenvector centrality by country in the long run IVN (left panel) and scatter plot of the rankings of eigenvector centrality in the IVN and the ITN. The colors correspond to the geographical region of the particular country as follows: America (red), Europe (green) and Asia-Pacific (yellow).

It is worth noting from the right panel of figure 6 that every Asian markets lie below the 45º line indicating that their centralities are systematically greater in the IVN than in the ITN. In other words, these economies show disproportional influence as volatility spreaders than as trade partners. The greater influences in the IVN shown by Asia markets have not always been the case. Figure 7 plots the moving average of the mean centrality by geographic regions. To build these series, I compute the long run IVN and the corresponding vector of centralities upon a set of 200-days long rolling windows with 1-day displacement steps. Note that the European and North American markets show larger mean centrality at the beginning of the analyzed period. However, the influence of Asian markets presents an upward trend that surpasses the centralities of European countries around mid Jul-2015 and the centralities North America countries by Aug-2015 while reaching its local maximum around the Chinese Black Monday (August 24, 2015). After one month of contraction, the influence of Asia markets has substantially increased placing that region at the top of this ranking of influence. On the other hand, the European and North American markets show a secular downward trend across time.

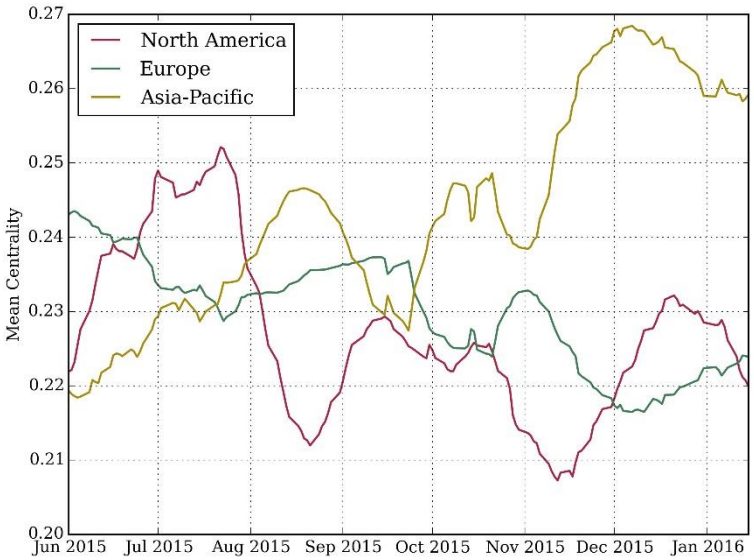

Figure 7: 20-days moving average of mean eigenvector centrality in the long run IVN grouped by geographic region and computed from 200-days long rolling windows with 1-day displacement steps.

The hypothesis of informational content of volatility spillovers is also consistent with a substantial overlapping of links between the IVN and the ITN indicating that volatility tends to flow across fundamentally connected economies. The pruned versions of IVN and the ITN present network densities of 25% and 31% where the number links that simultaneously exist in these structures is 15.[44] The following test is proposed in order to determine the likelihood of such amount of overlapping. I create two random networks (Erdös-Renyi framework) each with the same node-size and link-size as for the empirical IVN and ITN. Then, I identify the connections that simultaneously exists in both of these random replications. I repeat this procedure 10.000 times and compute the proportion of cases in which the amount of link's overlapping is equal or greater than 15. Since Erdös-Renyi framework provides networks made by chance, this ratio resembles a p-value in a traditional hypothesis test where the null hypothesis refers to non-systematic overlapping. For this case, the corresponding p-value is 4.5% indicating a low probability to observe this amount of link's overlapping between IVN and ITN under the null.

Finally, table 3 reports OLS estimations that results from regressing the weights attached to the links in the IVN on the weights of the same links in the ITN. Assuming that the informational content of volatility spillover's hypothesis holds, we should expect a positive and significant coefficient for the

[44] The link-sizes of the pruned versions of IVN and the ITN are 34 and 42 respectively

explanatory variable. Therefore, strong connections between countries as measured by trade links results in strong channels through which the volatility spreads. Indeed, this is the case since the value of the slope coefficient is 0.0142 with t-statistic of 3.36 while the constant term is not statistically different from zero at conventional levels. Figure D.1 in Appendix D presents the scatter plot with the regression results as a solid line showing this positive association.

	Coefficient	Stand Dev	p-value
Cons	-0.0733	0.0441	0.0989
Link-Weigths ITN	0.0142	0.0042	0.0010
F-test (p-value)		0.0010	
R-square		0.0777	
Num. Observations		136	

Table 3: OLS estimations of a regression where the dependent variable is the link-weigths in the IVN and the independent is the link-weigths in the ITN.

5.3 The Granger IVN

The salient features of the Granger IVN are studied in this section. Table 4 reports the corresponding adjacency matrix including in its last row the mean of the non-zero off-diagonal coefficients serving as a broad indicator of the country's relevance in the network (see Appendix E for a graphical representation of the network). The market with the largest mean impact is Hong Kong (0.11) mostly explained by its effects on the Chinese economy (0.24). In the second order of magnitude, economies like United Kingdom (0.08), Netherlands (0.08), Singapore (0.07), Japan (0.06) and France (0.06) represent other fundamental participants in this regards. Moreover, economies like Sweden and United Kingdom assume an exogenous role in the system since they are not affected by any of the rest of nodes in the network.

From a detailed inspection of table 4, it should be noted that Germany and Hong Kong strongly affects most of the economies located in the same continent. In particular, Germany affects 5 out of 9 European countries while Hong Kong impact on the rest of the Asian economies in the sample. In a different context, Hameed et al. (2015) defines firms whose fundamentals are highly correlated to those of peer firms as "bellwether firms". They show that when analysts revise a bellwether firm's

Noth America		CAN	USA	AUT	BEL	FRA	DEU	ITA	NLD	ESP	SWE	CHE	GBR	AUS	CHN	HK	JPN	SGP
Canada	CAN	0.18	-	-	-	-	-	-	0.01	-	-	-	-	0.01	-	-	-	-
United States	USA	0.02	0.16	-	-	-	-	-	-	-	-	-	-	-	-	-	0.01	0.00
Europe																		
Austria	AUT	-	-	-	-	-	-	-	-	-	-	-	-	-	-	-	-	-
Belgium	BEL	-	-	0.06	0.06	0.10	0.05	-	-	-	-	-	-	-	-	-	-	-
France	FRA	0.00	-	0.00	0.02	0.15	0.05	0.07	0.06	0.04	0.02	-	-	0.00	-	-	-	-
Germany	DEU	0.01	0.04	0.05	0.04	0.05	0.21	-	0.13	0.04	0.02	0.00	-	0.01	-	-	-	-
Italy	ITA	0.02	-	-	0.07	-	0.08	0.20	0.08	0.04	-	-	-	-	-	-	0.05	-
Netherlands	NLD	0.03	-	0.03	0.00	0.10	0.07	0.03	0.15	0.04	0.01	0.06	-	0.06	-	-	-	-
Spain	ESP	-	-	0.04	0.05	0.01	0.02	0.08	0.13	0.16	0.01	-	0.05	-	-	-	0.06	-
Sweden	SWE	-	-	-	-	-	-	-	-	-	-	-	-	-	-	-	-	-
Switzerland	CHE	-	-	0.02	-	-	-	-	-	-	-	0.11	-	-	-	-	-	-
United Kingdom	GBR	-	-	-	-	-	-	-	-	-	-	-	0.02	-	-	-	-	-
Asia-Pacific																		
Australia	AUS	0.08	0.02	-	-	-	-	-	0.06	-	0.04	0.05	0.06	0.07	0.07	0.02	-	0.08
China	CHN	-	-	-	-	-	-	-	-	-	-	-	0.05	-	0.12	0.24	-	0.12
Hong Kong	HK	-	0.03	-	-	-	-	0.00	-	-	0.02	-	-	-	0.07	0.22	0.10	0.13
Japan	JPN	-	0.00	-	-	-	-	-	-	-	-	-	-	-	0.04	0.06	0.24	0.04
Singapore	SGP	-	0.03	-	-	-	-	-	-	0.07	0.02	0.08	0.16	-	0.03	0.12	0.09	0.23
Mean Coefficient		0.03	0.02	0.03	0.03	0.06	0.05	0.05	0.08	0.05	0.02	0.05	0.08	0.02	0.05	0.11	0.06	0.07

Table 4: Adjacency matrix of the Granger IVN

earning forecast, it changes the prices of other firms significantly; however, the reverse effect is not supported by the data. For the particular case analyzed in this study, countries like Germany and Hong Kong resemble "bellwether countries" in the spirit of Hameed et al. (2015). It seems interesting to determine to which extent analyst coverage is plausible explanation for this empirical finding. I leave this open question as a future research line.

Additionally, note that table 4 reports that non-zero lead-lags coefficients tend to be more frequently found between countries from the same geographic area. From a network theory perspectives, this indicates that the Granger IVN is organized in communities where countries from the same continent are tightly interconnected among them but weakly interconnected across continents. This intuition is confirmed by means of a positive assortativity coefficient (see section 3.1) equal to 0.447 that result from grouping together economies from the same geographic region. Therefore, the probability of finding a non-null volatility lead-lag coefficient between pairs of countries located in the same continent is larger than what it would be expected by chance. One plausible explanation for these pattern of interconnectivity is further investigated in section 6.

6. Evidence of Gradual Diffusion of Information across International Markets

The evidence presented in section 5.3 indicates that the Granger IVN is organized in communities of countries grouped by continents. This non-random arrangement of connections is consistent with the hypothesis of a gradual diffusion of news in informational segmented markets (Menzly and Ozbas (2010)). More specifically, it might be the case that specialized investors following a specific group of markets incorporate rapidly the information related to those target economies in the prices of the corresponding ETFs while processing the information arising from other markets with some delay. To formally test this hypothesis, I propose the empirical information diffusion model given in (8) which is a generalization of the econometric specification presented in Rapach, Strauss, and Zhou (2013, p. 1650).

$$\hat{\varepsilon}_t = (\theta \circ \lambda)\eta_t + [(\mathbf{1} - \theta) \circ \lambda]\eta_{t-1} \tag{8}$$

where $\hat{\varepsilon}_t$ is the volatility residual (shocks of volatility) vector in period t as defined in (5), $\circ$ stands for the Hadamard product, $\mathbf{1}$ is an $n \times n$ matrix of ones and η_t is a n-dimensional multivariate Gaussian white noise of the form $\phi_n(\emptyset, \sigma_\eta^2 I_n)$ representing the arrival of news to the markets. The

element λ_{ij} from the $n \times n$ matrix λ measures the impacts of unit informational shocks from country j to country i while the element θ_{ij} from $n \times n$ matrix θ measures the frictional diffusion of information. Therefore, the total unit shock from country j to country i in period t, denoted by $\lambda_{ij}\eta_{jt}$, is contemporaneously absorbed by $\hat{\varepsilon}_{it}$ in a proportion equal to θ_{ij} while the remaining part is incorporated with a delay in period $t+1$ through the term $(1-\theta_{ij})\lambda_{ij}\eta_{jt}$. To simplify notation, let us denote $(\theta \circ \lambda)$ by Ω_a and $[(\mathbf{1}-\theta) \circ \lambda]$ by Ω_b leading to

$$\hat{\varepsilon}_t = \Omega_a \eta_t + \Omega_b \eta_{t-1} \tag{9}$$

Note that the original parameter's matrices θ and λ can be recovered by expressing them in terms of Ω_a and Ω_b as follows

$$\theta = \Omega_a \circ \left[(\Omega_a + \Omega_b)_{ij}\right]^{-1} \tag{10}$$

$$\lambda = \Omega_a + \Omega_b \tag{11}$$

After solving (9) in terms of η_t and lagging the resulting expression by one period, equation (12) is obtained which justifies the VAR representation provided in (1) assuming an auto-correlated structure in the error term.

$$\hat{\varepsilon}_t = (\Omega_b \Omega_a^{-1})\hat{\varepsilon}_{t-1} + \Omega_a \eta_t + (\Omega_b \Omega_a^{-1} \Omega_b)\eta_{t-2} \tag{12}$$

I obtain maximum likelihood estimators $\left(\widehat{\Omega}_a, \widehat{\Omega}_b, \hat{\sigma}_\eta^2\right)$ for the model (9) by numerically solving the optimization problem given in (13) (see Appendix F for a detailed derivation of these expressions).

$$\left(\widehat{\Omega}_a, \widehat{\Omega}_b, \hat{\sigma}_\eta^2\right) = \underset{\substack{\Omega_a, \Omega_b \in \mathbb{R}_+^{NxN} \\ \sigma_\eta^2 \in \mathbb{R}_+}}{\operatorname{argmax}} \; log\mathcal{L}$$

$$log\mathcal{L} = -\frac{1}{2}\left[T\{N(\log 2\pi + \log \sigma_\eta^2) + 2\log|\Omega_a|\} + \sum_{t=1}^{T} (\hat{\varepsilon}_t - \mu_t)' \frac{(\Omega_a \Omega_a')^{-1}}{\sigma_\eta^2} (\hat{\varepsilon}_t - \mu_t)\right] \tag{13}$$

$$\mu_t = \begin{cases} \emptyset, & t = 1 \\ \sum_{i=1}^{t-1} (-1)^{i+1} (\Omega_b \Omega_a^{-1})^i \, \hat{\varepsilon}_{t-i}, & t > 1 \end{cases}$$

I contrast the gradual diffusion of information hypothesis by means of likelihood ratio tests estimating model (9) on a continent-by-continent basis. To circumvent the curse of dimensionality problem, the number of countries included in this empirical exercise is considerably reduced accounting for only those markets representing more than 2% of the worldwide market capitalization. In particular, the European subsample is composed by France, Germany, Switzerland and United Kingdom while the Asian subsample comprises China, Hong Kong and Japan. Table 5 presents the likelihood estimations of $\widehat{\Omega}_a$ and $\hat{\sigma}_\eta^2$ in panel A and estimation of $\widehat{\Omega}_b$ in panel B.

		Panel A: Ω_a and σ_η^2								
Noth America		CAN	USA	FRA	DEU	CHE	GBR	CHN	HK	JPN
Canada	CAN	1.453	0.058							
United States	USA	0.061	1.171							
				σ_η^2= 0.20						
Europe										
France	FRA			0.000	0.522	1.363	0.112			
Germany	DEU			0.000	1.446	0.262	0.143			
Switzerland	CHE			0.180	0.000	0.000	1.616			
United Kingdom	GBR			1.526	0.000	0.000	0.000			
				σ_η^2= 0.08						
Asia-Pacific										
China	CHN							0.787	0.000	1.306
Hong Kong	HK							1.432	0.369	0.001
Japan	JPN							0.046	1.413	0.134
				σ_η^2= 0.16						
		Panel B: Ω_b								
Noth America		CAN	USA	FRA	DEU	CHE	GBR	CHN	HK	JPN
Canada	CAN	0.264	0.004							
United States	USA	0.118	0.231							
Europe										
France	FRA			0.006	0.194	0.254	0.034			
Germany	DEU			0.000	0.328	0.152	0.117			
Switzerland	CHE			0.125	0.038	0.062	0.272			
United Kingdom	GBR			0.223	0.000	0.079	0.000			
Asia-Pacific										
China	CHN							0.428	0.031	0.143
Hong Kong	HK							0.314	0.210	0.107
Japan	JPN							0.140	0.323	0.148

Table 5: Maximum likelihood estimators of Ω_a , Ω_b and σ_η^2

The hypothesis of gradual diffusion of information is formally stated as follows in terms of Ω_b. First, let us assume that countries i and j are fundamentally interrelated, $\lambda \neq \emptyset$. From equation (8) note that the contemporaneous informational shock vector η_t is entirely and instantaneously absorbed by the vector $\hat{\varepsilon}_t$ as long as $\theta = \mathbf{1}$. Then, the null hypothesis of instantaneous diffusion is $H_0: \theta = \mathbf{1}$ while the alternative gradual diffusion hypothesis is $H_1: \theta \neq \mathbf{1}$. In accordance with equation (10), these two hypotheses are written in term of Ω_b as follows: $H_0: \Omega_b = \emptyset$ and $H_1: \Omega_b \neq \emptyset$.[45]

The values of the log likelihood function for the restricted and unrestricted models, the likelihood ratio statistic and the p-values for the gradual diffusion of information tests are reported in table 6. The hypothesis of instantaneous diffusion is rejected at any sensible level of significance for each of the geographical area. Therefore, this result provides some support to the frictional transmission of information hypothesis as a plausible explanation of the volatility lead-lag coefficients among economies that are reported in table 4.

	Log Likelihood			Countries	Parameters	Restrictions	DF	P-value
	Unrestricted	Restricted	Ratio					
Noth America	- 1,146.32	- 1,178.64	64.64	2	9	4	5	0.00%
Europe	- 1,348.87	- 1,402.07	106.40	4	33	16	17	0.00%
Asia-Pacific	- 1,633.03	- 1,704.96	143.86	3	19	9	10	0.00%

Table 6: Likelihood ratio test for gradual diffusion of information hypothesis

7. Conclusion

The major concern of this study is to shed some light on the nature of volatility spillovers among major capital markets around the world by relying on network theory concepts. I introduce two networks, the International Volatility Network (IVN) and the International Trade Network (ITN), whose nodes stand for a set of large-cap financial markets. The links of the former structure captured significant volatility correlations between pairs of ETFs replicating MSCI market indices of the selected economies. Since the IVN is built in a time series setting, three different versions of this network are identified accounting for the short-run, Granger and long-run interconnections. To obtain sparse estimations of the IVNs, Lasso-related techniques are implemented in this regard. On

[45] This is true since $\Omega_a, \Omega_b \in \mathbb{R}_+^{NxN}$

the other hand, the links from the latter structures captures fundamental relationships across countries as measured by their bilateral trade flows.

The first results show that the long-run IVN and the ITN resemble each other closely evidencing that volatility tends to spread across fundamentally connected countries. The hypothesis is supported upon three empirical observations: (i) a positive and statistically significant correlation between the centrality of countries across these two networks, (ii) a large amount of link's overlapping between the IVN and the ITN that is inconsistent with random arrangements of connections and (iii) a positive and statistically significant correlation between the weights of the same links across these structures. Moreover, I also observe that Asian markets show larger centralities in the IVN than in the ITN thus indicating greater influences of these economies as volatility spreaders than as trade partners.

The second result comes from a detailed analysis of the connections in the Granger IVN. I find that lead-lag volatility coefficients are more likely and stronger between pairs of countries located in the same continent. In network terms, this implies that the Granger IVN is organized in communities where markets from the same geographic area are tightly interconnected among them but loosely interconnected across those areas. Moreover, the pattern of volatility lead-lags found in the data is consistent with the notion of specialized investors reacting fast to innovation arising from target markets while processing the information from other markets with some delay. I formally test this hypothesis through the estimation of an econometric model addressing this behavior. The strong rejection of the null hypothesis of instantaneous diffusion of news against the alternative hypothesis of gradual diffusion of information corresponds to the third results of the paper.

Reference

Alizadeh, S., T. Brandt, and F. X. Diebold, 2002, Rrange-Based Estimation of Stochastic Volatility Models, *The Journal of Finance* 57, 1047–1092.

Andersen, T., T. Bollerslev, F. X. Diebold, and P. Labys, 2003, Modeling and forcasting realized volatility, *Econometrica* 71, 579–625.

Barigozzi, M., and C. Brownlees, 2016, Nets: Network Estimation for Time Series, *SSRN - Working Paper*, 1–43.

Bekaert, G., R. Hodrick, and X. Zhang, 2012, Aggregate Idiosyncratic Volatility, *Journal of Financial and Quantitative Analysis* 47, 1155–1185.

Billio, M., M. Getmansky, A. W. Lo, and L. Pelizzon, 2012, Econometric measures of connectedness and systemic risk in the finance and insurance sectors, *Journal of Financial Economics* 104, 535–559.

Bonacich, P., 1972, Factoring and weighting approaches to status scores and clique identification, *The Journal of Mathematical Sociology* 2, 113–120.

Bonacich, P., 1987, Power and Centrality: A Family of Measures, *American Journal of Sociology* 92, 1170–1182.

Bonacich, P., 2007, Some unique properties of eigenvector centrality, *Social Networks* 29, 555–564.

Diebold, F. X., and K. Yilmaz, 2009, Measuring Financial Asset Return and Volatility Spillovers , With Application to Global Equity Markets, *The Economic Journal* 119, 158–171.

Diebold, F. X., and K. Yilmaz, 2012, Better to give than to receive: Predictive directional measurement of volatility spillovers, *International Journal of Forecasting* 28, 57–66.

Diebold, F. X., and K. Yilmaz, 2014, On the network topology of variance decompositions: Measuring the connectedness of financial firms, *Journal of Econometrics* 182, 119–134.

Diebold, F. X., and K. Yilmaz, 2015, Trans-Atlantic Volatility Connectedness Among Financial Institutions, .

Dimpfl, Thomas, and R.C. Jung, 2012, Financial market spillovers around the globe, *Applied Financial Economics* 22, 45–57.

Friedman, J., T. Hastie, and R. Tibshirani, 2008, Sparse inverse covariance estimation with the graphical lasso., *Biostatistics (Oxford, England)* 9, 432–41.

Garman, M., and M. Klass, 1980, On the Estimation of Security Price Volatilities from Historical Data, *The Journal of Business* 53, 67–68.

Gastineau, G., 2010, *The Exchange-Traded Funds Manual* (John Wiley & Sons, Inc., Hoboken, NJ, USA).

Hamao, Y., R. Masulis, and V. Ng, 1990, Correlations in Price Changes and Volatility across International Stock Markets, *Review of Financial Studies* 3, 281–307.

Hameed, A., R. Morck, J. Shen, and B. Yeung, 2015, Information, Analysts, and Stock Return Comovement, *Review of Financial Studies* 28, 3153–3187.

Hautsch, N., J. Schaumburg, and M. Schienle, 2015, Financial Network Systemic Risk Contributions, *Review of Finance* 9, 685–738.

Hughen, J., and P. Mathew, 2009, The efficiency of international information flow: Evidence from

the ETF and CEF prices, *International Review of Financial Analysis* 18, 40–49.

Investment Company Institute, ed., 2015, *Investment Company Fact Book* (Investment Company Institute).

Jackson, M. O., 2010, *Social and Economic Networks* (Princeton University Press).

Jung, R.C., and R. Maderitsch, 2014, Structural breaks in volatility spillovers between international financial markets: Contagion or mere interdependence?, *Journal of Banking & Finance* 47, 331–342.

Khorana, A., E. Nelling, and J. Tester, 1998, The emergence of country index funds, *Journal of Portfolio Management* 24, 78–84.

King, M., and S. Wadhwani, 1990, Transmission of Volatility between Stock Markets, *Review of Financial Studies* 3, 5–33.

Lin, W., R. Engle, and T. Ito, 1994, Do Bulls and Bears Move Across Borders ? International Transmission of Stock Returns and Volatility, *Review of Financial Studies* 7, 507–538.

Menzly, Lior, and Oguzhan Ozbas, 2010, Market segmentation and cross-predictability of returns, *Journal of Finance* 65, 1555–1580.

Newman, M. E. J., 2003, Mixing patterns in networks, *Physical Review E* 67, 026126.

Newman, M. E. J., 2004, Analysis of weighted networks, *Physical Review E*.

Newman, M. E. J., 2010, *Networks: An Introduction Oxford University Press* (Oxford University Press).

Peralta, G., 2015, Network-based measures as leading indicators of market instability: the case of the Spanish stock market, *Journal of Network Theory in Finance* 1, 91–122.

Rapach, D., J. Strauss, and G. Zhou, 2013, International Stock Return Predictability: What Is the Role of the United States?, *The Journal of Finance* 68, 1633–1662.

Strohsal, T., and E. Weber, 2012, The Signal of Volatility. Duscussion Paper.

Tibshirani, R., 1996, Regression Shrinkage and Selection via Lasso, *Journal of the Royal Statistical Society: Series B (Statistical Methodology)* 58, 267–288.

Tse, Chi K., J. Liu, and F. C. M. Lau, 2010, A network perspective of the stock market, *Journal of Empirical Finance* 17, 659–667.

Tse, Y., and V. Martinez, 2007, Price discovery and informational efficiency of international iShares funds, *Global Finance Journal* 18, 1–15.

Zou, H., 2006, The Adaptive Lasso and Its Oracle Properties, *Journal of the American Statistical Association* 101, 1418–1429.

Appendix A: Estimation Methodology for the IVN

A.1 General Procedure for estimation of coefficients

1) OLS estimation of the coefficients $\widehat{\boldsymbol{\beta}}_{\boldsymbol{ols}}$
2) Estimation of $\hat{\beta}_i$ on a row-by-row basis by optimizing (10) and selecting (λ_1, γ) by means of 3-fold cross validation where $\widehat{w}_j = \left(\left|\hat{\beta}_{j,ols}\right|\right)^{-\gamma}$
3) Estimate Adaptive LASSO $\hat{\beta}_{i,alasso}$ (see A.2 below)
4) Estimate residuals from the Adaptive LASSO regressions
5) Apply Graphical LASSO upon the residuals from step 4 and selecting λ_2 by means of 3-fold cross validation

A.2 Estimation of Adaptive Lasso (Scikit-learn in Python)

1) Compute $\boldsymbol{X}^* = \boldsymbol{X}/\widehat{\boldsymbol{w}}$
2) $\widehat{\boldsymbol{\beta}}^*_{\boldsymbol{alasso}} = \arg\min_{\beta}(\|\boldsymbol{y} - \boldsymbol{X}^*\boldsymbol{\beta}\|_2^2 + \lambda_1\|\boldsymbol{\beta}\|_1)$
3) The corrected estimated coefficients from Adaptive Lasso are thus given by $\widehat{\boldsymbol{\beta}}_{\boldsymbol{alasso}} = \widehat{\boldsymbol{\beta}}^*_{\boldsymbol{alasso}}/\widehat{\boldsymbol{w}}$

Appendix B: Trading Hours by Countries

Region-Country		Local Time Open	Local Time Close	UTC Open	UTC Close	Trading Hours (UTC)
Australia						
Australia	AUS	10:00	16:00	0:00	6:00	
Asia						
Japan	JPN	9:00	15:00	0:00	6:00	
China	CHN	9:30	15:00	1:30	7:00	
Hong Kong	HK	9:30	16:00	1:30	8:00	
Singapore	SGP	9:00	17:00	1:00	9:00	
Europe						
Austria	AUT	8:55	17:35	7:55	16:35	
Sweden	SWE	9:00	17:30	8:00	16:30	
Belgium	BEL	9:00	17:30	8:00	16:30	
France	FRA	9:00	17:30	8:00	16:30	
Germany	DEU	9:00	17:30	8:00	16:30	
Italy	ITA	9:00	17:30	8:00	16:30	
Netherlands	NLD	9:00	17:30	8:00	16:30	
Spain	ESP	9:00	17:30	8:00	16:30	
Switzerland	CHE	9:00	17:30	8:00	16:30	
United Kingdom	GBR	8:00	16:30	8:00	16:30	
North America						
Canada	CAN	9:30	16:00	14:30	21:00	
United States	USA	9:30	16:00	14:30	21:00	

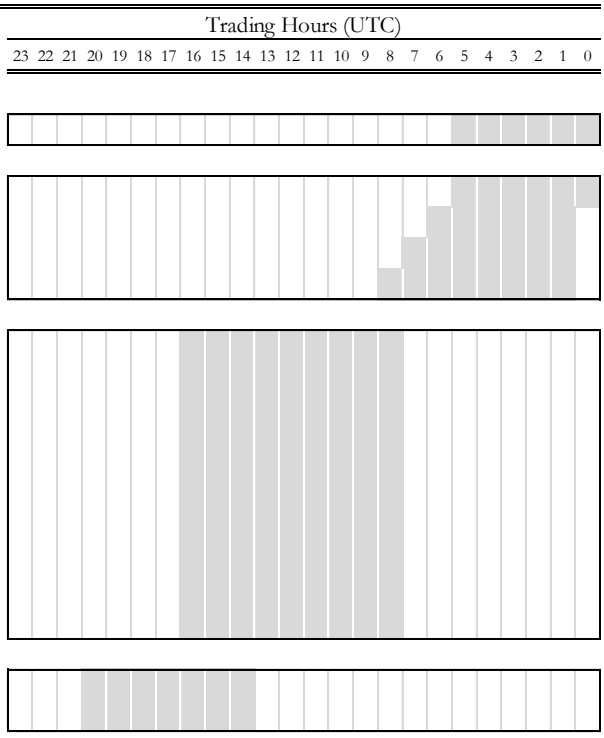

Table B.1: Trading hours by countries sorted by UTC opening

Appendix C: Descriptive Statistics for the Annualized Volatility and Volatility Residuals

Countries	Mean	Median	Min	Max	Std	Skewness	Kurtosis	Autocorrelation			
								Lag 1	Lag 5	Lag 10	Lag 20
Noth America											
Canada	11.0%	9.6%	1.9%	73.3%	6.2%	2.92	17.88	0.51	0.42	0.22	0.18
United States	9.3%	8.1%	2.0%	88.3%	6.0%	4.70	47.11	0.50	0.26	0.11	0.08
Europe											
Austria	8.9%	7.9%	1.8%	48.9%	4.6%	2.65	14.46	0.27	0.16	0.13	0.04
Belgium	8.1%	7.3%	1.5%	46.3%	4.1%	2.57	14.09	0.32	0.16	0.09	0.06
France	9.7%	8.6%	2.2%	54.2%	5.1%	2.27	10.64	0.36	0.24	0.11	0.10
Germany	9.9%	8.9%	2.9%	54.5%	5.1%	2.08	9.77	0.42	0.25	0.13	0.14
Italy	12.3%	11.0%	3.6%	46.6%	5.7%	1.94	5.75	0.37	0.23	0.11	0.07
Netherlands	8.2%	7.3%	1.8%	63.9%	4.7%	3.55	31.52	0.40	0.24	0.14	0.13
Spain	11.3%	10.2%	2.8%	49.6%	5.6%	1.86	5.86	0.36	0.18	0.06	0.07
Sweden	9.6%	8.5%	2.6%	49.0%	4.8%	2.42	11.02	0.40	0.20	0.07	0.09
Switzerland	7.7%	6.8%	1.8%	49.9%	4.1%	3.04	19.80	0.40	0.19	0.14	0.14
United Kingdom	8.7%	7.9%	1.8%	44.9%	4.5%	2.51	10.99	0.48	0.31	0.14	0.13
Asia-Pacific											
Australia	9.4%	8.1%	1.2%	46.3%	5.2%	2.34	9.22	0.48	0.39	0.25	0.19
China	10.9%	9.4%	2.4%	97.2%	6.6%	4.57	45.61	0.53	0.23	0.11	0.13
Hong Kong	8.3%	7.2%	2.1%	81.1%	5.1%	5.68	66.71	0.42	0.19	0.10	0.07
Japan	8.4%	7.3%	2.3%	48.5%	4.5%	2.27	10.85	0.55	0.35	0.19	0.13
Singapore	7.4%	6.5%	1.5%	53.4%	4.4%	3.79	26.87	0.46	0.24	0.16	0.12
Global											
First PC	19.4%	17.4%	8.0%	131.0%	9.1%	4.02	35.58	0.53	0.28	0.12	0.11

Table C.1: Descriptive statistics Annualized Volatility for period 2013-6 to 2016-1

Countries	Mean	Median	Min	Max	Std	Skewness	Kurtosis	Autocorrelation			
								Lag 1	Lag 5	Lag 10	Lag 20
Noth America											
Canada	0.000	0.007	-2.431	2.513	0.666	-0.069	0.509	0.259	0.206	0.150	0.017
United States	0.000	0.022	-2.323	2.613	0.540	-0.191	1.093	0.238	0.151	0.107	0.011
Europe											
Austria	0.000	-0.001	-2.379	2.435	0.628	-0.053	1.270	0.114	0.044	0.079	0.062
Belgium	0.000	0.013	-2.687	2.169	0.545	-0.132	1.171	0.137	0.130	0.060	0.086
France	0.000	0.009	-1.759	1.914	0.421	0.033	1.047	0.271	0.212	0.165	0.093
Germany	0.000	-0.003	-1.648	1.270	0.428	-0.132	0.379	0.308	0.309	0.238	0.158
Italy	0.000	-0.038	-1.531	1.673	0.461	0.249	0.299	0.261	0.226	0.186	0.108
Netherlands	0.000	0.010	-1.706	1.270	0.436	-0.262	0.580	0.237	0.140	0.099	0.089
Spain	0.000	-0.015	-1.288	1.564	0.458	-0.025	0.156	0.230	0.075	0.148	0.053
Sweden	0.000	0.009	-1.967	1.668	0.471	-0.054	1.081	0.081	0.061	0.047	0.036
Switzerland	0.000	0.008	-1.693	2.594	0.460	0.270	1.858	0.186	0.048	-0.055	-0.007
United Kingdom	0.000	-0.004	-1.772	1.581	0.431	-0.070	0.986	0.147	0.060	0.079	-0.045
Asia-Pacific											
Australia	0.000	0.026	-2.419	1.717	0.521	-0.228	0.815	0.121	0.059	0.136	0.037
China	0.000	-0.008	-1.889	2.604	0.651	0.036	0.320	0.311	0.217	0.191	0.143
Hong Kong	0.000	0.005	-2.208	2.651	0.628	0.001	0.559	0.357	0.229	0.193	0.169
Japan	0.000	0.013	-2.280	1.824	0.601	-0.273	0.209	0.325	0.268	0.219	0.170
Singapore	0.000	0.021	-2.205	3.198	0.673	-0.073	0.791	0.279	0.292	0.207	0.221
Global											
First PC											

Table C.2: Descriptive statistics Volatility Residuals for period 2013-6 to 2016-1

Appendix D: Regression between the link's weights across the IVN and ITN

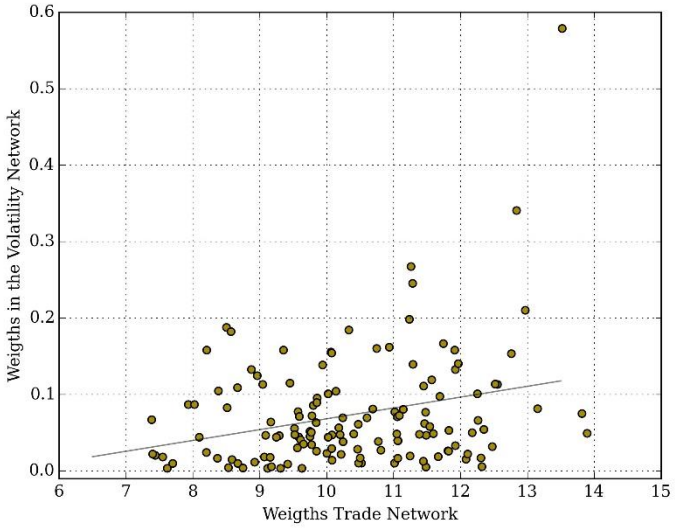

Figure D.1: Scatter plot between the weights of the links in the IVN and in the ITN. The solid line correspond to the results of OLS estimation as reported by table 3.

Appendix E: Plot of the Granger IVN

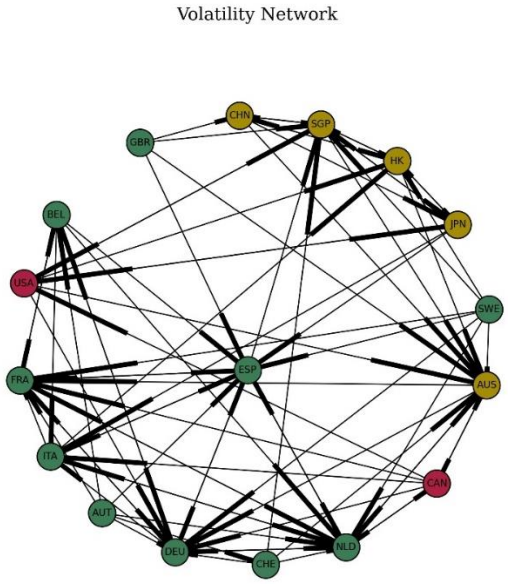

Figure E.1: Granger IVN

Appendix F: Log likelihood function of the Gradual Diffusion of Information Model

Let us starts from equation (9) from section 6 where $\hat{\varepsilon}_t, \eta_t \in \mathbb{R}^N$ and $t = 1,2,\dots,T$

$$\hat{\varepsilon}_t = \Omega_a \eta_t + \Omega_b \eta_{t-1} \tag{F.1}$$

Assuming $\eta_0 = \emptyset$ and $\eta_t \sim \phi_N\left(\emptyset, \sigma_\eta^2 I_N\right)$, the next expressions can be obtained by successive replacements

Period of time	Volatility Shock	Distribution
1	$\hat{\varepsilon}_1 = \Omega_a \eta_1$	$\phi_N\left(\emptyset, \sigma_\eta^2(\Omega_a \Omega_a')\right)$
2	$\hat{\varepsilon}_2 = \Omega_a \eta_2 + \Omega_b \Omega_a^{-1} \hat{\varepsilon}_1$	$\phi_N\left(\Omega_b \Omega_a^{-1} \hat{\varepsilon}_1, \sigma_\eta^2(\Omega_a \Omega_a')\right)$
3	$\hat{\varepsilon}_3 = \Omega_a \eta_3 + \Omega_b \Omega_a^{-1} \hat{\varepsilon}_2 - (\Omega_b \Omega_a^{-1})^2 \hat{\varepsilon}_1$	$\phi_N\left(\Omega_b \Omega_a^{-1} \hat{\varepsilon}_2 - (\Omega_b \Omega_a^{-1})^2 \hat{\varepsilon}_1, \sigma_\eta^2(\Omega_a \Omega_a')\right)$

In general term, the expressions for the volatility shock and the corresponding probability distribution for period t are

Period of time	Volatility Shock	Distribution
t	$\hat{\varepsilon}_t = \Omega_a \eta_t + \mu_t$	$\phi_N\left(\mu_t, \sigma_\eta^2(\Omega_a \Omega_a')\right)$

Where

$$\mu_t = \begin{cases} \emptyset, & t = 1 \\ \sum_{i=1}^{t-1} (-1)^{i+1} (\Omega_b \Omega_a^{-1})^i \hat{\varepsilon}_{t-i}, & t > 1 \end{cases}$$

Note that μ_t can be written as $\mu_t = \beta X_t$ where β is an $N \times N(T-1)$ matrix and X_t is an $N(T-1)$ dimensional vector of the form

$$\beta = [[\Omega_b \Omega_a^{-1}] \quad -[\Omega_b \Omega_a^{-1}]^2 \quad [\Omega_b \Omega_a^{-1}]^3 \quad \dots \quad (-1)^t (\Omega_b \Omega_a^{-1})^{t-1}]$$

$$X_t' = [\hat{\varepsilon}_{t-1} \quad \hat{\varepsilon}_{t-2} \quad \hat{\varepsilon}_{t-3} \quad \dots \quad \hat{\varepsilon}_1]$$

Therefore, the log of the density function of $\hat{\varepsilon}_t$ is

$$\log \phi_N\left(\mu_t, \sigma_\eta^2(\Omega_a\Omega_a')\right) = -\frac{1}{2}\left[N\log 2\pi + \log\left|\sigma_\eta^2\Omega_a\Omega_a'\right| + (\hat{\varepsilon}_t - \mu_t)'\frac{(\Omega_a\Omega_a')^{-1}}{\sigma_\eta^2}(\hat{\varepsilon}_t - \mu_t)\right]$$
$$= -\frac{1}{2}\left[N\left(\log 2\pi + \log\sigma_\eta^2\right) + 2\log|\Omega_a| + (\hat{\varepsilon}_t - \mu_t)'\frac{(\Omega_a\Omega_a')^{-1}}{\sigma_\eta^2}(\hat{\varepsilon}_t - \mu_t)\right]$$

Finally, the log likelihood function for the entire sample is

$$log\mathcal{L} = \sum_{t=1}^{T}\log\phi_N\left(\mu_t, \sigma_\eta^2\left(\Omega_a\Omega_a^{'}\right)\right)$$
$$= -\frac{1}{2}\left[T\left\{N\left(\log 2\pi + \log\sigma_\eta^2\right) + 2\log|\Omega_a|\right\} + \sum_{t=1}^{T}\left(\hat{\varepsilon}_t - \mu_t\right)'\frac{\left(\Omega_a\Omega_a^{'}\right)^{-1}}{\sigma_\eta^2}\left(\hat{\varepsilon}_t - \mu_t\right)\right]$$